ISM Dynamics and Star Formation

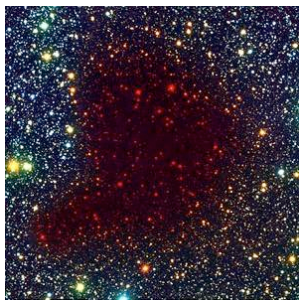
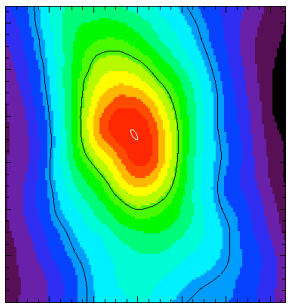

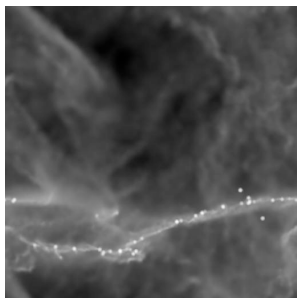

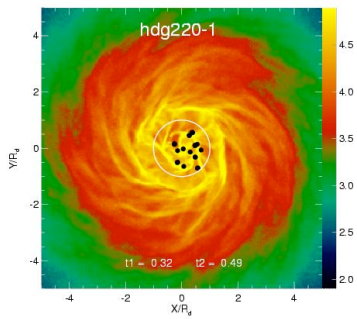

Ralf Klessen

Zentrum für Astronomie der Universität Heidelberg
Institut für Theoretische Astrophysik

thanks to ...

- many thanks to
  - Robi Banerjee (ITA)
  - Paul Clark (ITA)
  - Clare Dobbs (Exeter)
  - Christoph Federrath (ITA)
  - Simon Glover (ITA)
  - Thomas Greif (ITA)
  - Patrick Hennebelle (ENS)
  - Mordecai Mac Low (AMNH)
  - Dominik Schleicher (ITA)
  - Enrique Vazquez-Semadeni (UNAM)

agenda

- importance of *chemistry* and *thermodynamics* on formation and evolution of *molecular cloud* and their ability to *form stars*
  - formation of molecular clouds in galactic disks (H_2 & CO chemistry)
  - universal IMF: influence of thermodynamics

agenda

- importance of *chemistry* and *thermodynamics* on formation and evolution of *molecular cloud* and their ability to *form stars*
  - formation of molecular clouds in galactic disks (H_2 & CO chemistry)
  - universal IMF: influence of thermodynamics

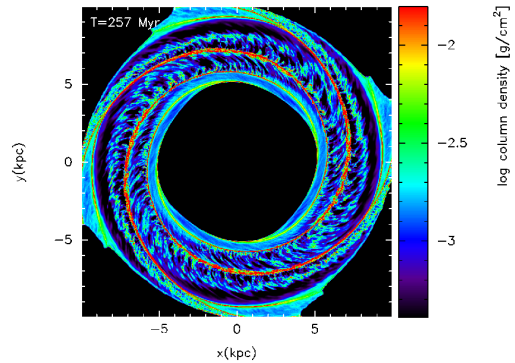

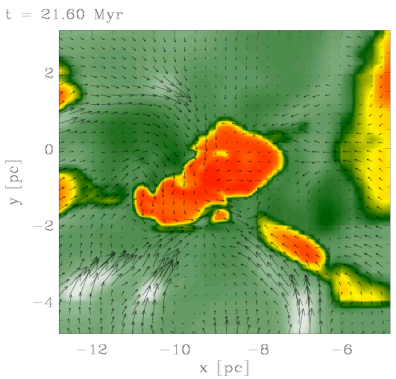

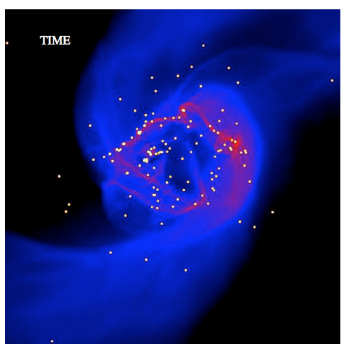

dynamical SF in a nutshell

- interstellar gas is highly *inhomogeneous*
  - *gravitational instability*
  - *thermal instability*
  - *turbulent compression* (in shocks $\delta\rho/\rho \propto \mathcal{M}^2$; in atomic gas: $\mathcal{M} \approx 1...3$)

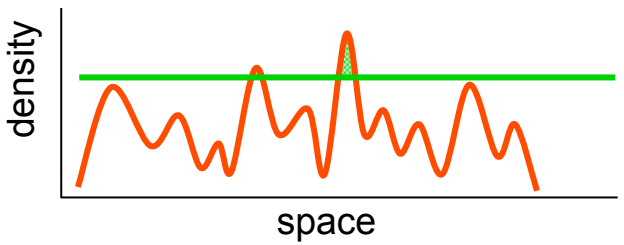

- cold *molecular clouds* can form rapidly in high-density regions at *stagnation points* of *convergent large-scale flows*
  - chemical *phase transition*: atomic → molecular
  - process is *modulated* by large-scale *dynamics* in the galaxy
- inside *cold clouds:* turbulence is highly supersonic ($\mathcal{M} \approx 1...20$)
  → *turbulence* creates large density contrast,
  gravity selects for collapse

→ ***GRAVOTUBULENT FRAGMENTATION***

- *turbulent cascade:* local compression *within* a cloud provokes collapse
  → formation of individual *stars* and *star clusters*

(e.g. Mac Low & Klessen, 2004, Rev. Mod. Phys., 76, 125-194)

molecular cloud formation

molecular cloud formation

- star formation on galactic scales
  → missing link so far:
  formation of molecular clouds
- questions
  - *where* and *when* do molecular clouds form?
  - *what* are their properties?
  - *how* does that correlation to star formation?
  - global correlations? → *Schmidt law*

molecular cloud formation

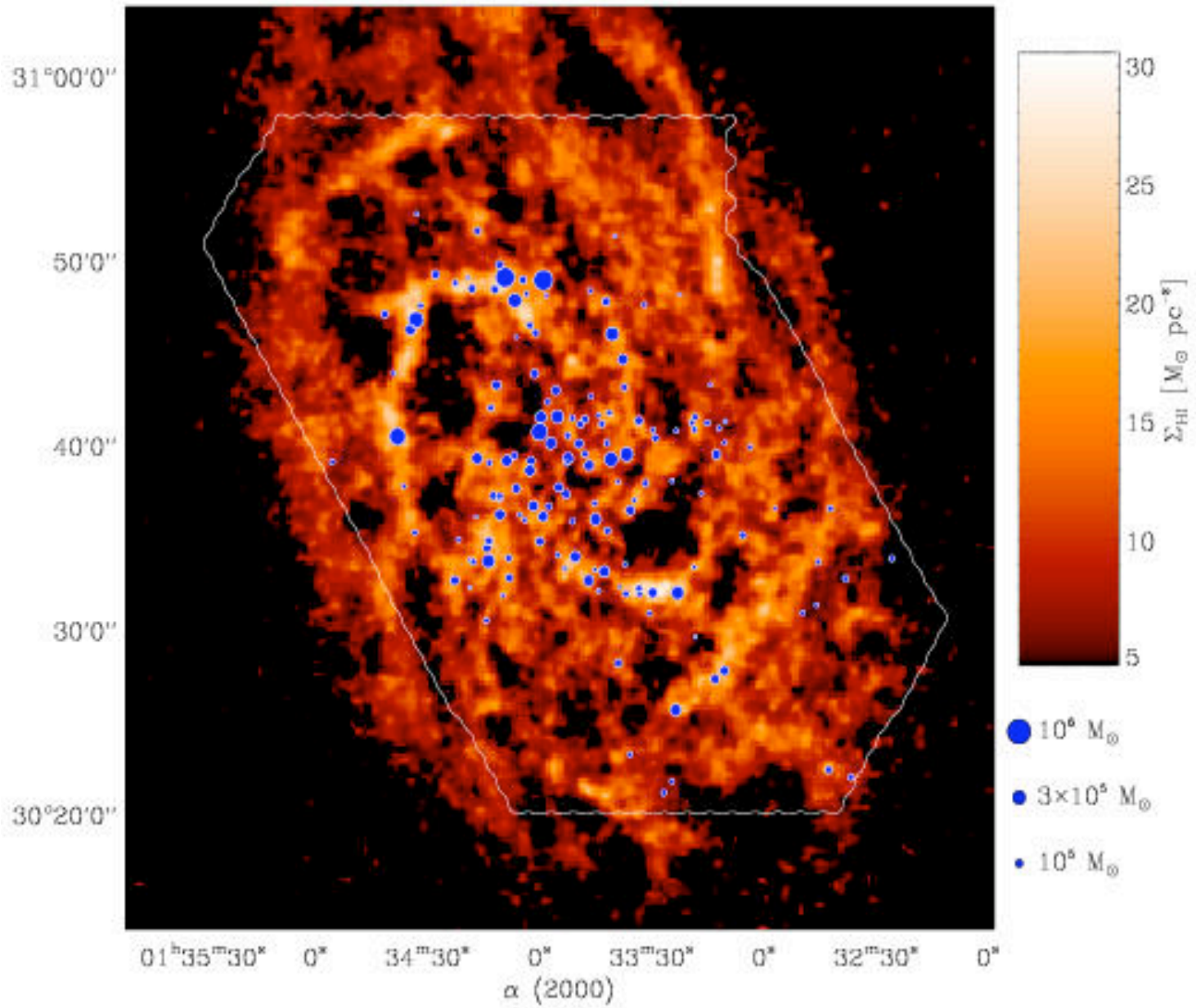

(Deul & van der Hulst 1987, Blitz et al. 2004)

Thesis:

Molecular clouds form at *stagnation points* of large-scale convergent flows, mostly triggered by global (or external) perturbations.

modeling galactic SF

SPH calculations of self-gravitating disks of stars and (isothermal) gas in dark-matter potential, sink particles measure local collapse --> star formation

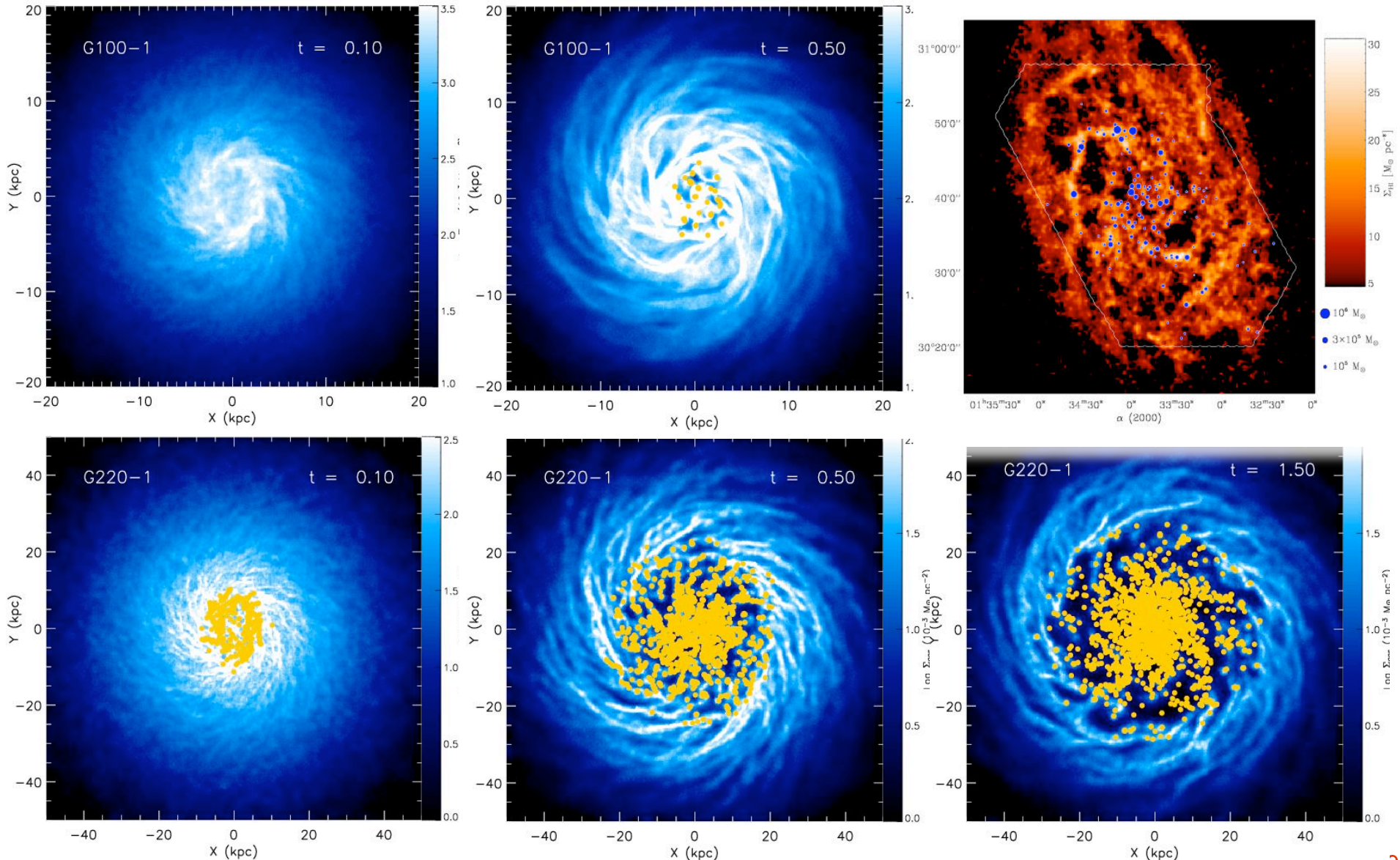

(Li, Mac Low, & Klessen, 2005, ApJ, 620,L19 - L22)

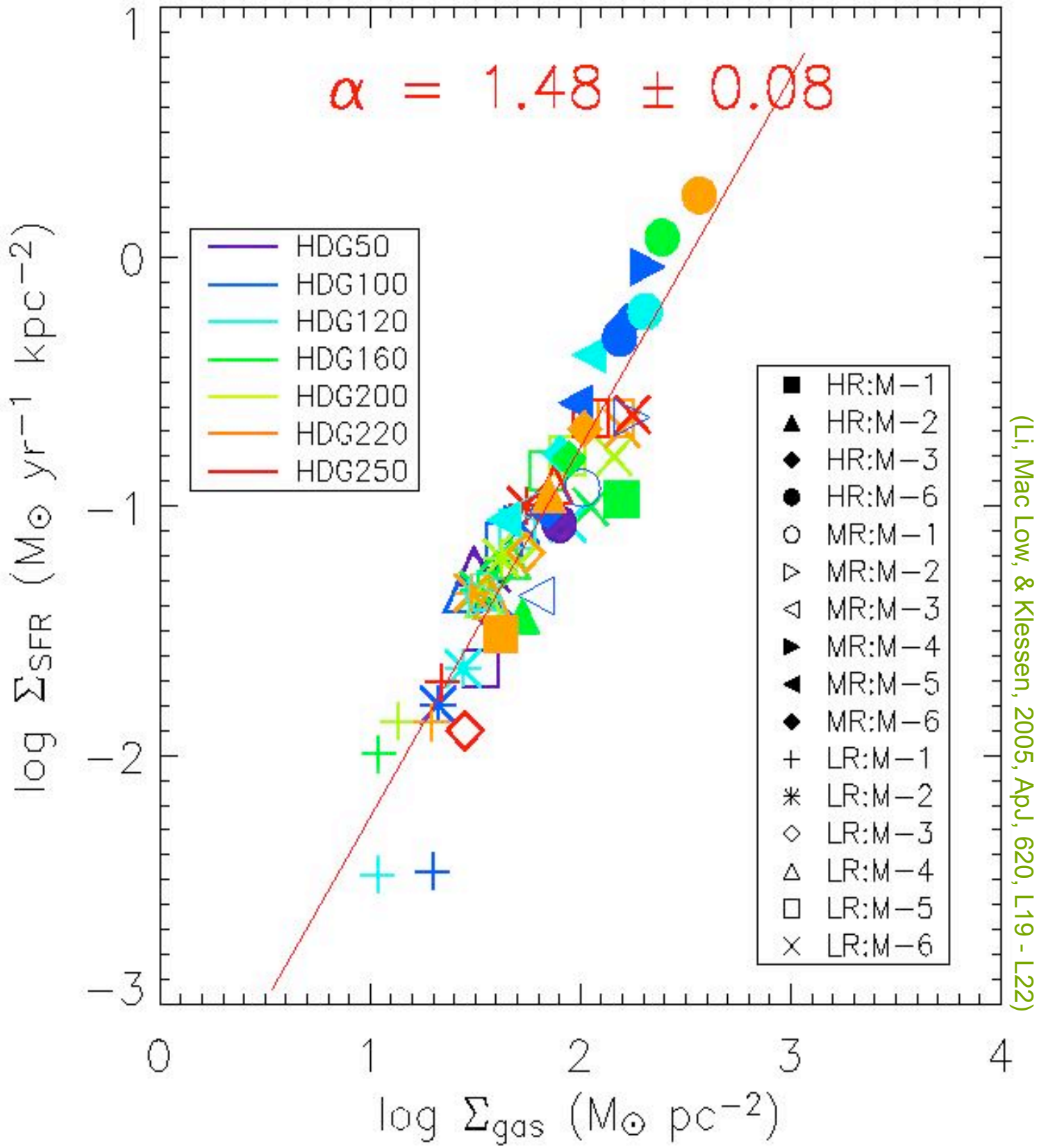

(Li, Mac Low, & Klessen, 2005, ApJ, 620, L19 - L22)

We find correlation between *star formation rate* and *gas surface density:*

$$\Sigma_{SFR} \propto \Sigma_{gas}^{1.5}$$

global Schmidt law

observed Schmidt law

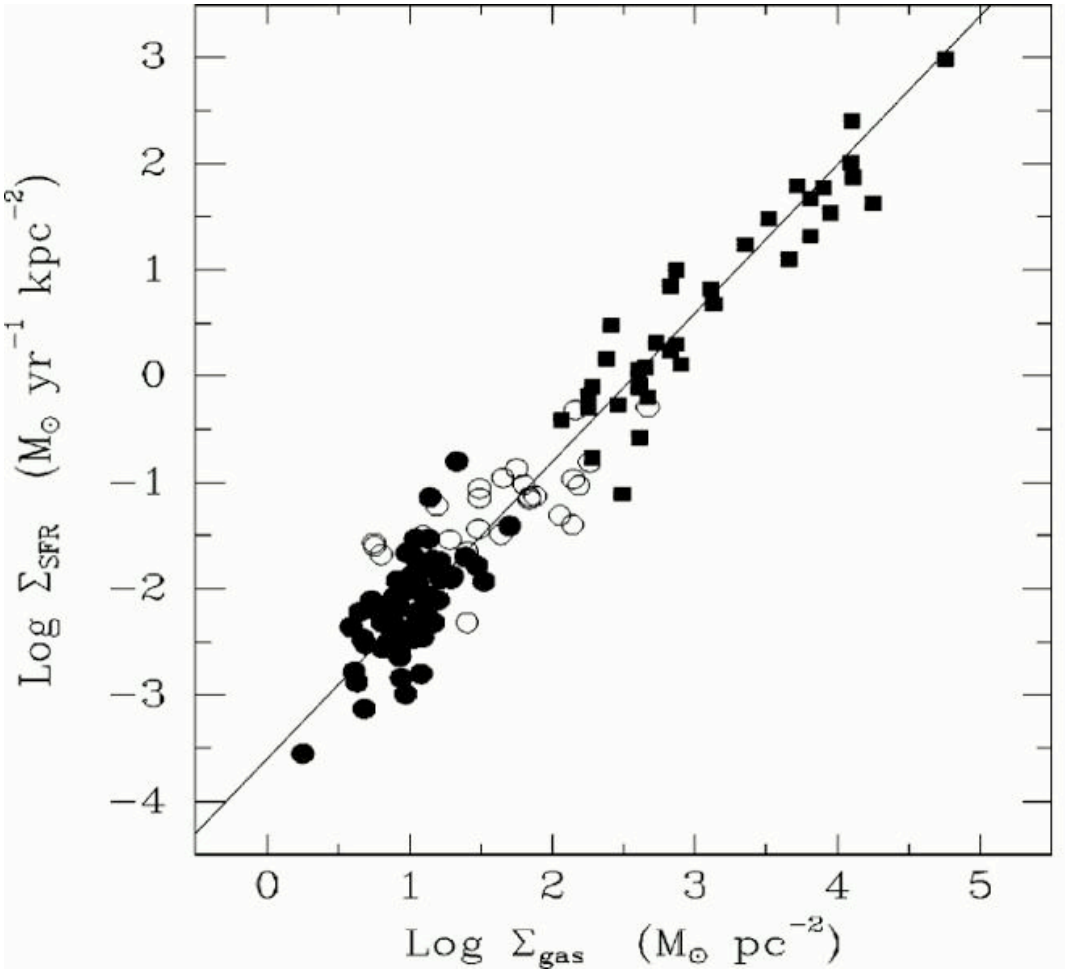

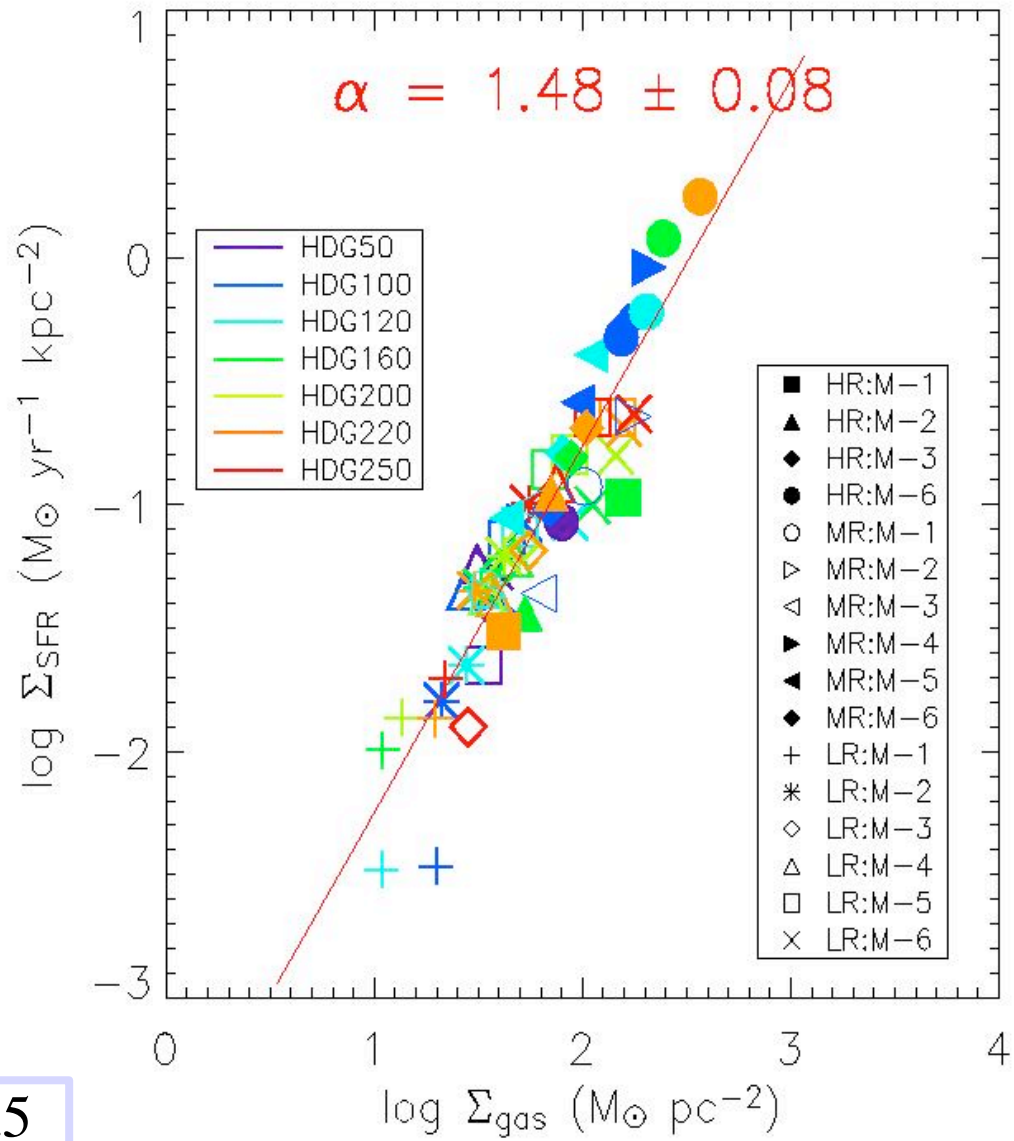

in both cases: $\Sigma_{SFR} \propto \Sigma_{gas}^{1.5}$

(from Kennicutt 1998)

local Schmidt law

Gravity only:
Local Schmidt law exhibits downturn!
Global one does not.

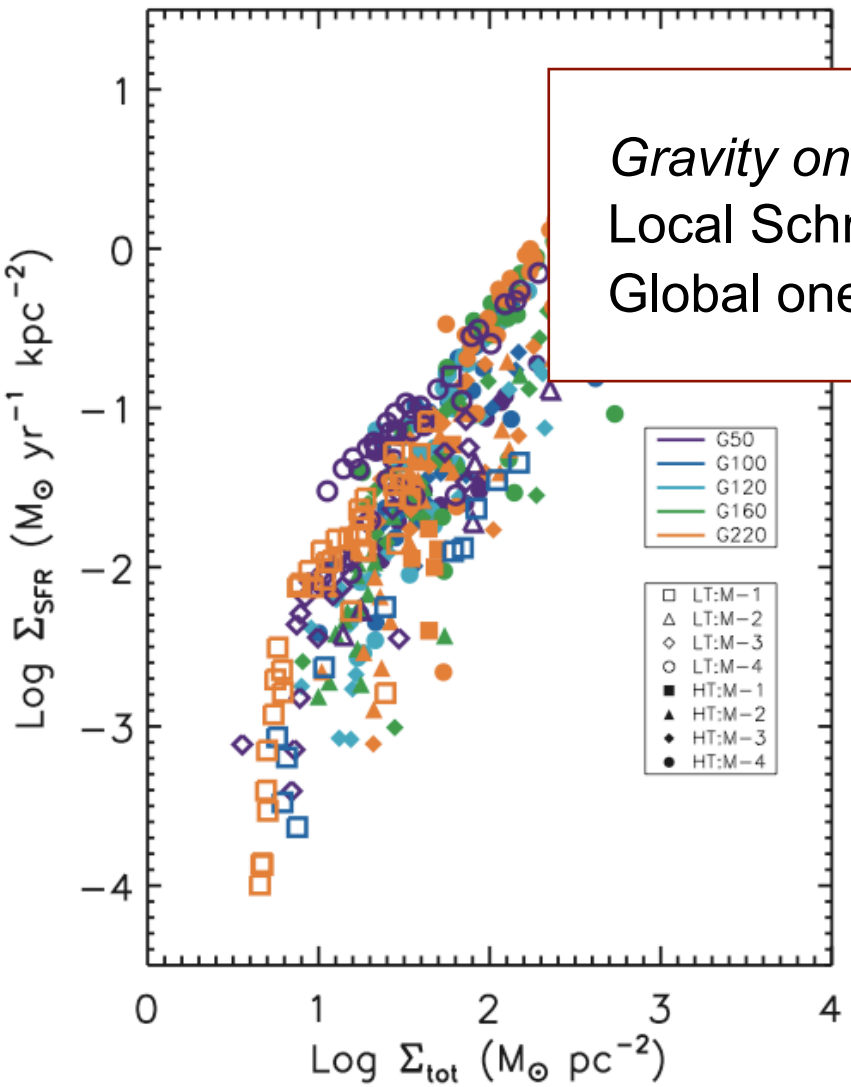

FIG. 11.—Local Schmidt laws of all models with $\tau_{SF} < 3$ Gyr. The legends are the same as in Fig. 5: the color of the symbol indicates the rotational velocity for each model as given in Table 1, the shape indicates the submodel classified by gas fraction, and open and filled symbols represent low- and high-T models, respectively.

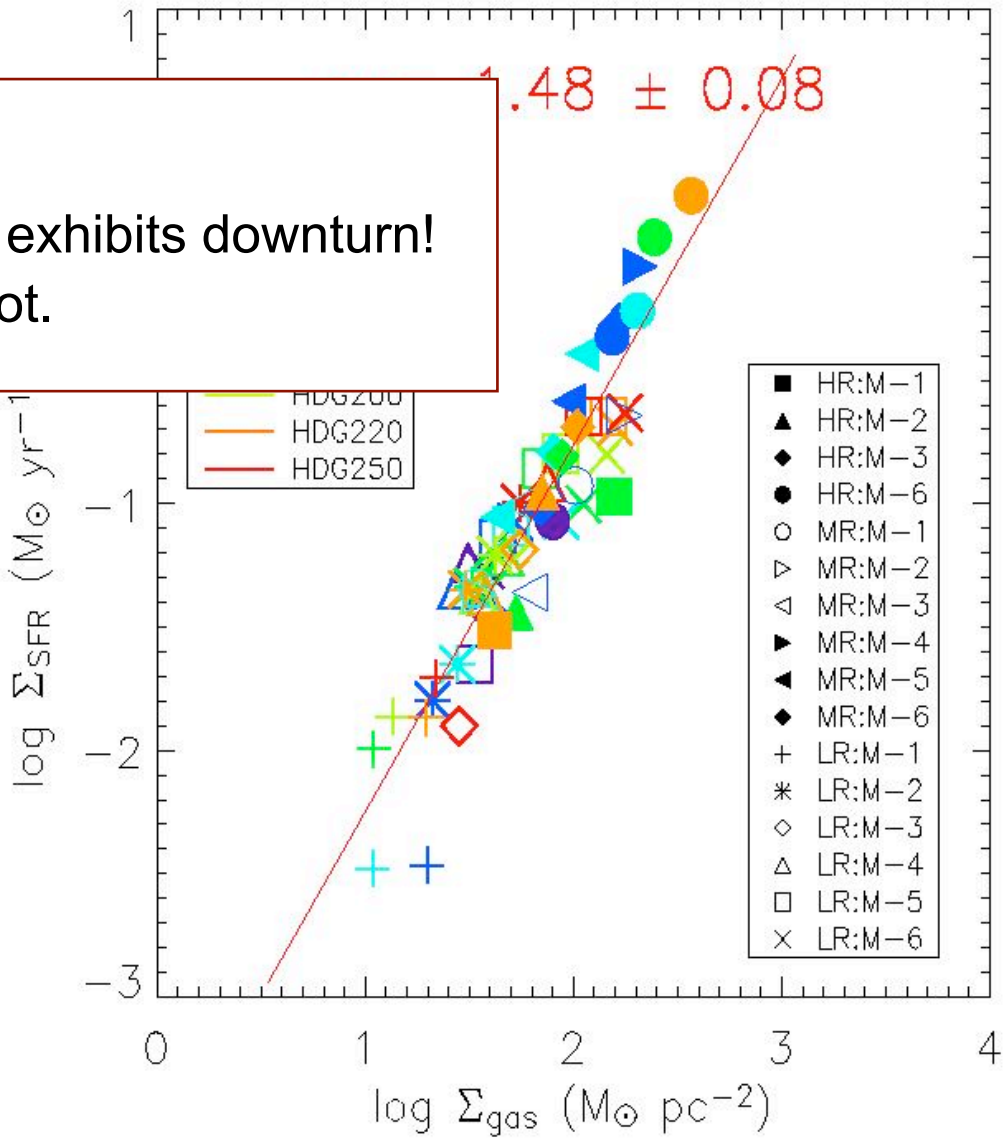

(Li et al. 2006)

correlation with large-scale perturbations

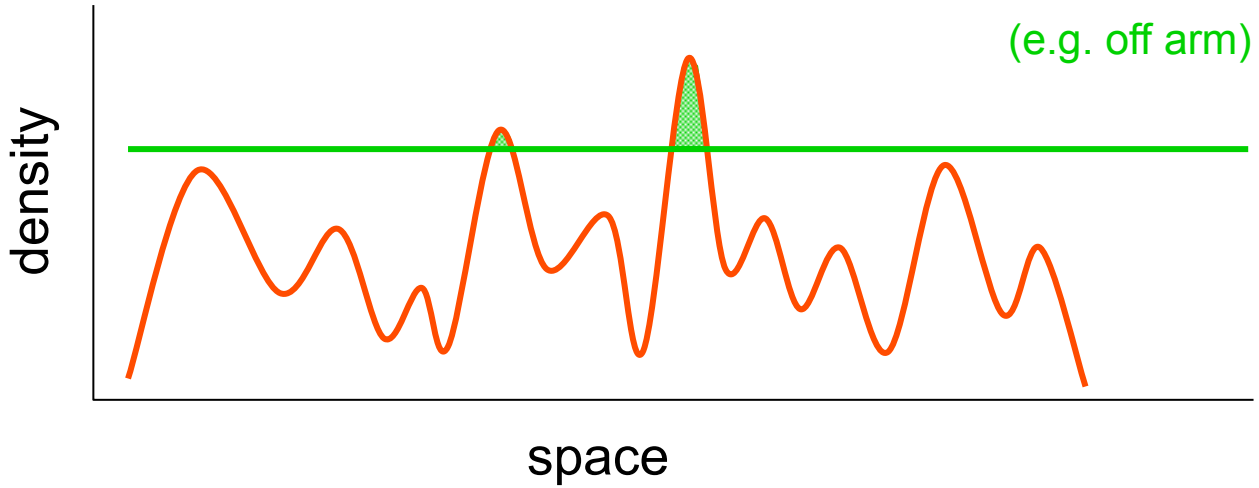

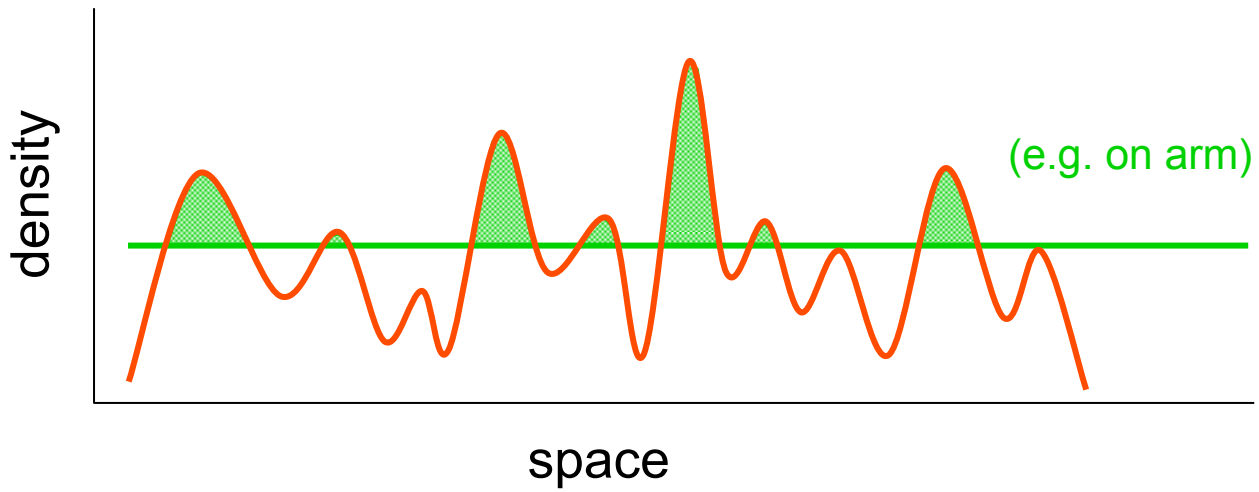

density/temperature fluctuations in warm atomar ISM are caused by *thermal/gravitational instability* and/or *supersonic turbulence*

some fluctuations are *dense* enough to *form* H_2 within "*reasonable time*"
→ *molecular cloud*

(Glover & Mac Low 2007a,b)

external perturbations (i.e. potential changes) *increase* likelihood

star formation on *global* scales

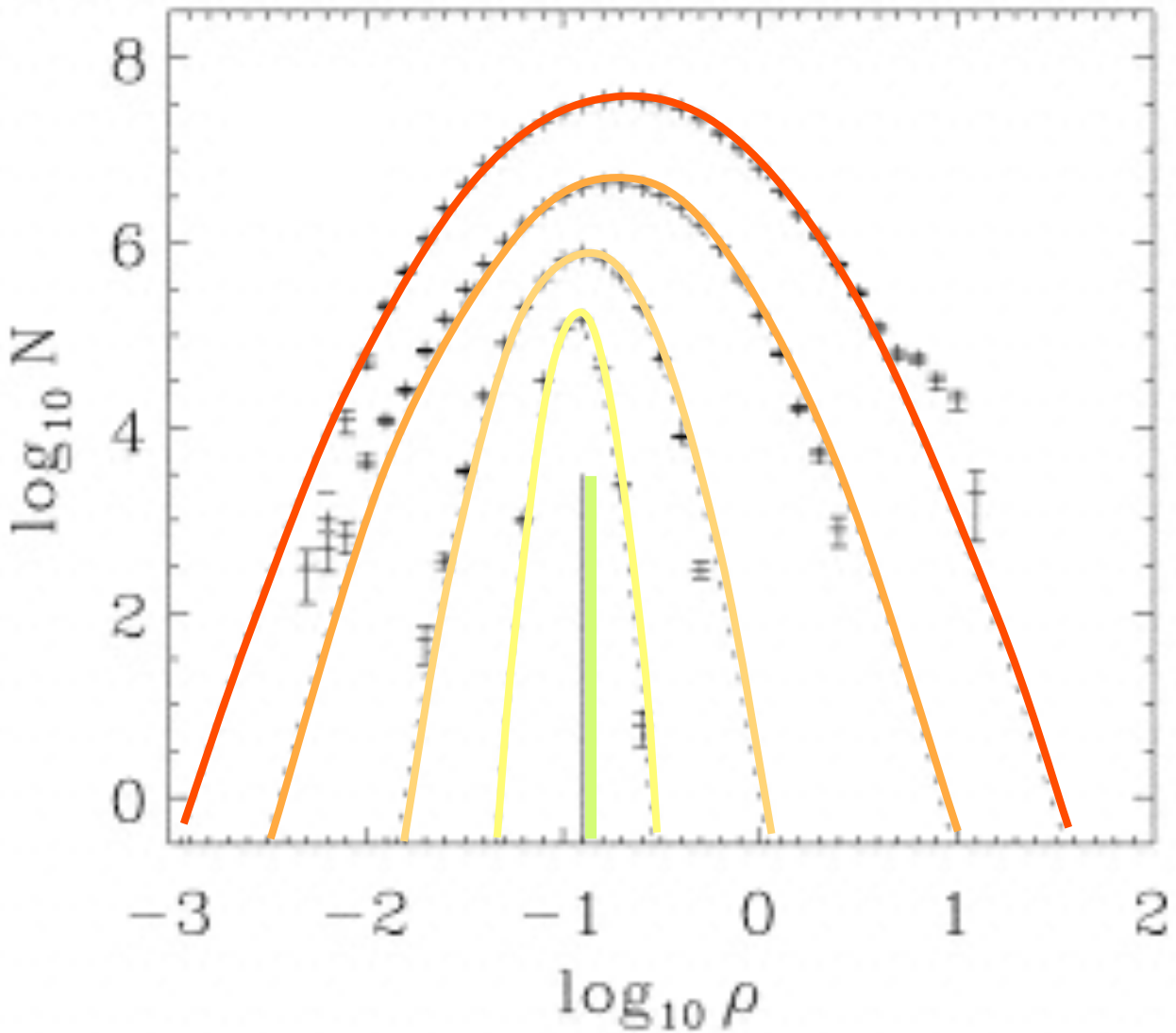

mass weighted ρ-pdf, each shifted by ΔlogN=1

(from Klessen, 2001; also Gazol et al. 2005, Krumholz & McKee 2005)

probability distribution function of the density *(ρ-pdf)*

varying rms Mach numbers:

M1 > M2 > M3 > M4 > 0

star formation on *global* scales

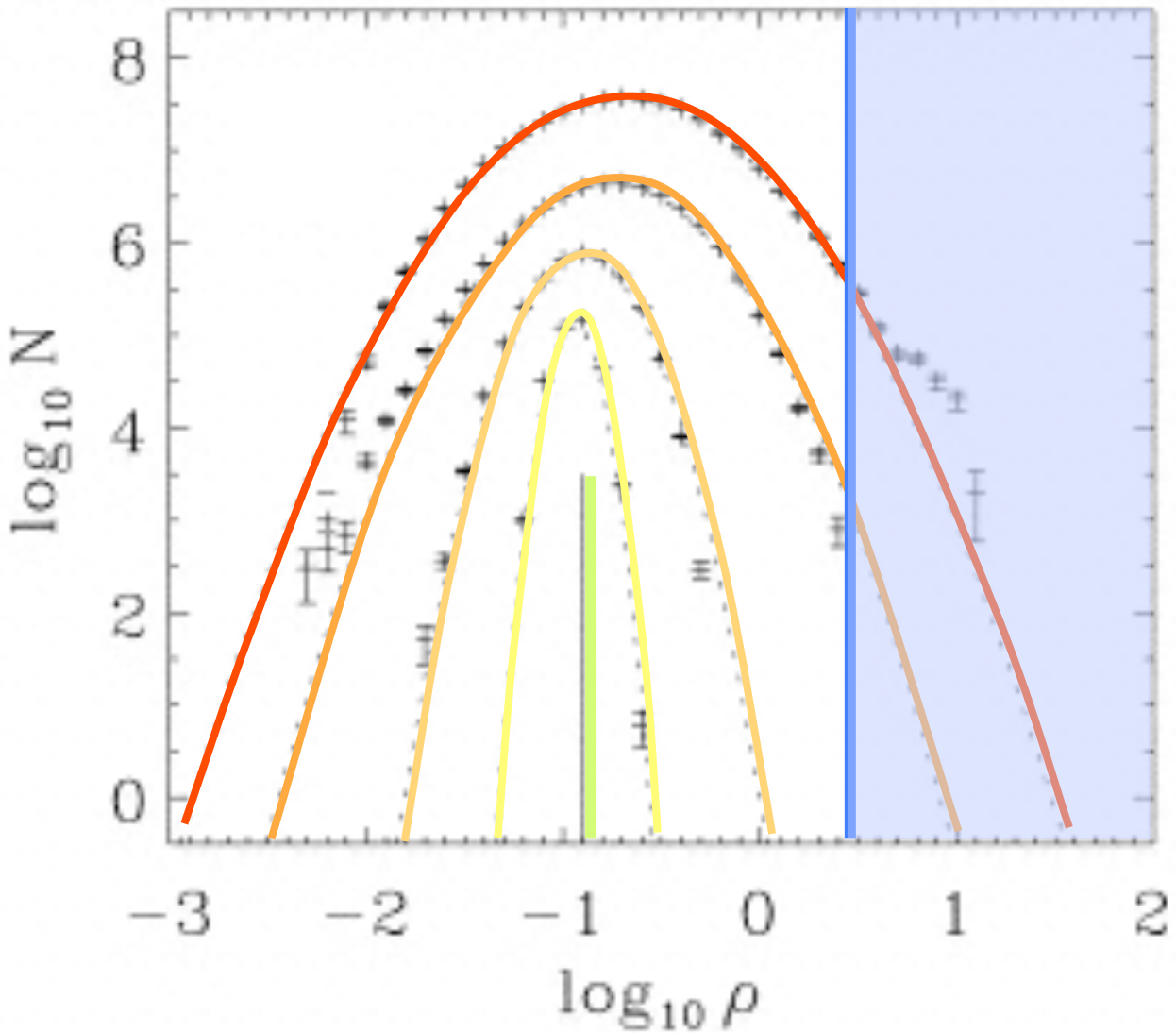

mass weighted ρ-pdf, each shifted by ΔlogN=1

(rate from Hollenback, Werner, & Salpeter 1971)

H_2 formation rate:

$$\tau_{H_2} \approx \frac{1.5\,\mathrm{Gyr}}{n_H / 1\mathrm{cm}^{-3}}$$

for $n_H \geq 100$ cm^{-3}, H_2 forms within 10 Myr, this is about the lifetime of typical MC's.

in turbulent gas, the H_2 fraction can become very high on short timescale

(for models with coupling between cloud dynamics and time-dependent chemistry, see Glover & Mac Low 2007a,b)

star formation on *global* scales

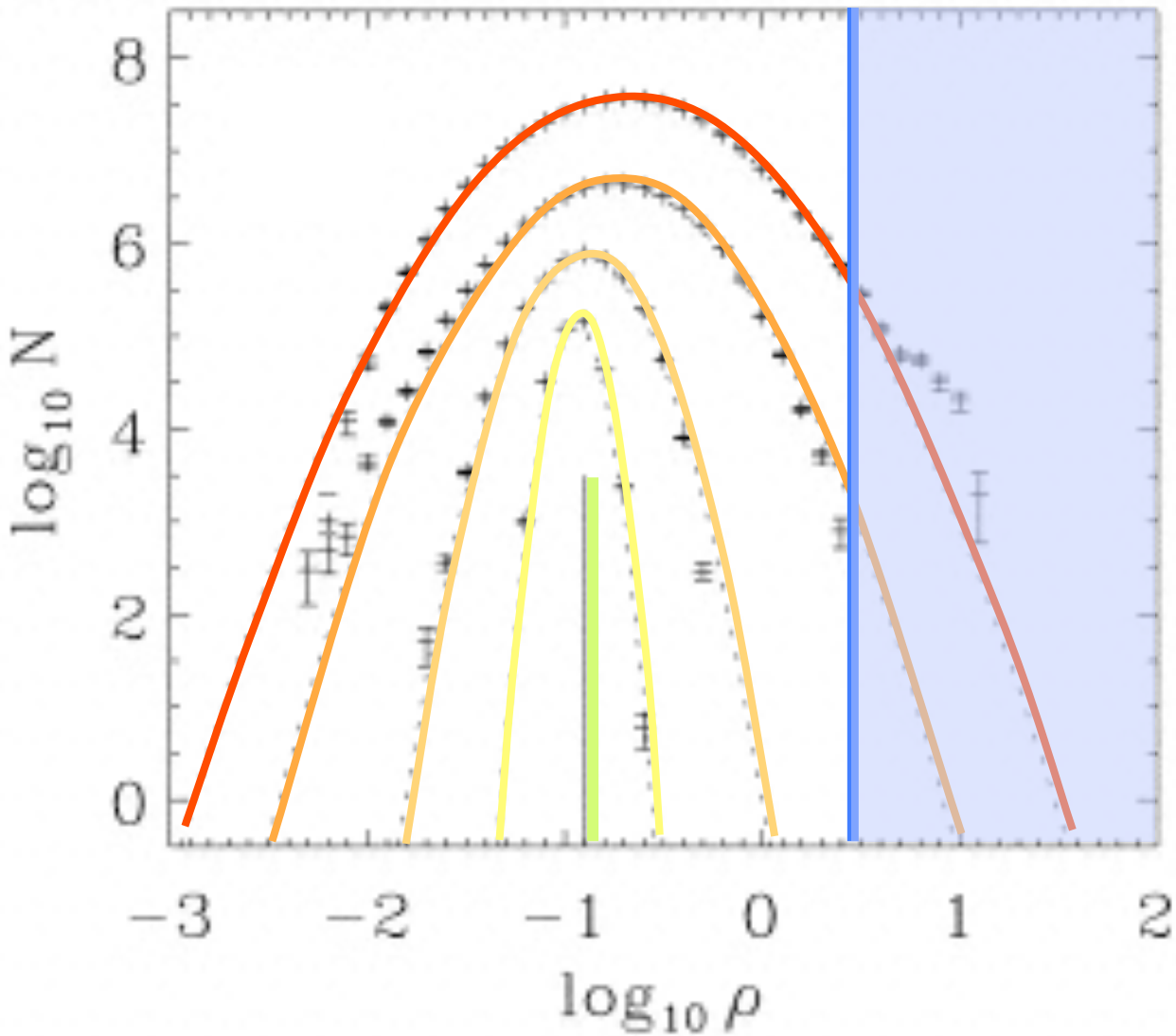

mass weighted ρ-pdf, each shifted by ΔlogN=1

(rate from Hollenback, Werner, & Salpeter 1971)

BUT: *it doesn't work*
(at least not so easy):

Chemistry has a memory effect!

H2 forms more quickly in high-density regions as it gets destroyed in low-density parts.

(for models with coupling between cloud dynamics and time-dependent chemistry, see Glover & Mac Low 2007a,b)

molecular cloud formation

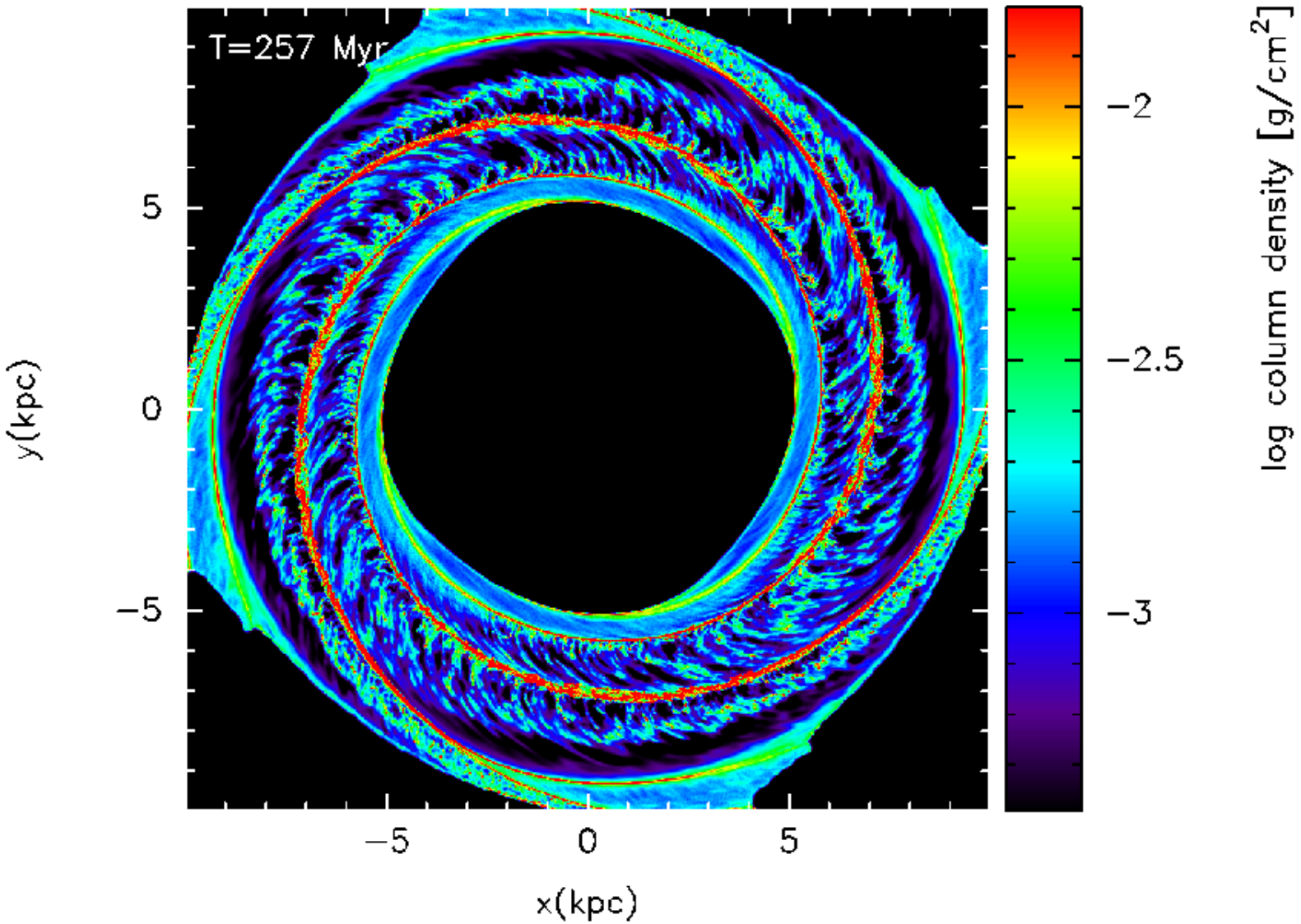

(from Dobbs, Glover, Clark, Klessen 2008)

molecular cloud formation

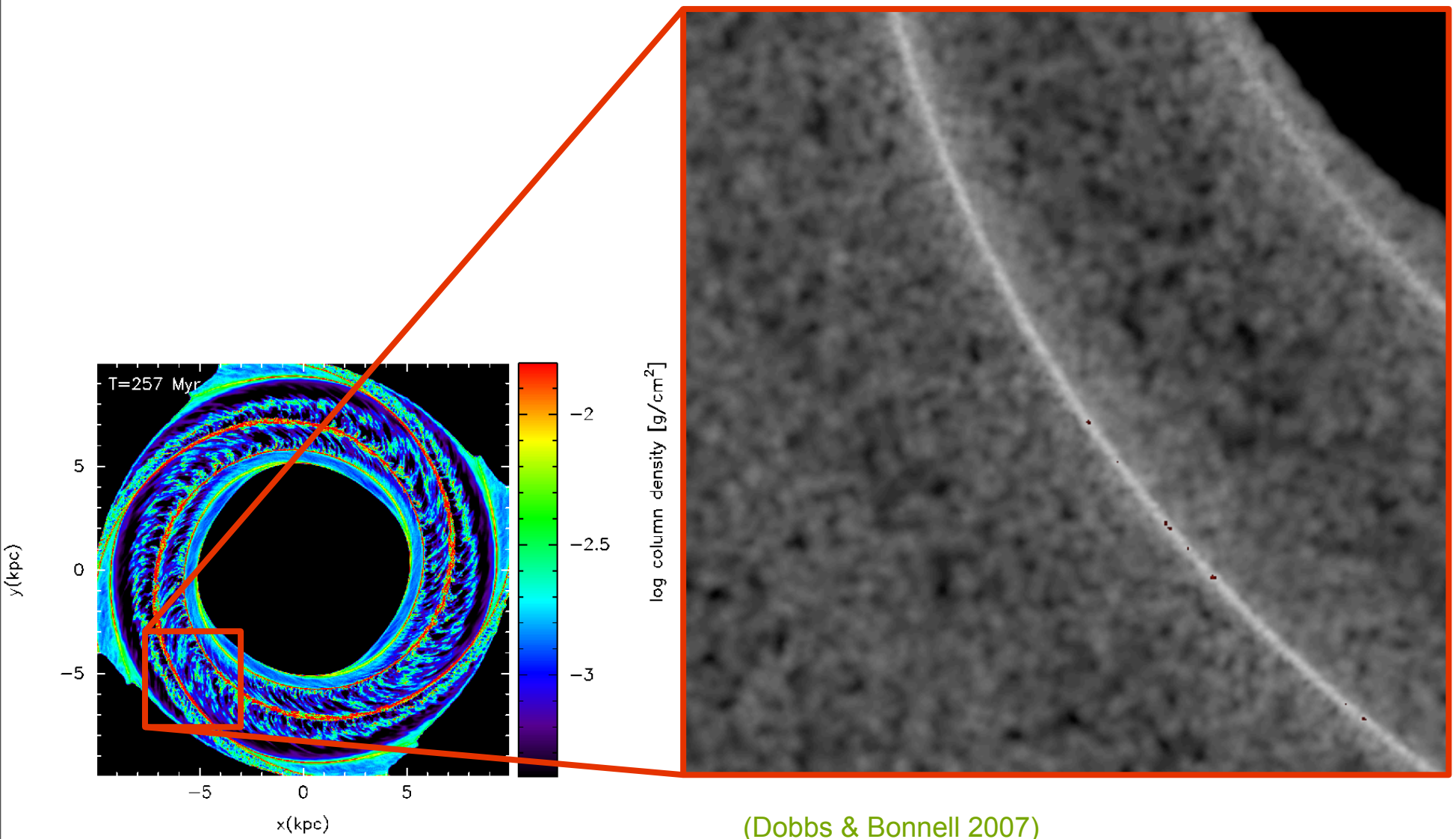

(Dobbs & Bonnell 2007)

molecular cloud formation

molecular gas fraction as function of time

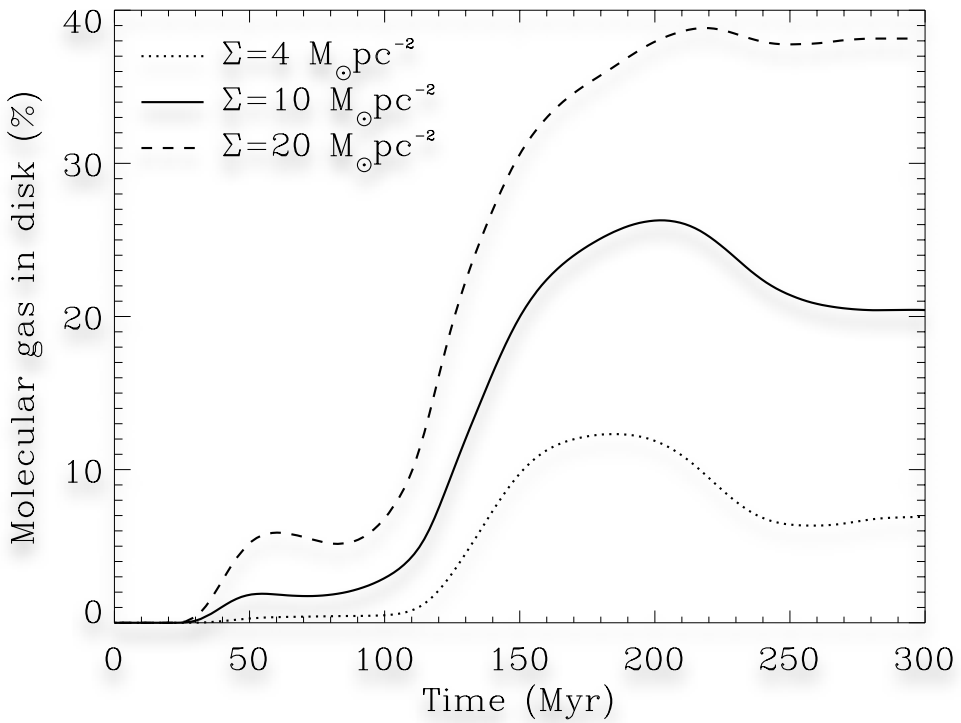

(Dobbs et al. 2008)

molecular gas fraction as function of density

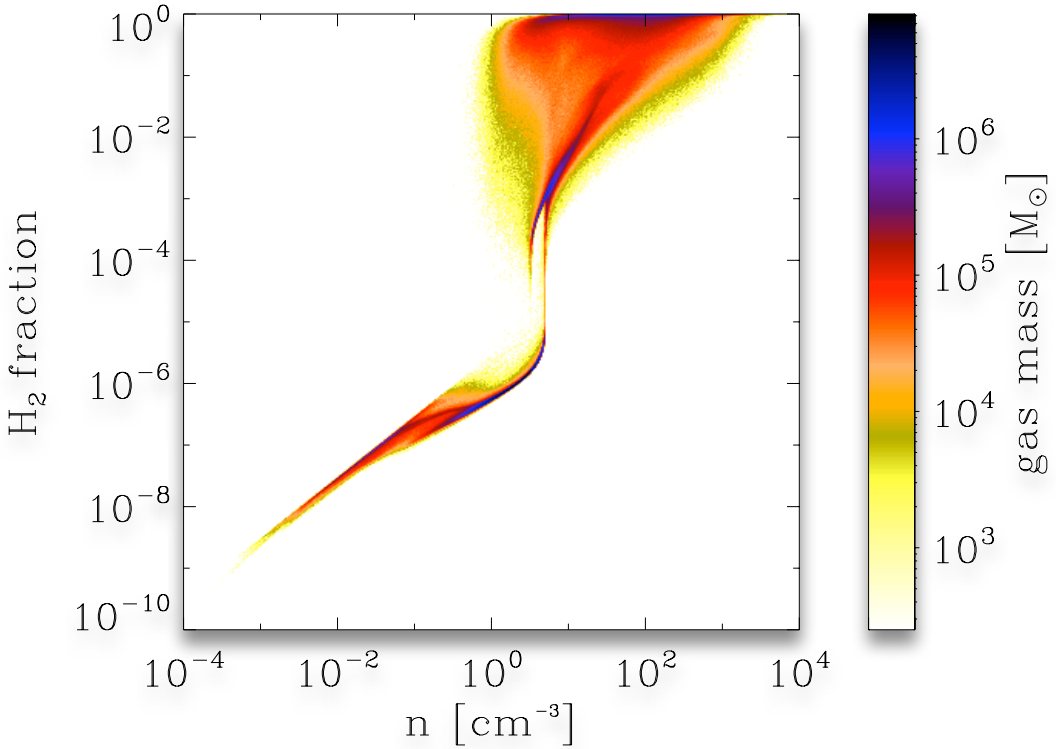

molecular cloud formation

molecular gas fraction of fluid element as function of time

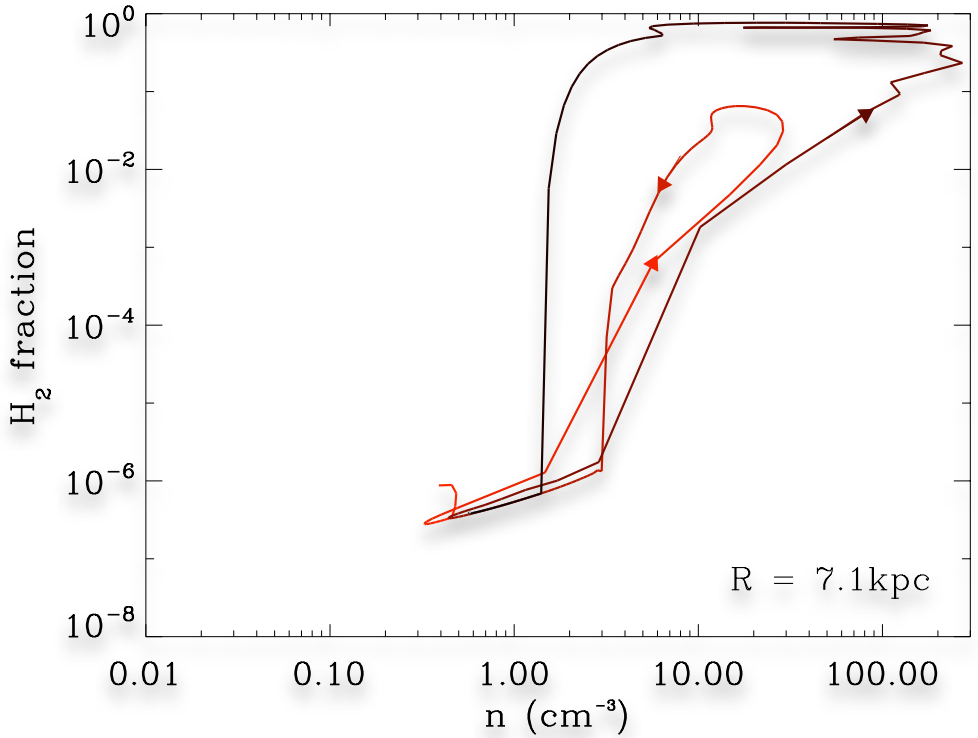

molecular gas fraction as function of density

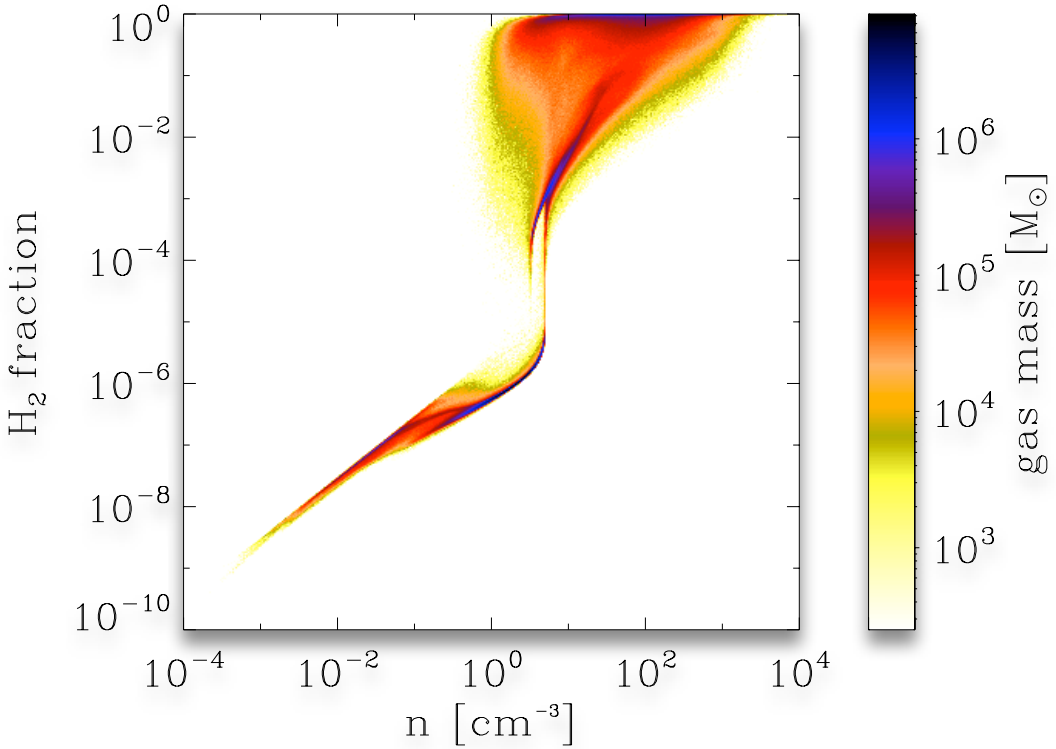

(Dobbs et al. 2008)

observed timescales

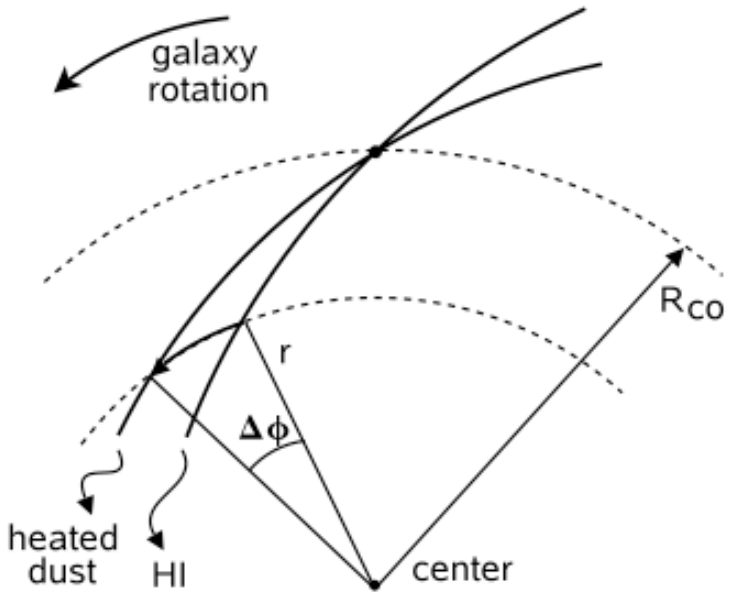

Tamburro et al. (2008)

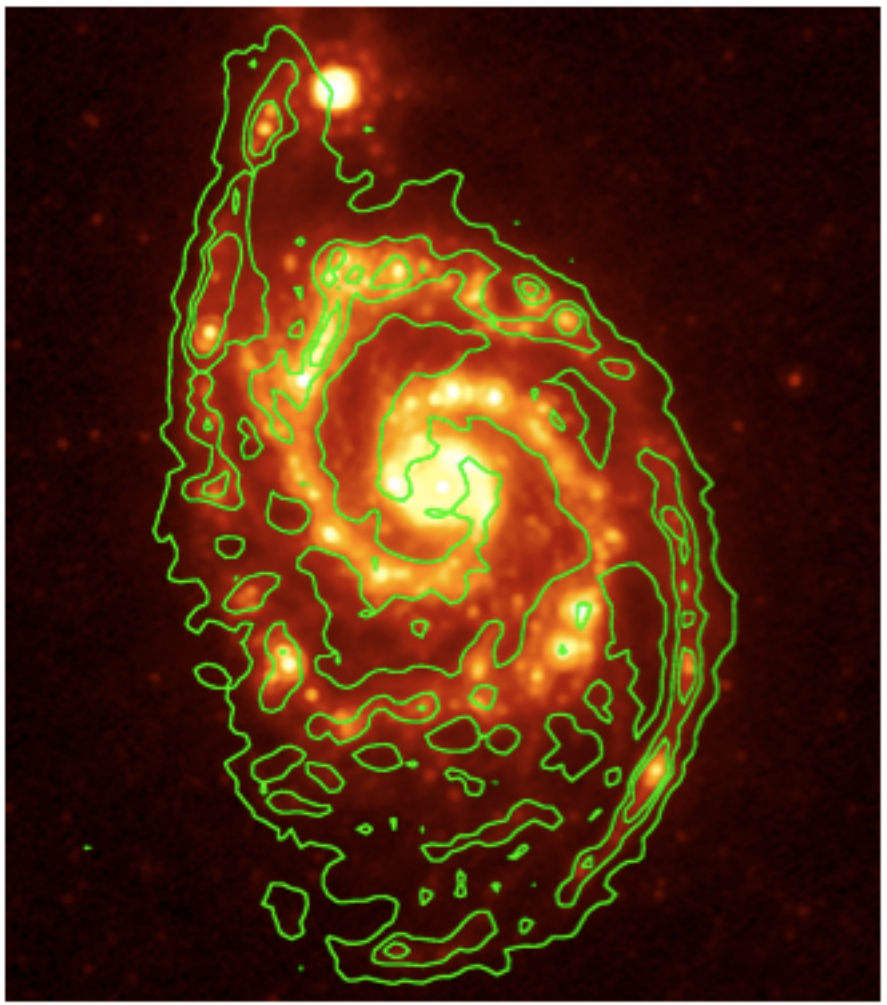

Fig. 1.— NGC 5194: the 24 μm band image is plotted in color scale; the H I emission map is overlayed with green contours.

observed timescales

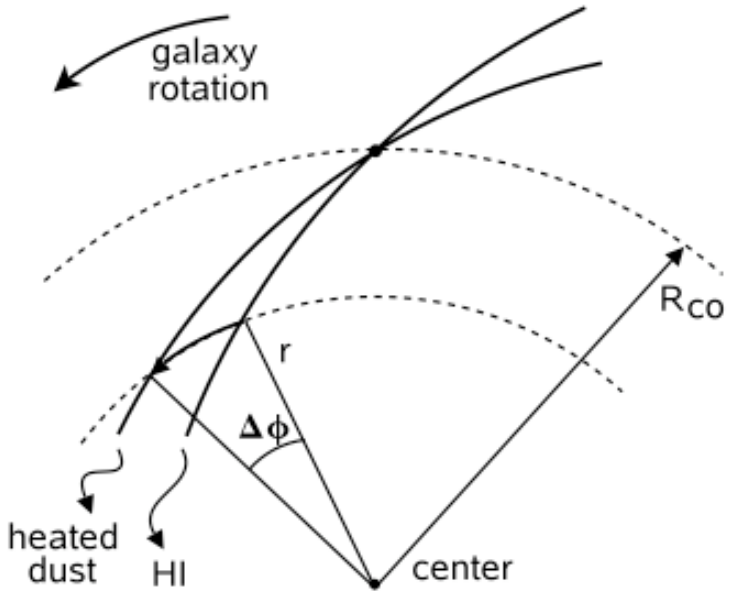

Tamburro et al. (2008)

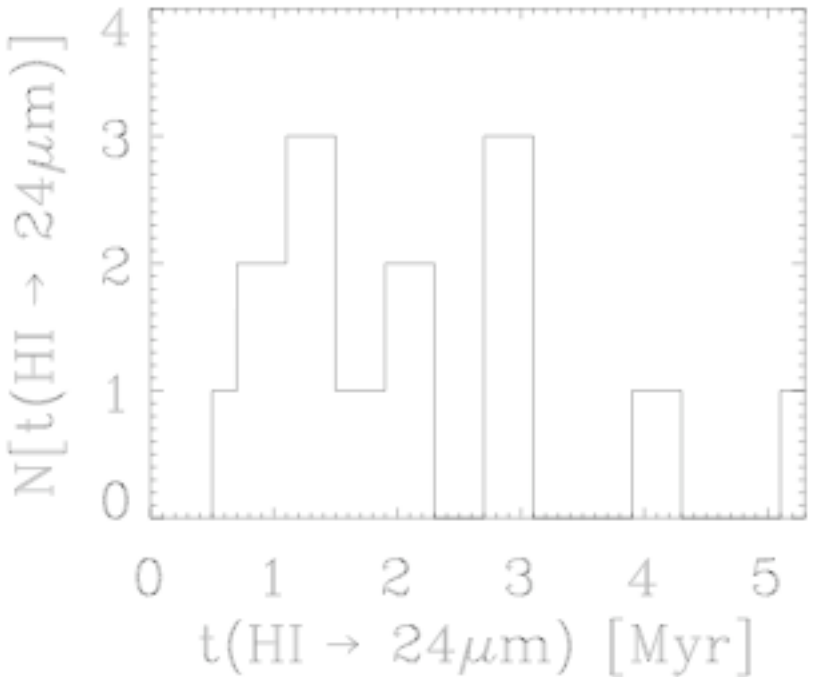

Fig. 5.— Histogram of the time scales $t_{\mathrm{HI}\mapsto 24\,\mu\mathrm{m}}$ derived from the fits in Figure 4 and listed in Table. 2 for the 14 sample galaxies listed in Table. 1. The timescales range between 1 and 4 Myr for almost all galaxies.

calculated timescales

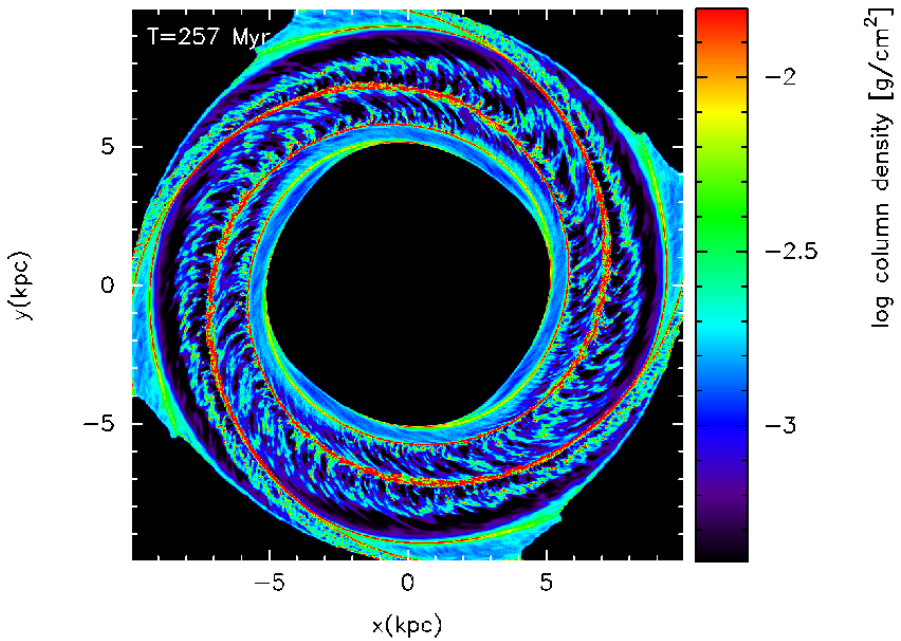

Dobbs et al. (2008)

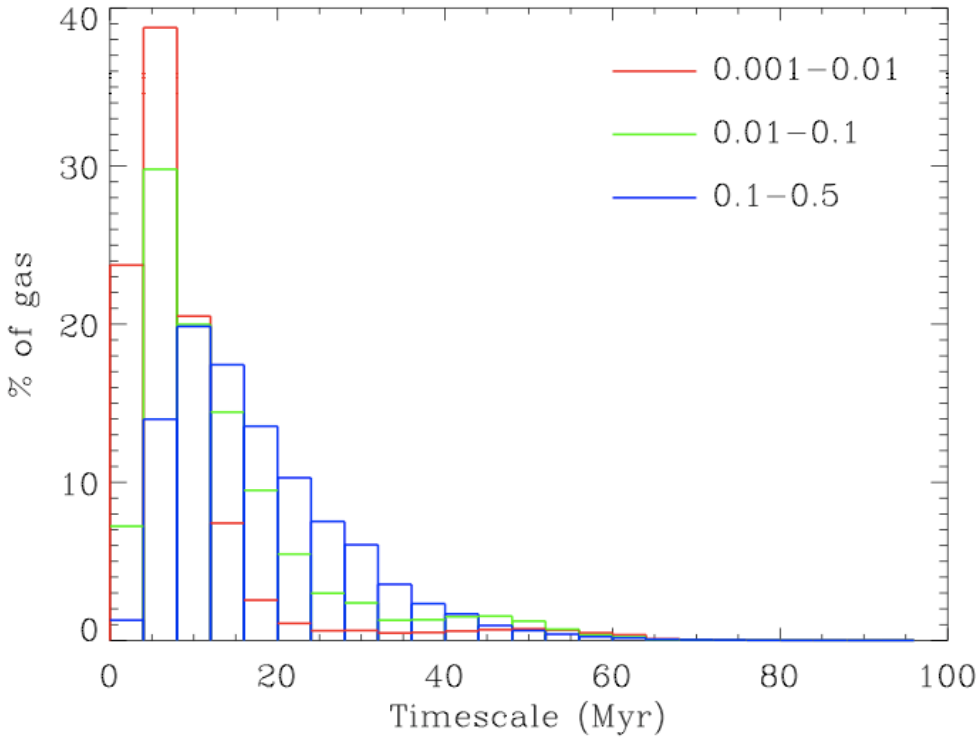

Figure 16. This histogram gives the distribution of timescales over which the gas reaches certain molecular gas fractions. The timescales denote the time for the H_2 fraction of a particle to increase from 0.001 to 0.01, 0.01 to 0.1 and 0.1 to 0.5, as indicated.

zooming in ...

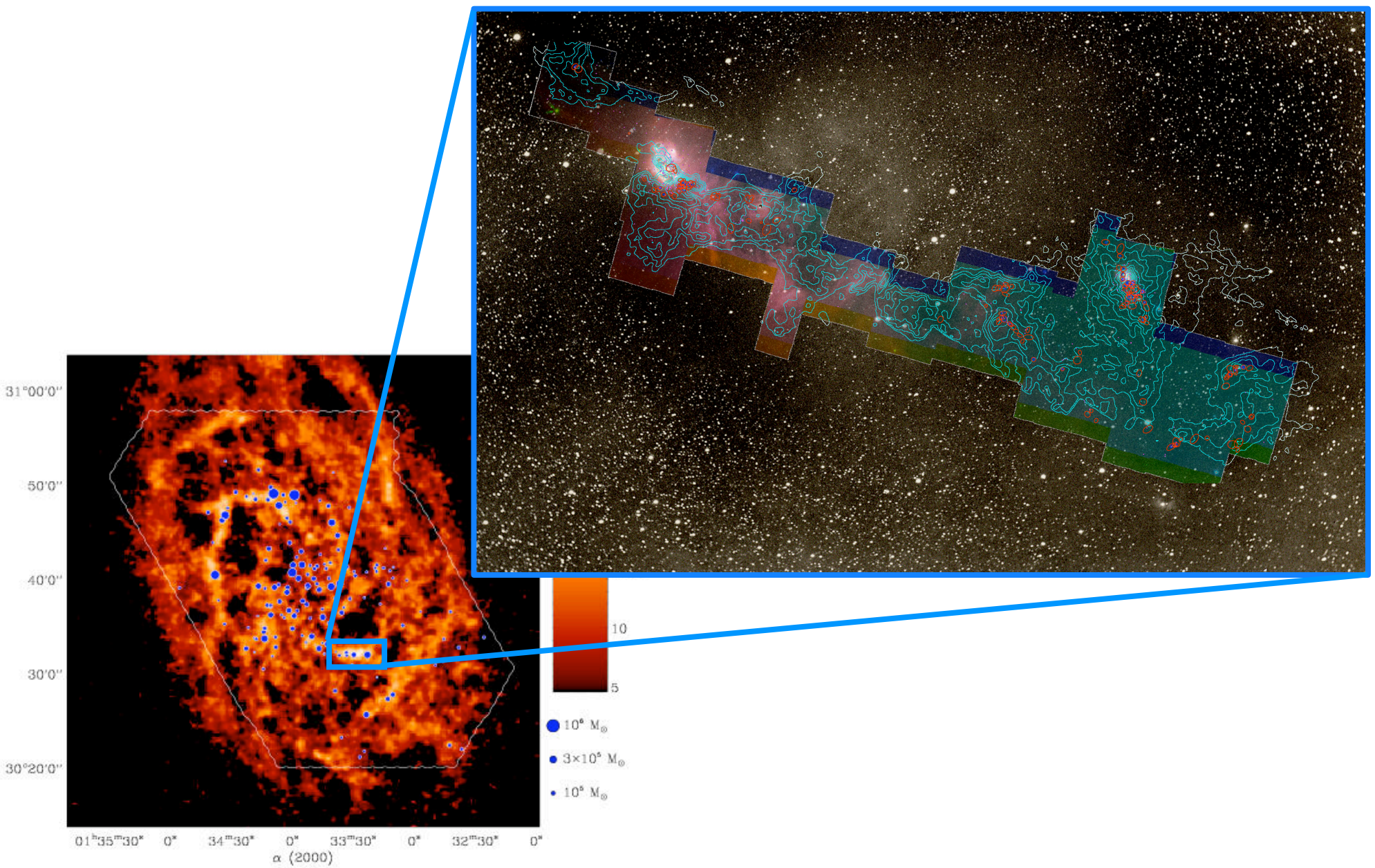
31°00'0"
50'0"
40'0"
30'0"
30°20'0"
01h35m30s
0s
34m30s
0s
33m30s
0s
32m30s
0s
α (2000)
10
5
10⁶ M⊙
3×10⁵ M⊙
10⁵ M⊙

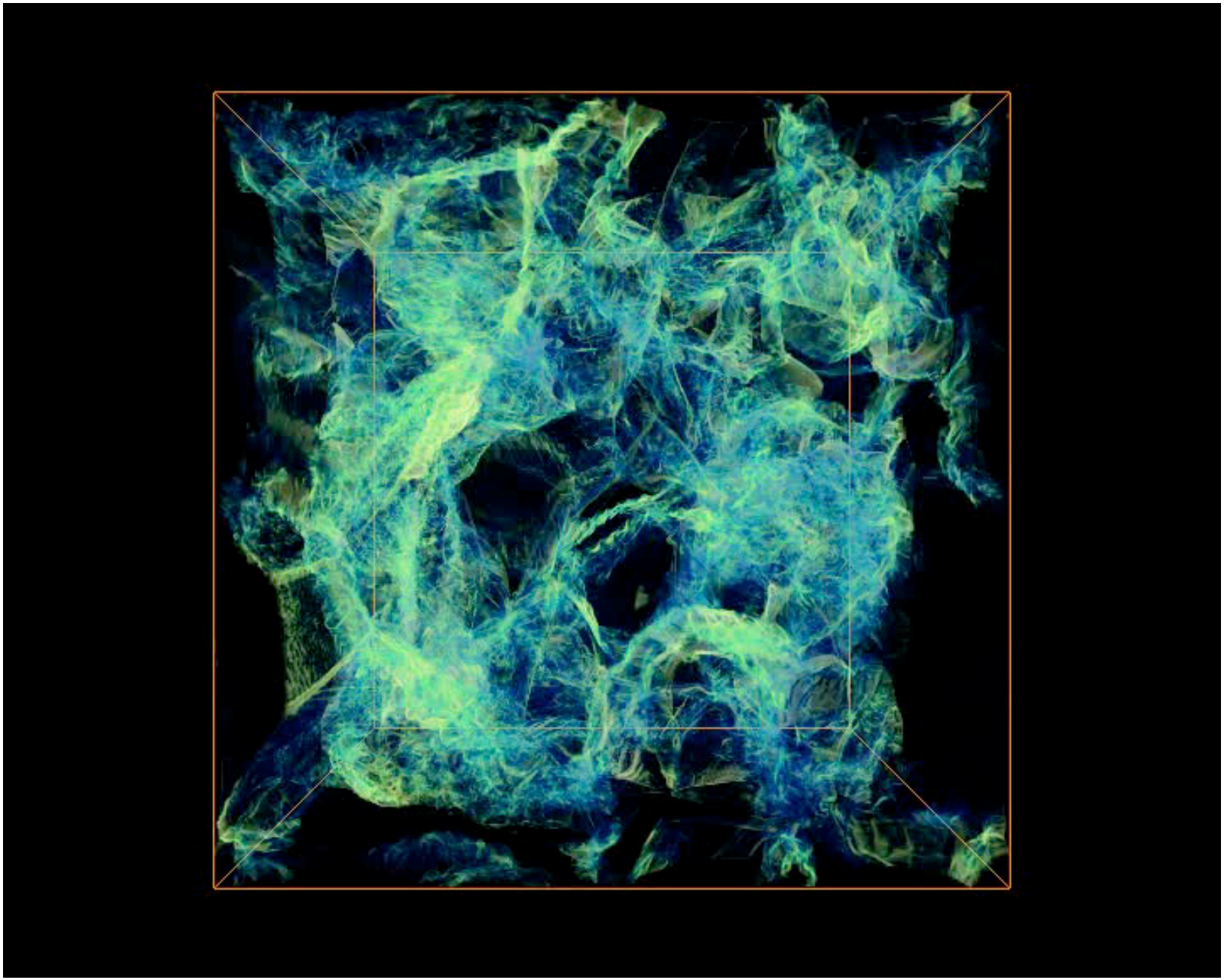

(movie from Christoph Federrath)

experimental set-up

6 ray approximation to external radiation field

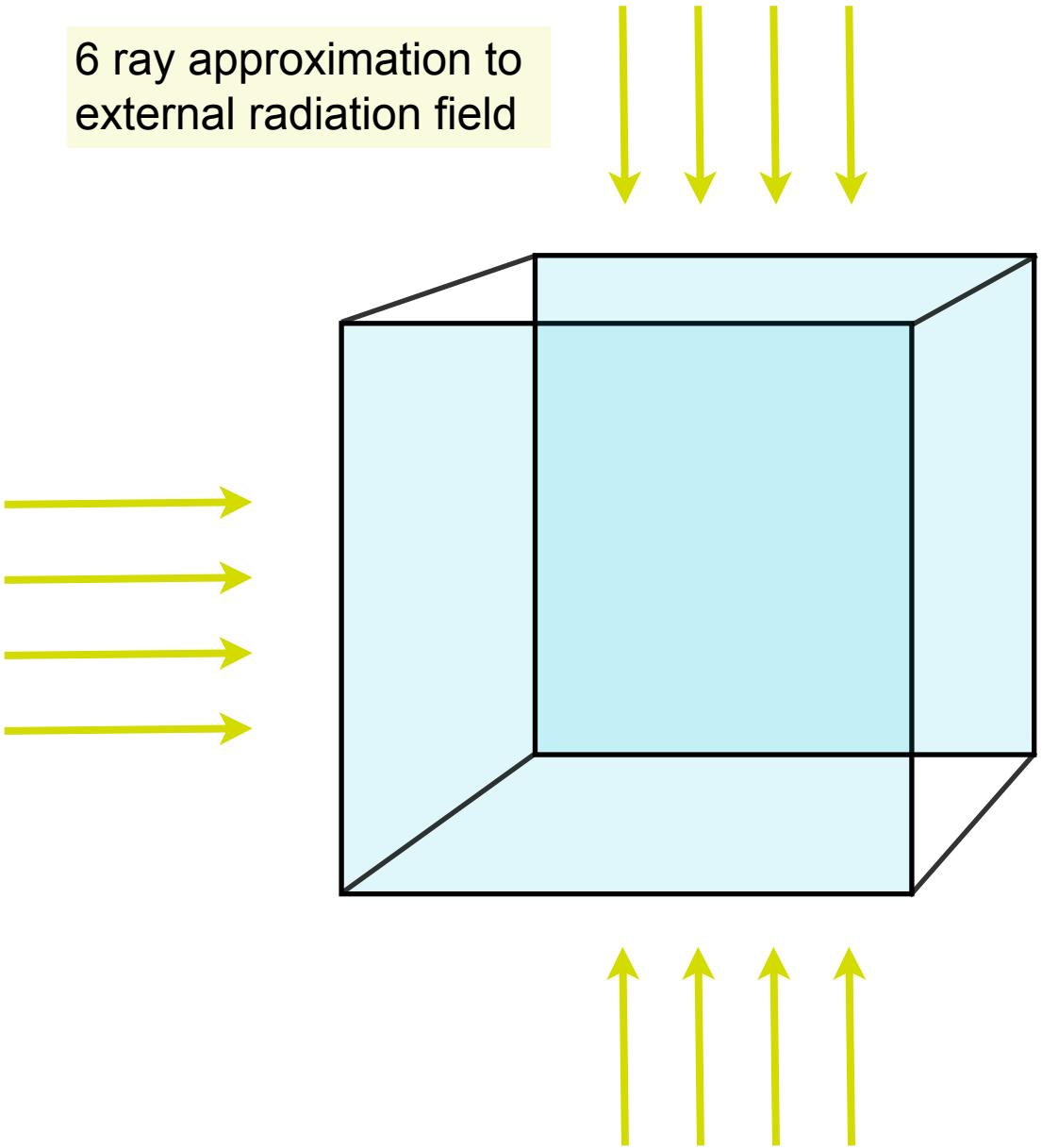

- AMR MHD (B = 2 muG)
- stochastic forcing (Ornstein-Uhlenbeck)
- self-gravity
- time-dependent chemistry
- cooling & heating processes
  --> thermodynamics done right!

- gives you mathematically well defined boundary conditions
  --> good for statistical studies

chemical model 0

- 32 chemical species
  - 17 in instantaneous equilibrium:

H^-, H_2^+, H_3^+, CH^+, CH_2^+, OH^+, H_2O^+, H_3O^+, CO^+, HOC^+, O^-, C^- and O_2^+

  - 19 full non-equilibrium evolution

e^-, H^+, H, H_2, He, He^+, C, C^+, O, O^+, OH, H_2O, CO,

C_2, O_2, HCO^+, CH, CH_2 and CH_3^+

- 218 reactions
- various heating and cooling processes

(Glover, Federrath, Mac Low, Klessen, in prep)

chemical model 1

Process	
Cooling:	
C fine structure lines	Atomic data – Silva & Viegas (2002)
	Collisional rates (H) – Abrahamsson, Krems & Dalgarno (2007)
	Collisional rates (H_2) – Schroder et al. (1991)
	Collisional rates (e^-) – Johnson et al. (1987)
	Collisional rates (H^+) – Roueff & Le Bourlot (1990)
C^+ fine structure lines	Atomic data – Silva & Viegas (2002)
	Collisional rates (H_2) – Flower & Launay (1977)
	Collisional rates (H, $T < 2000$ K) – Hollenbach & McKee (1989)
	Collisional rates (H, $T > 2000$ K) – Keenan et al. (1986)
	Collisional rates (e^-) – Wilson & Bell (2002)
O fine structure lines	Atomic data – Silva & Viegas (2002)
	Collisional rates (H) – Abrahamsson, Krems & Dalgarno (2007)
	Collisional rates (H_2) – see Glover & Jappsen (2007)
	Collisional rates (e^-) – Bell, Berrington & Thomas (1998)
	Collisional rates (H^+) – Pequignot (1990, 1996)
H_2 rovibrational lines	Le Bourlot, Pineau des Forêts & Flower (1999)
CO and H_2O rovibrational lines	Neufeld & Kaufman (1993); Neufeld, Lepp & Melnick (1995)
OH rotational lines	Pavlovski et al. (2002)
Gas-grain energy transfer	Hollenbach & McKee (1989)
Recombination on grains	Wolfire et al. (2003)
Atomic resonance lines	Sutherland & Dopita (1993)
H collisional ionization	Abel et al. (1997)
H_2 collisional dissociation	See Table B1
Compton cooling	Cen (1992)
Heating:	
Photoelectric effect	Bakes & Tielens (1994); Wolfire et al. (2003)
H_2 photodissociation	Black & Dalgarno (1977)
UV pumping of H_2	Burton, Hollenbach & Tielens (1990)
H_2 formation on dust grains	Hollenbach & McKee (1989)
Cosmic ray ionization	Goldsmith & Langer (1978)

(Glover, Federrath, Mac Low, Klessen, in prep)

chemical model 2

(Glover, Federrath, Mac Low, Klessen, in prep)

Table B2. List of photochemical reactions included in our chemical model

No.	Reaction	Optically thin rate (s^{-1})	γ	Ref.
166	$H^- + \gamma \rightarrow H + e^-$	$R_{166} = 7.1 \times 10^{-7}$	0.5	1
167	$H_2^+ + \gamma \rightarrow H + H^+$	$R_{167} = 1.1 \times 10^{-9}$	1.9	2
168	$H_2 + \gamma \rightarrow H + H$	$R_{168} = 5.6 \times 10^{-11}$	See §2.2	3
169	$H_3^+ + \gamma \rightarrow H_2 + H^+$	$R_{169} = 4.9 \times 10^{-13}$	1.8	4
170	$H_3^+ + \gamma \rightarrow H_2^+ + H$	$R_{170} = 4.9 \times 10^{-13}$	2.3	4
171	$C + \gamma \rightarrow C^+ + e^-$	$R_{171} = 3.1 \times 10^{-10}$	3.0	5
172	$C^- + \gamma \rightarrow$			
173	$CH + \gamma \rightarrow$			
174	$CH + \gamma \rightarrow$			
175	$CH^+ + \gamma$			
176	$CH_2 + \gamma$			
177	$CH_2 + \gamma$			
178	$CH_2^+ + \gamma$			
179	$CH_3^+ + \gamma$			
180	$CH_3^+ + \gamma$			
181	$C_2 + \gamma \rightarrow$			
182	$O^- + \gamma$			
183	$OH + \gamma$			
184	$OH + \gamma$			
185	$OH^+ + \gamma$			
186	$H_2O + \gamma$			
187	$H_2O + \gamma$			
188	$H_2O^+ + \gamma$			
189	$H_2O^+ + \gamma$			
190	$H_2O^+ + \gamma$			
191	$H_2O^+ + \gamma$			
192	$H_3O^+ + \gamma$			
193	$H_3O^+ + \gamma$			
194	$H_3O^+ + \gamma$			
195	$H_3O^+ + \gamma$			
196	$O_2 + \gamma \rightarrow$			
197	$O_2 + \gamma \rightarrow O + O$	$R_{197} = 7.0 \times 10^{-10}$	1.8	7
198	$CO + \gamma \rightarrow C + O$	$R_{198} = 2.0 \times 10^{-10}$	See §2.2	13

Table B3. List of reactions included in our chemical model that involve cosmic rays or cosmic-ray induced UV emission

No.	Reaction	Rate ($s^{-1}\zeta_H^{-1}$)	Ref.
199	$H + \text{c.r.} \rightarrow H^+ + e^-$	$R_{199} = 1.0$	—
200	$He + \text{c.r.} \rightarrow He^+ + e^-$	$R_{200} = 1.1$	1
201	$H_2 + \text{c.r.} \rightarrow H^+ + H + e^-$	$R_{201} = 0.037$	1
202	$H_2 + \text{c.r.} \rightarrow H + H$	$R_{202} = 0.22$	1
203	$H_2 + \text{c.r.} \rightarrow H^+ + H^-$	$R_{203} = 6.5 \times 10^{-4}$	1
204	$H_2 + \text{c.r.} \rightarrow H_2^+ + e^-$	$R_{204} = 2.0$	1
205	$C + \text{c.r.} \rightarrow C^+ + e^-$	$R_{205} = 3.8$	1
206	$O + \text{c.r.} \rightarrow O^+ + e^-$	$R_{206} = 5.7$	1
207	$CO + \text{c.r.} \rightarrow CO^+ + e^-$	$R_{207} = 6.5$	1
208	$C + \gamma_{\text{c.r.}} \rightarrow C^+ + e^-$	$R_{208} = 2800$	2
209	$CH + \gamma_{\text{c.r.}} \rightarrow C + H$	$R_{209} = 4000$	3
210	$CH^+ + \gamma_{\text{c.r.}} \rightarrow C^+ + H$	$R_{210} = 960$	3
211	$CH_2 + \gamma_{\text{c.r.}} \rightarrow CH_2^+ + e^-$	$R_{211} = 2700$	1
212	$CH_2 + \gamma_{\text{c.r.}} \rightarrow CH + H$	$R_{212} = 2700$	1
213	$C_2 + \gamma_{\text{c.r.}} \rightarrow C + C$	$R_{213} = 1300$	3
214	$OH + \gamma_{\text{c.r.}} \rightarrow O + H$	$R_{214} = 2800$	3
215	$H_2O + \gamma_{\text{c.r.}} \rightarrow OH + H$	$R_{215} = 5300$	3
216	$O_2 + \gamma_{\text{c.r.}} \rightarrow O + O$	$R_{216} = 4100$	3
217	$O_2 + \gamma_{\text{c.r.}} \rightarrow O_2^+ + e^-$	$R_{217} = 640$	3
218	$CO + \gamma_{\text{c.r.}} \rightarrow C + O$	$R_{218} = 0.21 T^{1/2} x_{H_2} x_{CO}^{-1/2}$	4

HI to H2 conversion rate

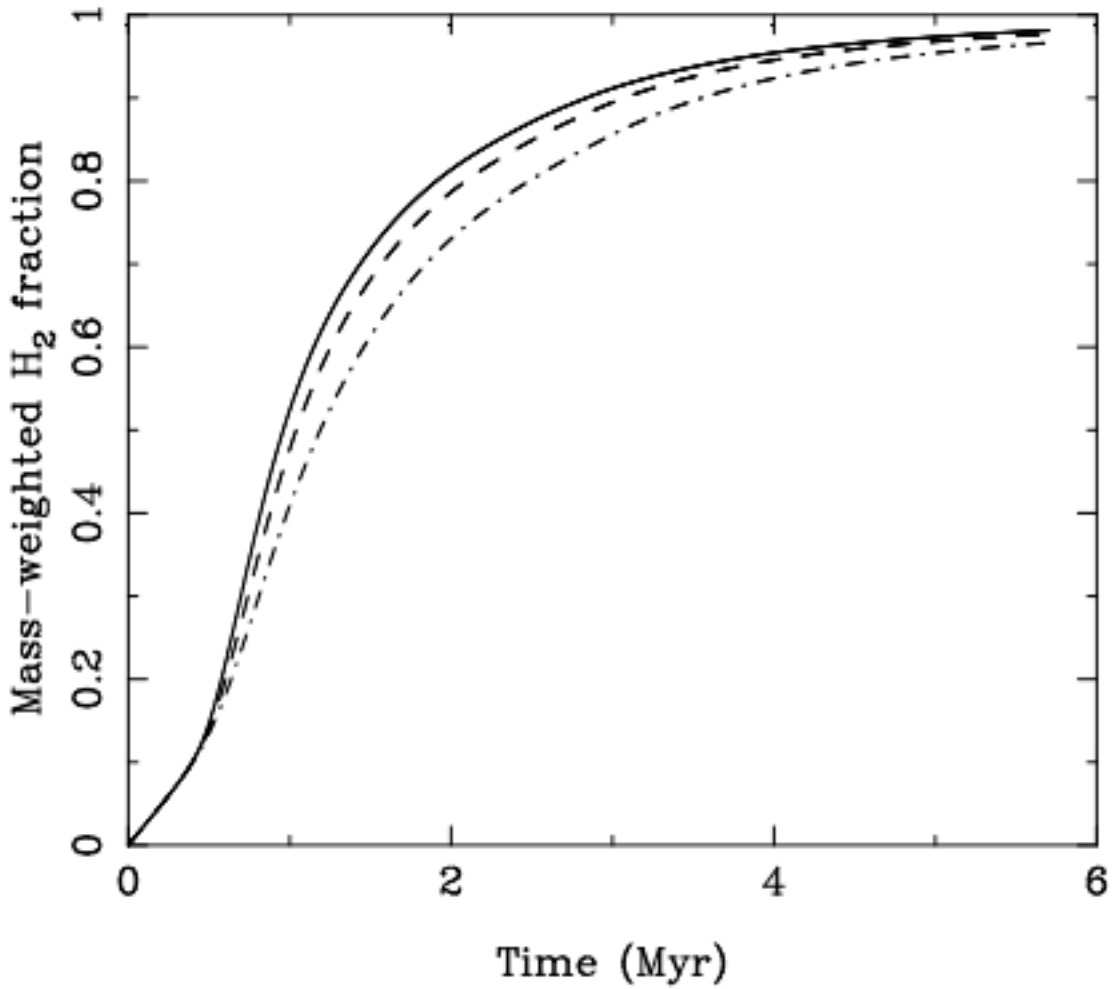

Figure 4. Time evolution of the mass-weighted H_2 abundance in simulations R1, R2 and R3, which have numerical resolutions of 64^3 zones (dot-dashed), 128^3 zones (dashed) and 256^3 zones (solid), respectively.

(Glover, Federrath, Mac Low, Klessen, in prep)

HI to H2 conversion rate

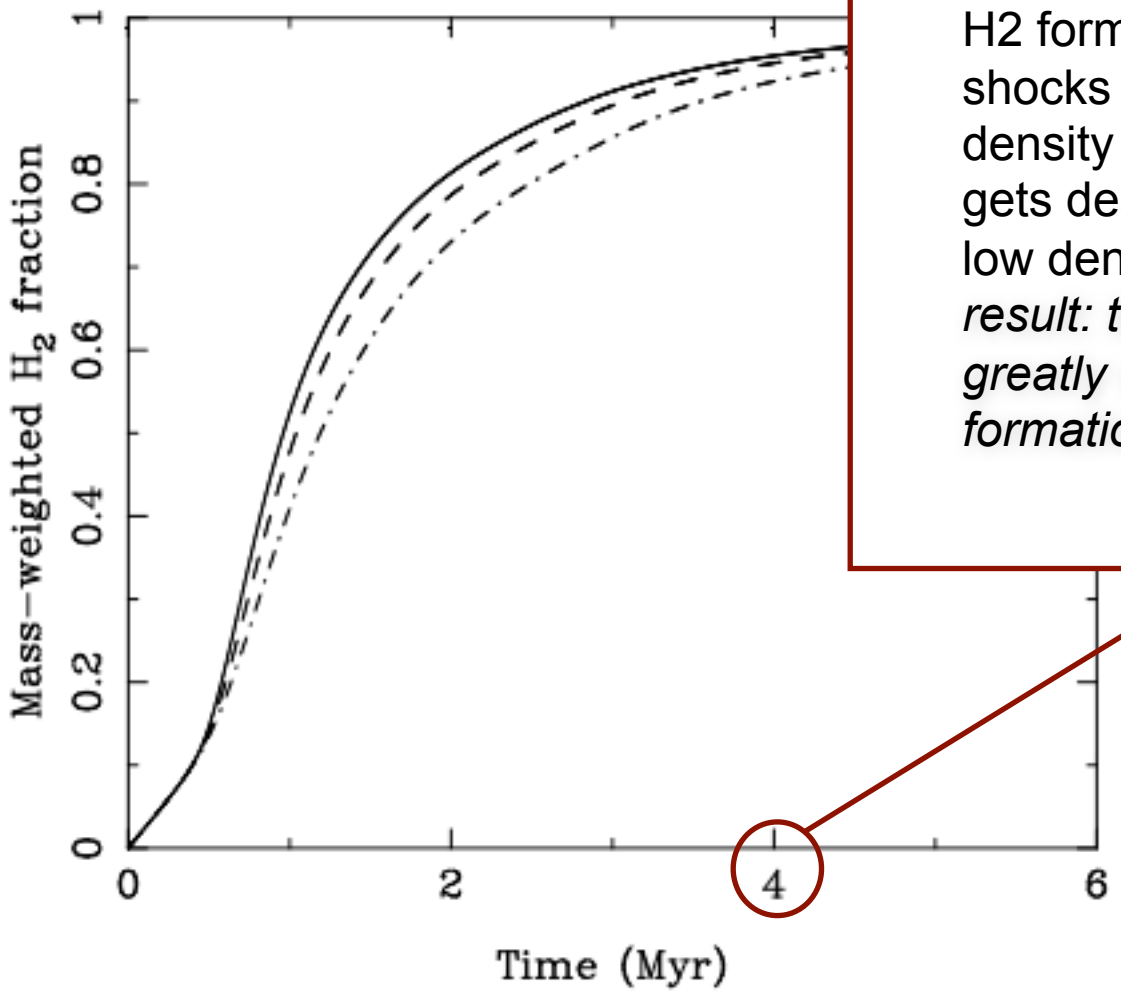

H2 forms rapidly in shocks / transient density fluctuations / H2 gets destroyed slowly in low density regions / *result: turbulence greatly enhances H2-formation rate*

Figure 4. Time evolution of the mass-weighted H_2 abundance in simulations R1, R2 and R3, which have numerical resolutions of 64^3 zones (dot-dashed), 128^3 zones (dashed) and 256^3 zones (solid), respectively.

(Glover, Federrath, Mac Low, Klessen, in prep)

HI to H2 conversion rate

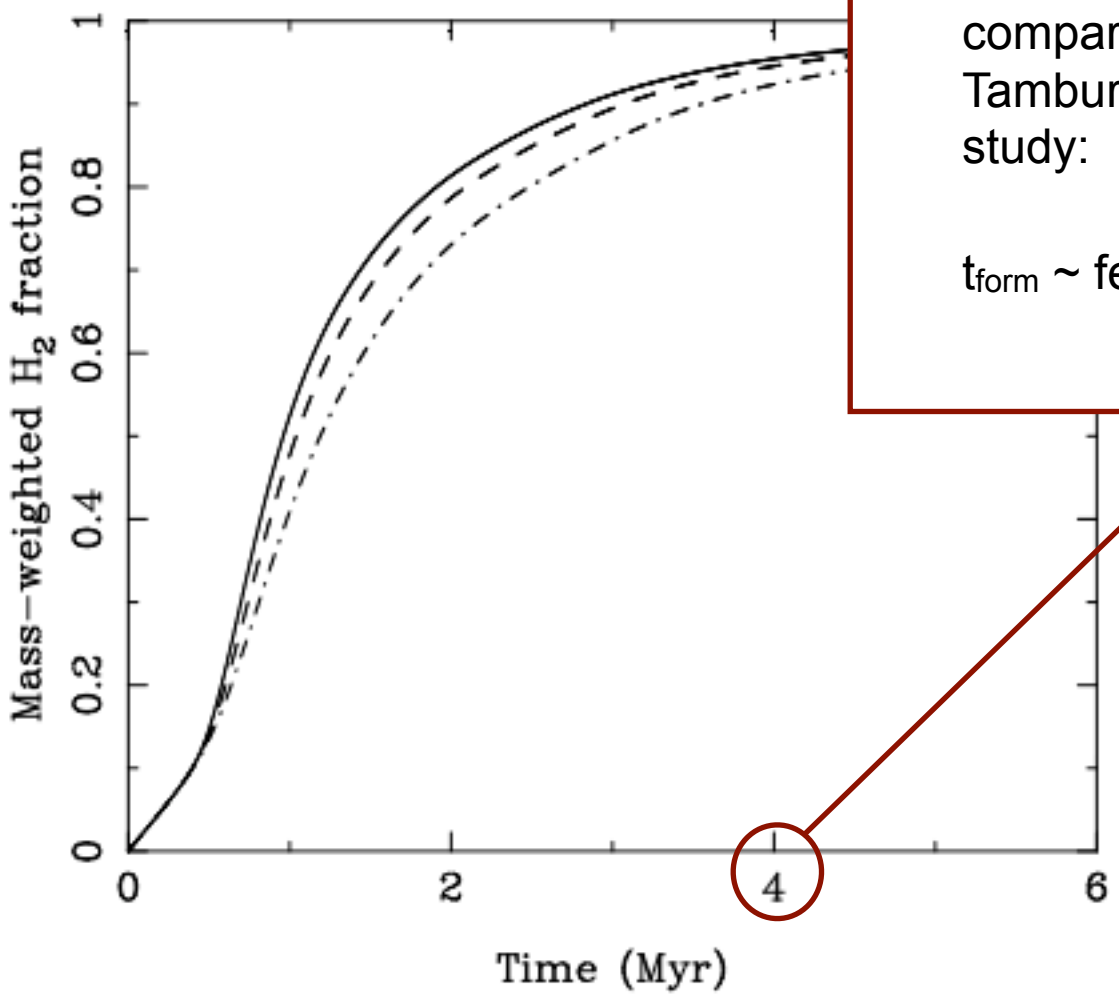

compare to data from Tamburro et al. (2008) study:

t_{form} ~ few x 10^6 years

Figure 4. Time evolution of the mass-weighted H_2 abundance in simulations R1, R2 and R3, which have numerical resolutions of 64^3 zones (dot-dashed), 128^3 zones (dashed) and 256^3 zones (solid), respectively.

(Glover, Federrath, Mac Low, Klessen, in prep)

CO, C^+ formation rates

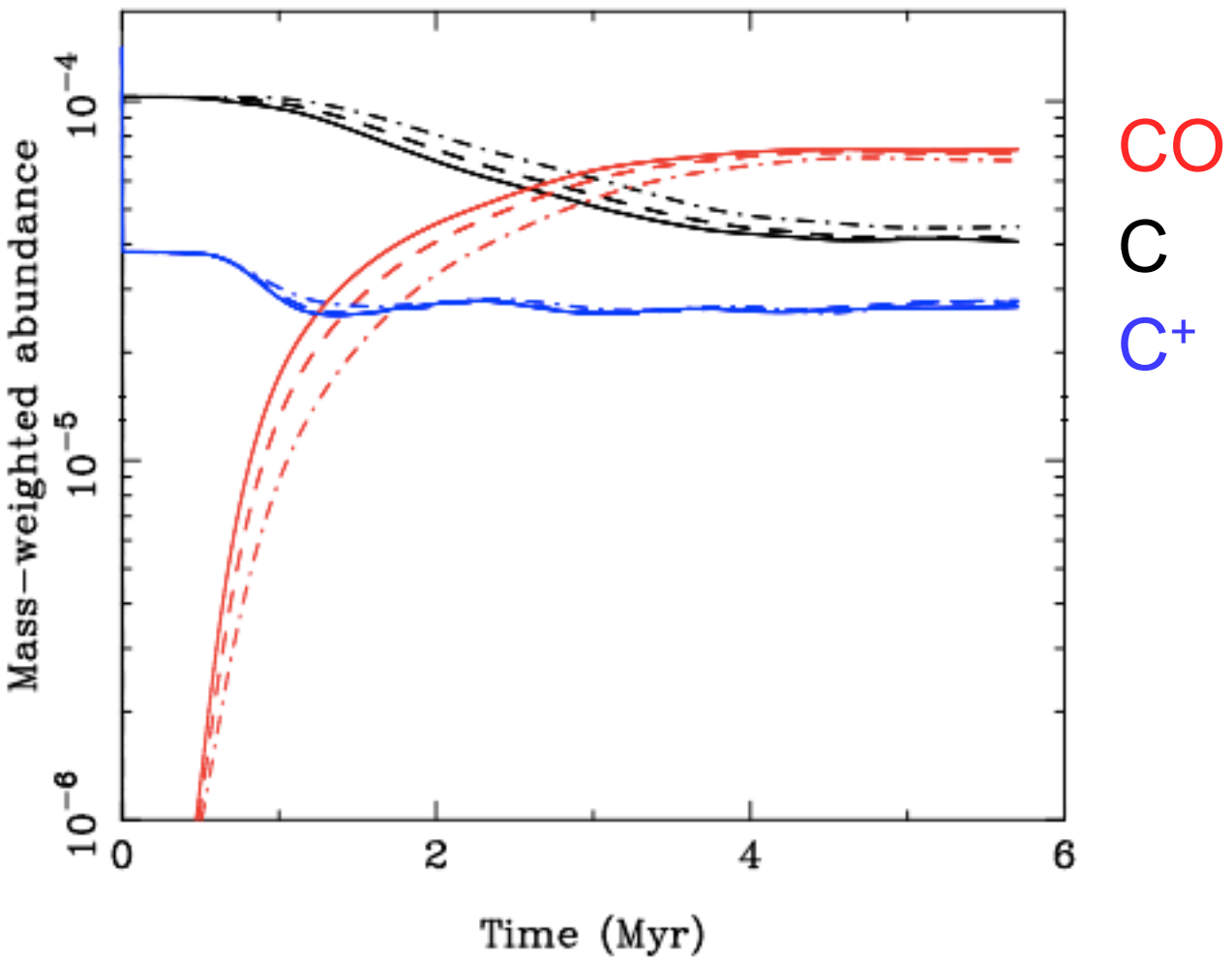

Figure 5. Time evolution of the mass-weighted abundances of atomic carbon (black lines), CO (red lines), and C^+ (blue lines) in simulations with numerical resolutions of 64^3 zones (dot-dashed), 128^3 zones (dashed) and 256^3 zones (solid).

(Glover, Federrath, Mac Low, Klessen, in prep)

effects of chemistry 1

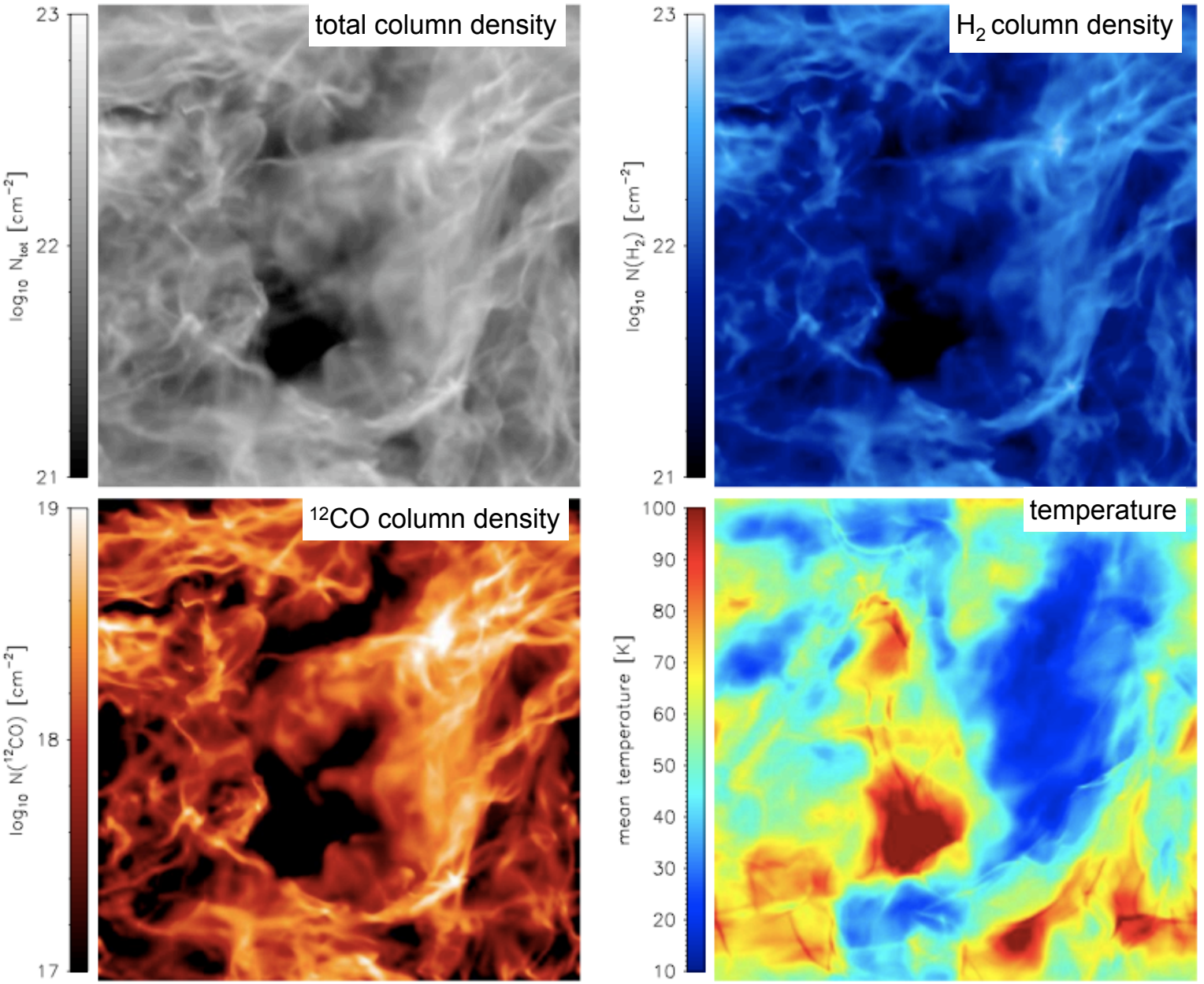

(Glover, Federrath, Mac Low, Klessen, in prep)

effects of chemistry 2

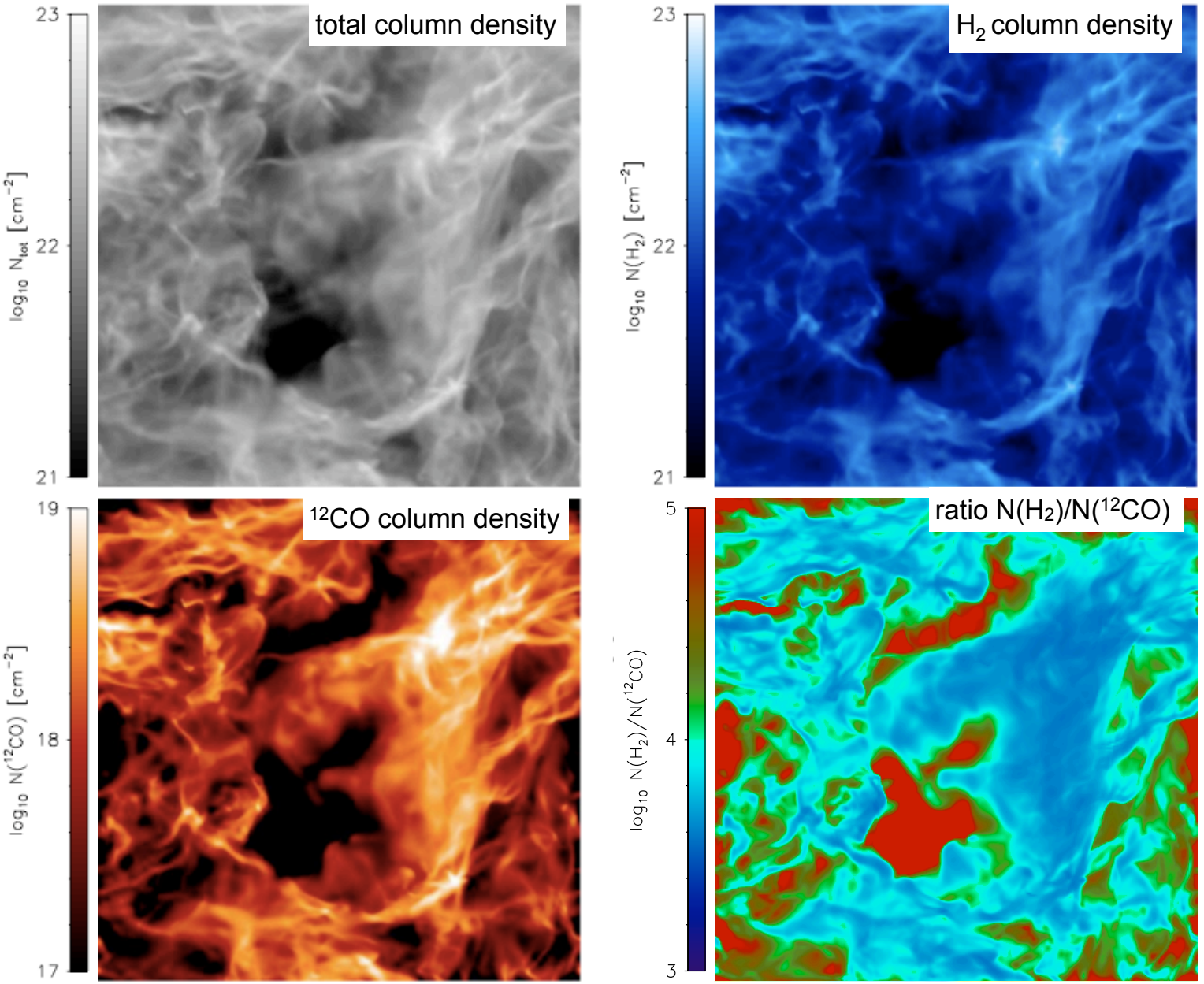

(Glover, Federrath, Mac Low, Klessen, in prep)

effects of chemistry 3

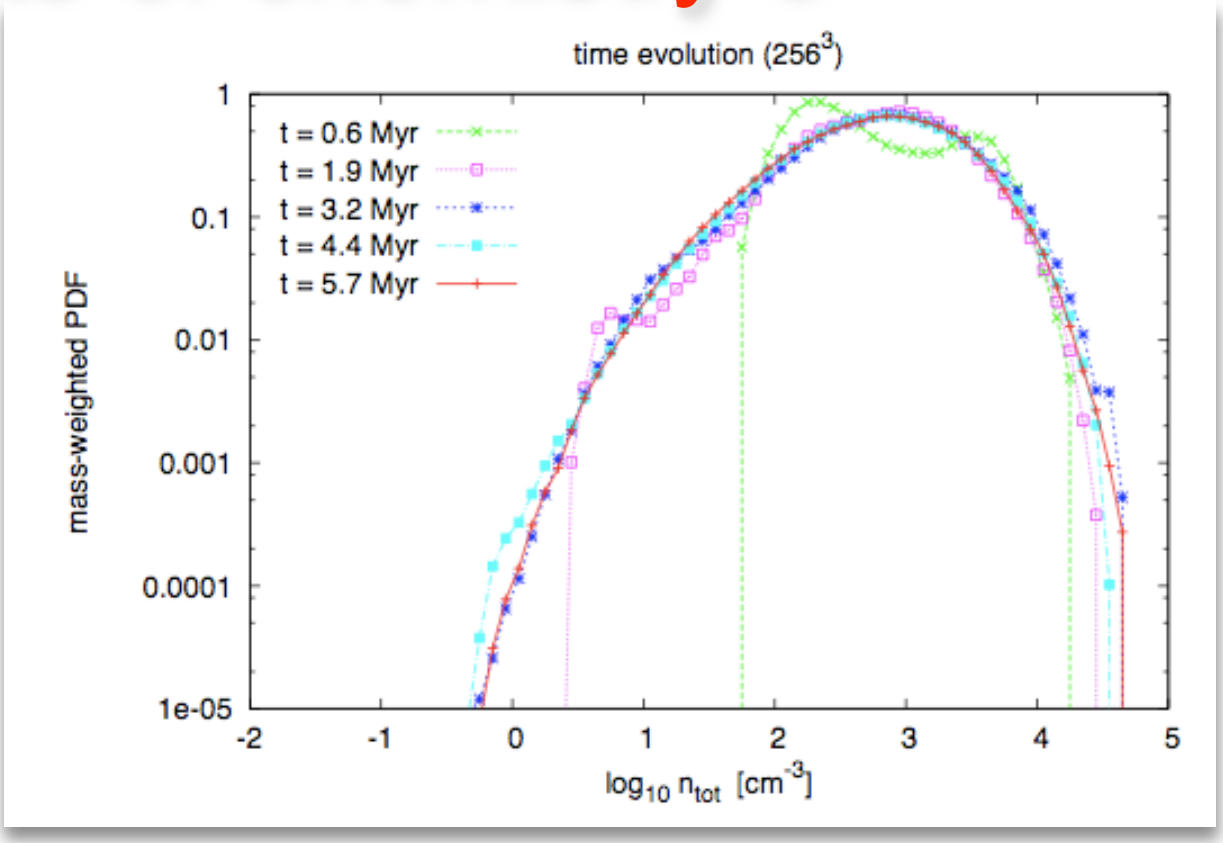

(Glover, Federrath, Mac Low, Klessen, in prep)

effects of chemistry 3

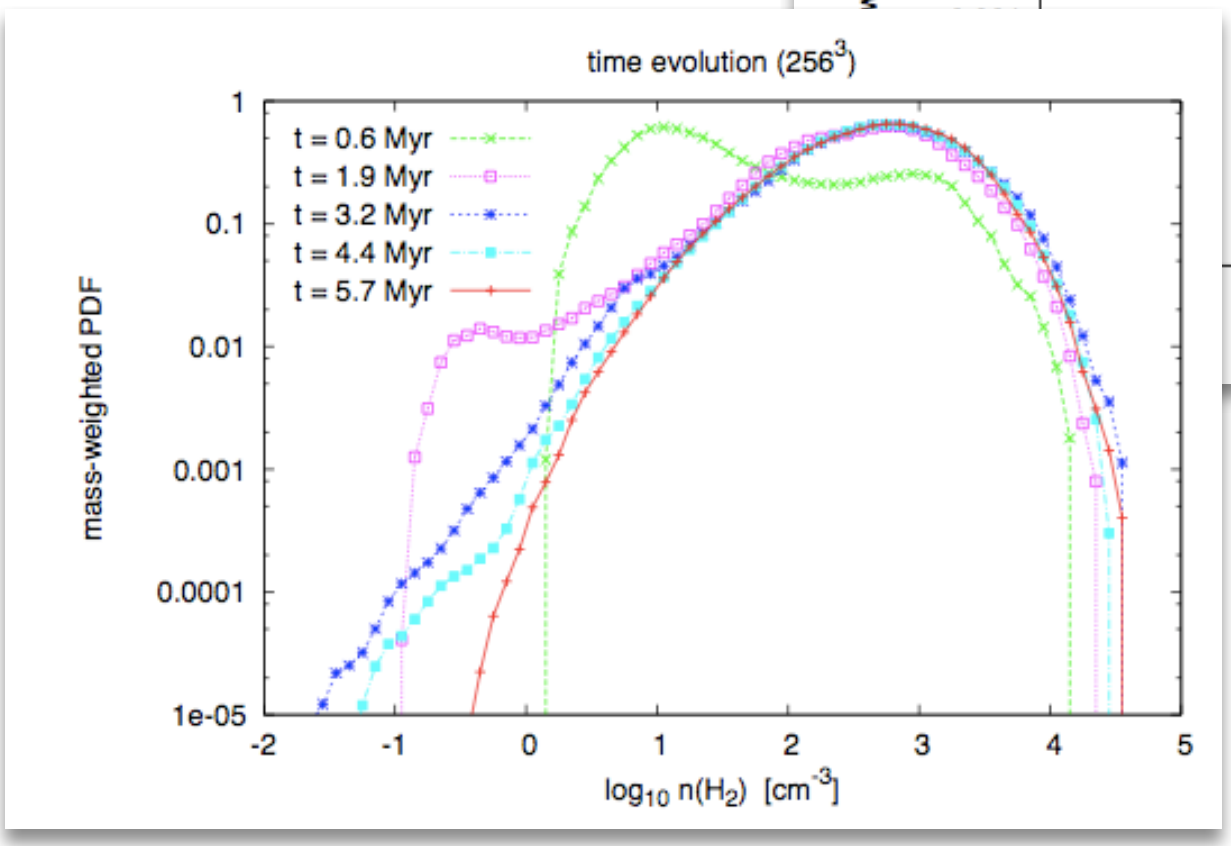

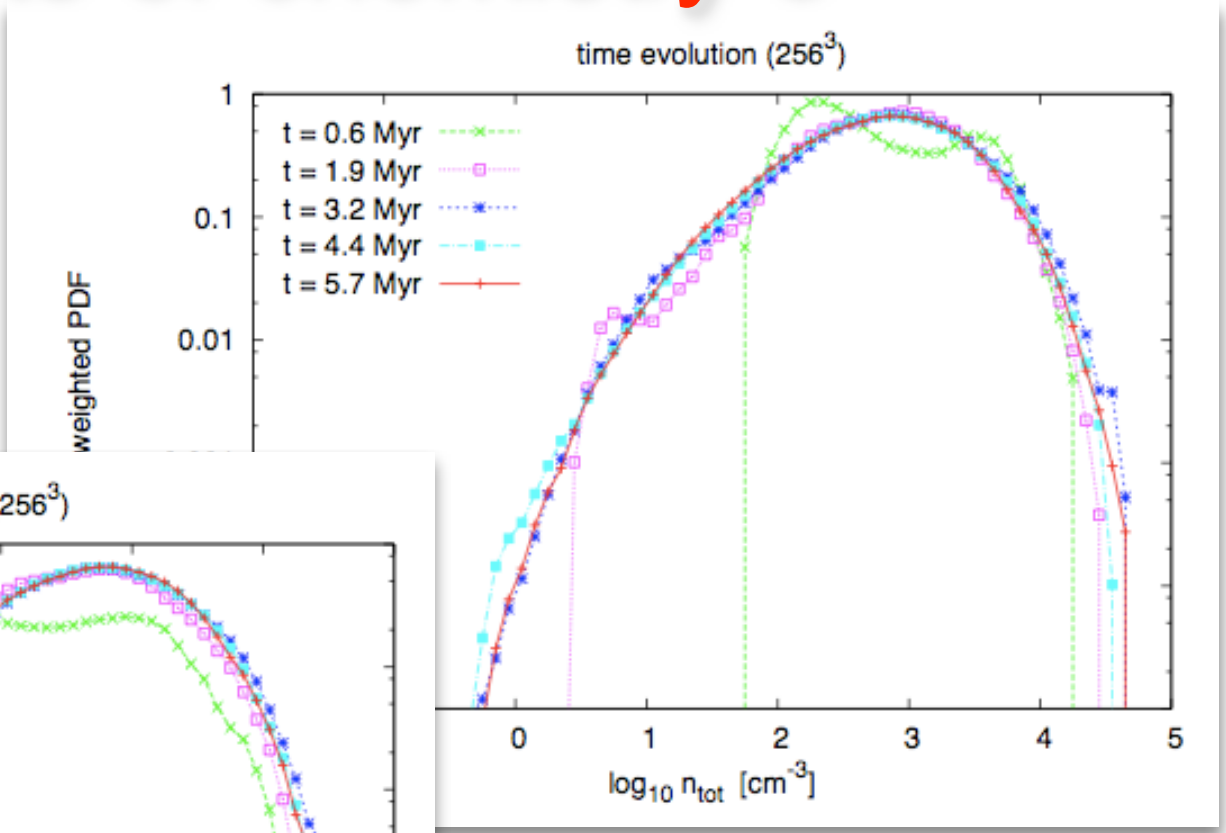

(Glover, Federrath, Mac Low, Klessen, in prep)

effects of chemistry 3

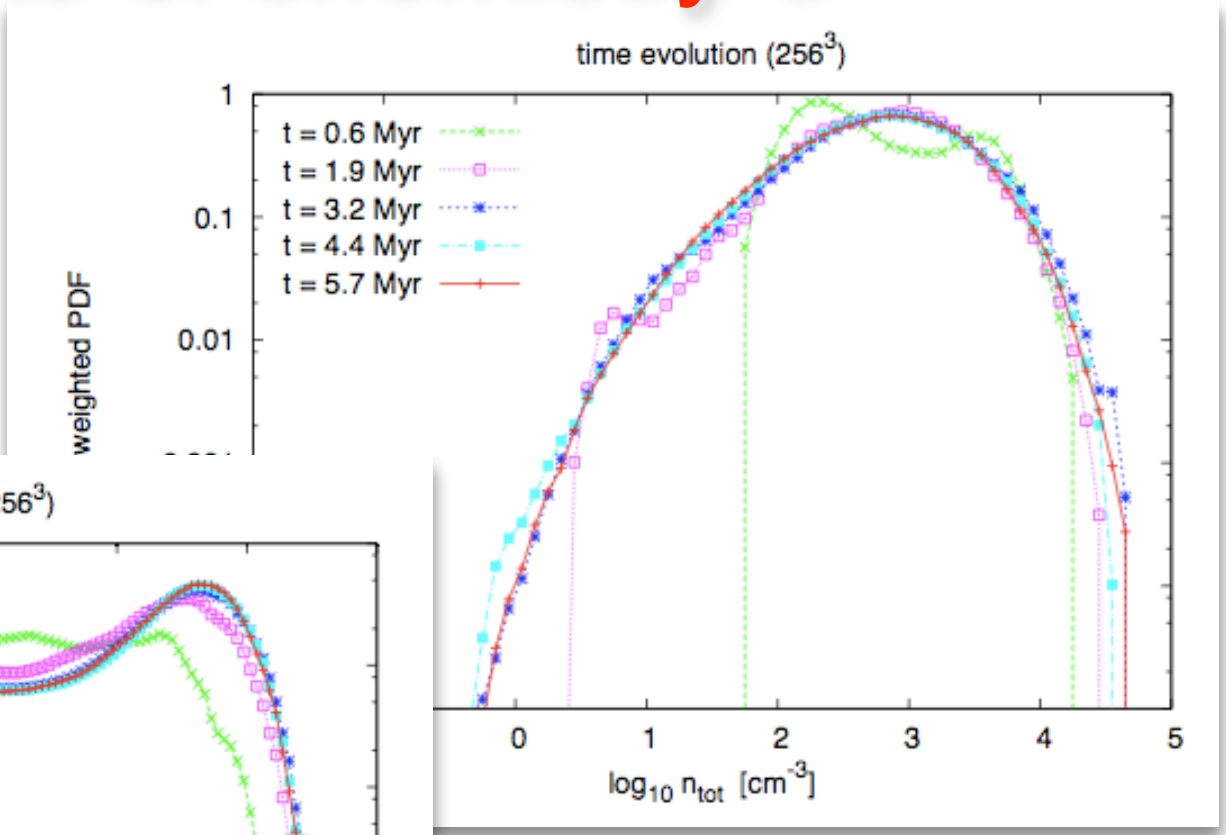

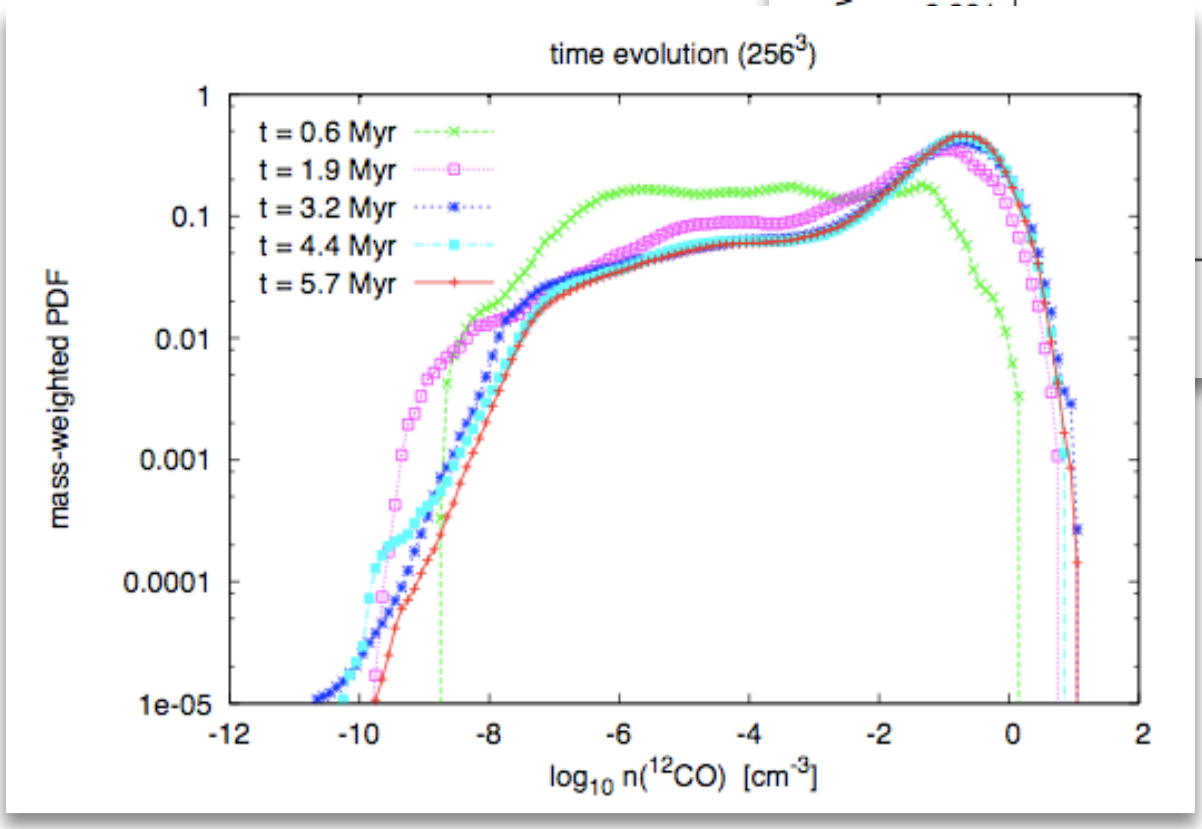

(Glover, Federrath, Mac Low, Klessen, in prep)

effects of chemistry 3

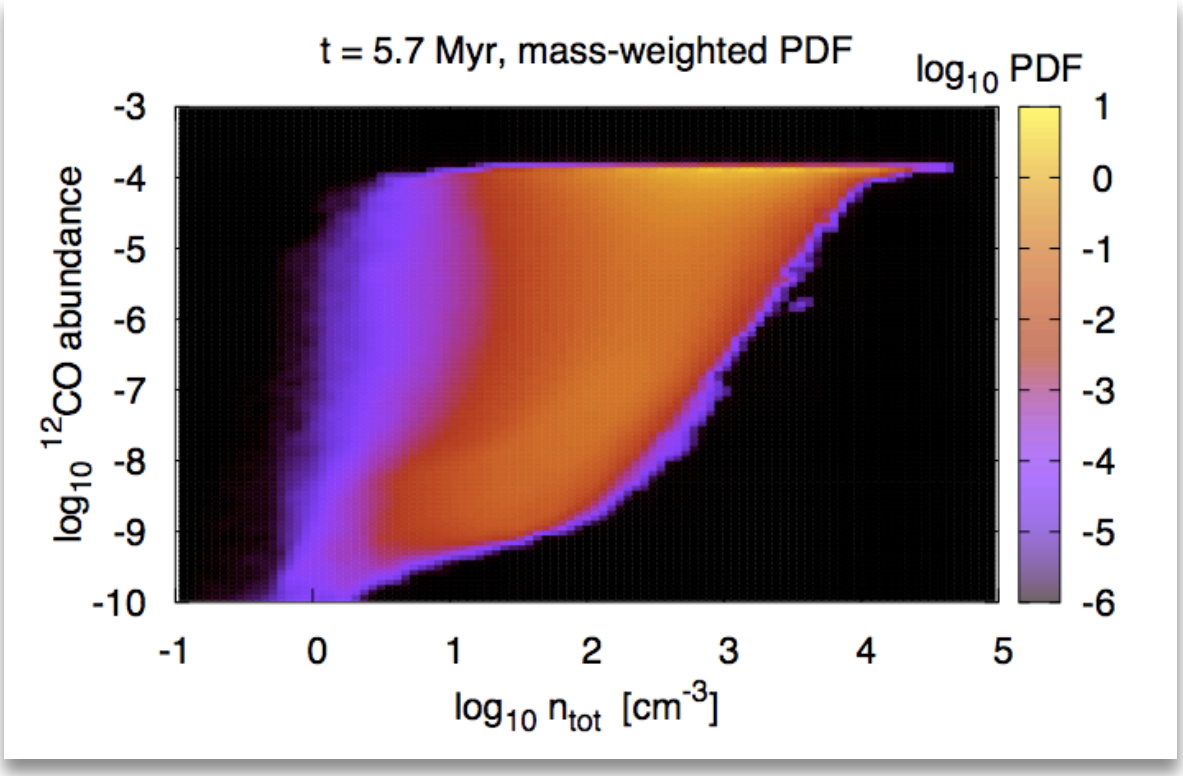

(Glover, Federrath, Mac Low, Klessen, in prep)

effects of chemistry 3

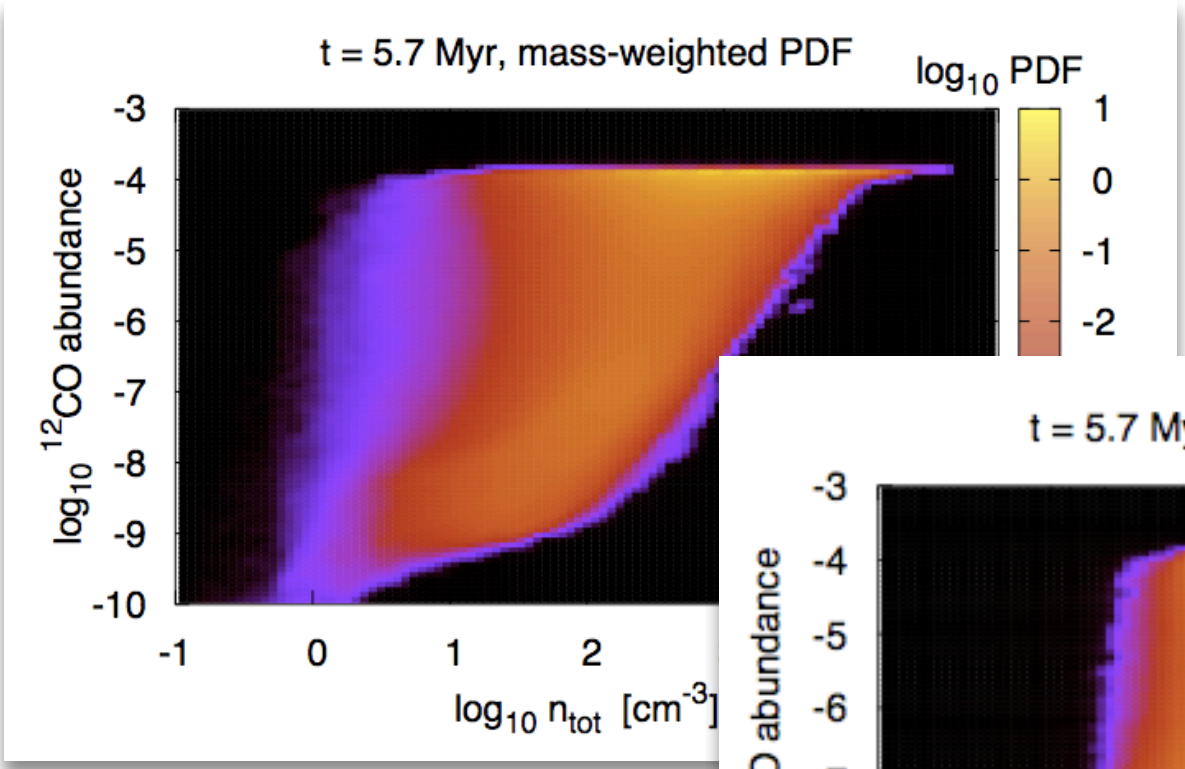

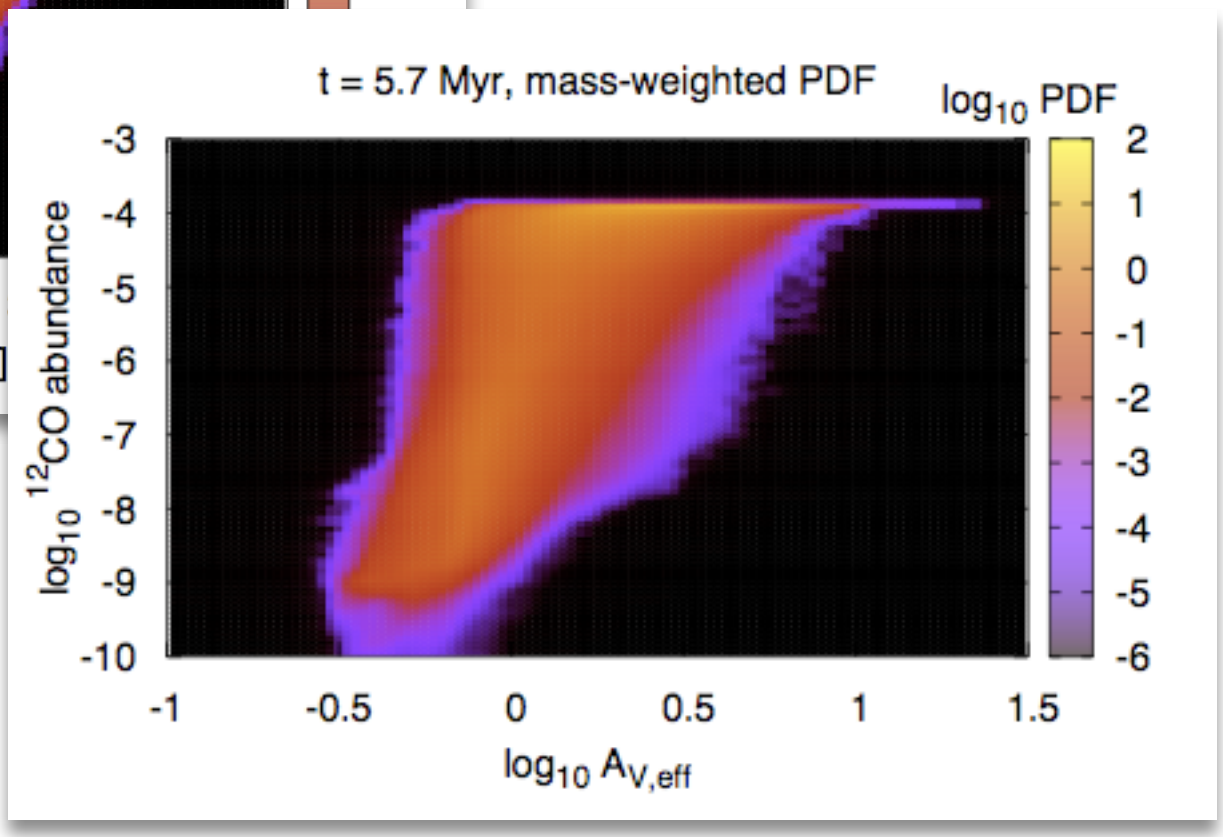

(Glover, Federrath, Mac Low, Klessen, in prep)

density pdf

1200^3 hydrodynamic simulation

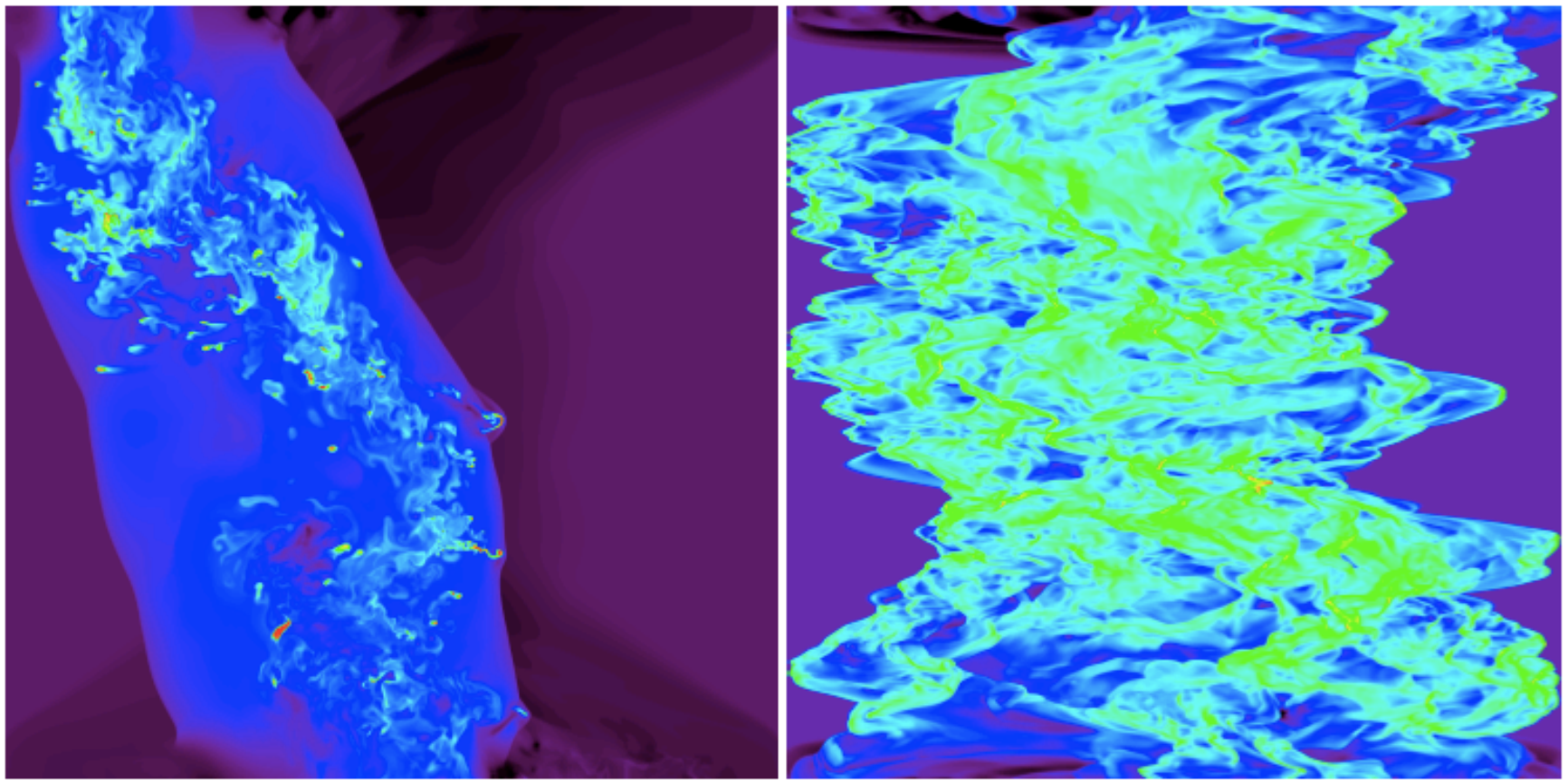

Fig. 3. Density cut through the simulations. The left plot corresponds to the 2-phase run and the right one to the isothermal run. Dark-blue, blue, green and red correspond respectively to densities of the order of 1 cm^{-3}, 3 cm^{-3}, 20 cm^{-3} and 100 cm^{-3}.

(Audit & Hennebelle, submitted)

density pdf

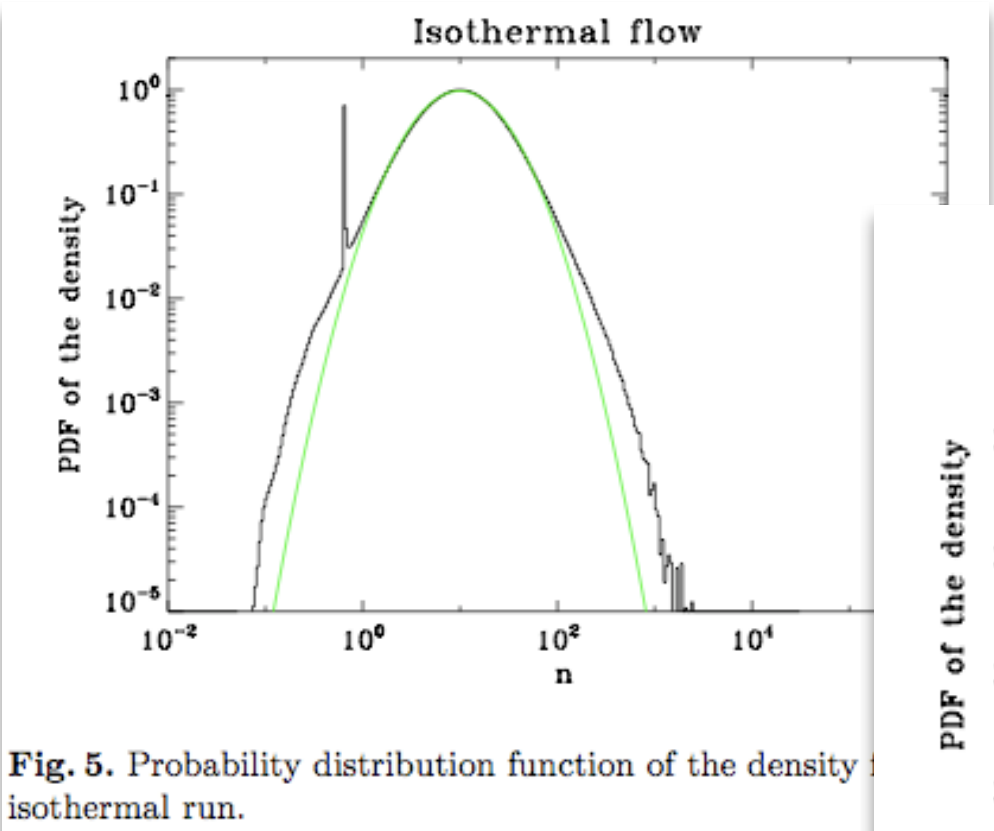

Fig. 5. Probability distribution function of the density
isothermal run.

(Audit & Hennebelle, submitted)

1200^3 hydrodynamic simulation

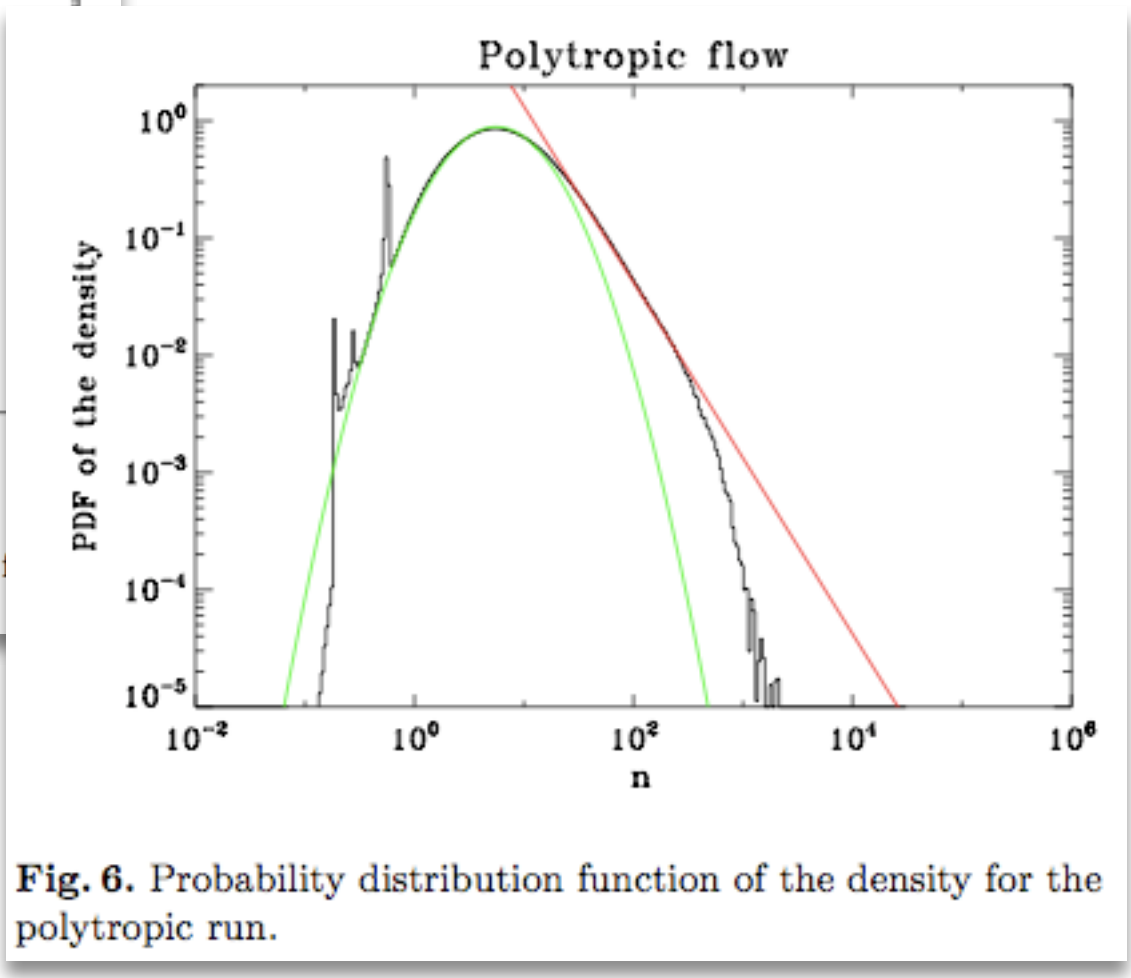

Fig. 6. Probability distribution function of the density for the polytropic run.

dilatational vs. solenoidal

density as function of time / cut through 1024^3 cube simulation (FLASH)

compressive
larger structures, higher ρ-contrast

rotational
smaller structures, small ρ-pdf

Federrath, Klessen, Schmidt (2008a,b)

dilatational vs. solenoidal

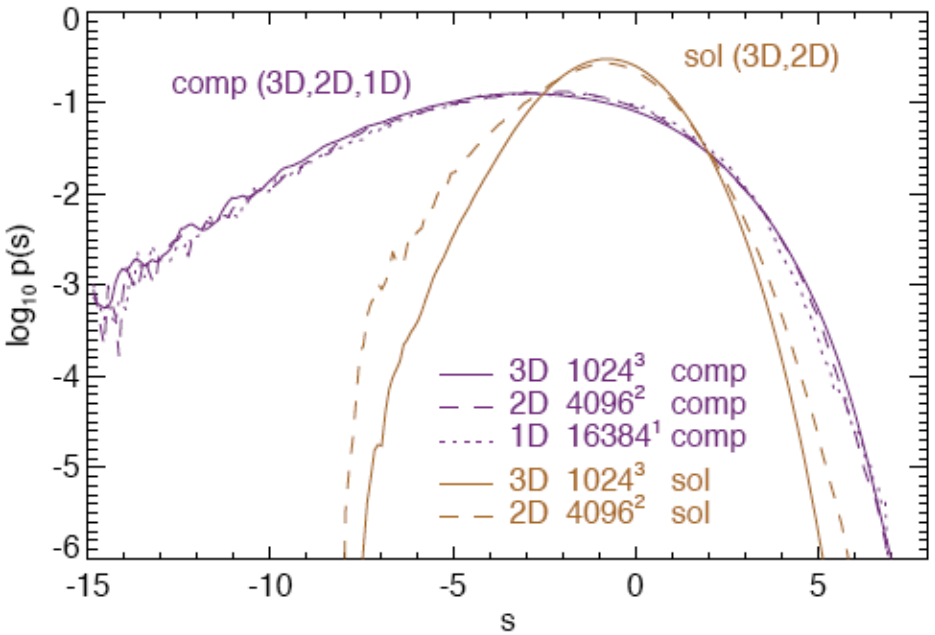

FIG. 3.— Volume-weighted density PDFs $p(s)$ obtained from 3D, 2D and 1D simulations with compressive forcing and from 3D and 2D simulations using solenoidal forcing. Note that in 1D, only compressive forcing is possible as in the study by Passot & Vázquez-Semadeni (1998). As suggested by eq. (5), compressive forcing yields almost identical density PDFs in 1D, 2D and 3D with $b\sim1$, whereas solenoidal forcing leads to a density PDF with $b\sim1/2$ in 2D and with $b\sim1/3$ in 3D.

- density pdf depends on "dimensionality" of driving
  - relation between width of pdf and Mach number

$$\sigma_\rho / \rho_0 = b\mathcal{M}$$

  - with b depending on ζ via

$$b = 1 + \left[\frac{1}{D} - 1\right]\zeta = \begin{cases} 1 - \frac{2}{3}\zeta & \text{, for } D = 3 \\ 1 - \frac{1}{2}\zeta & \text{, for } D = 2 \\ 1 & \text{, for } D = 1 \end{cases}$$

  - with ζ being the ratio of dilatational vs. solenoidal modes:

$$\mathcal{P}_{ij}^{\zeta} = \zeta\mathcal{P}_{ij}^{\perp} + (1-\zeta)\mathcal{P}_{ij}^{\parallel} = \zeta\delta_{ij} + (1-2\zeta)\frac{k_i k_j}{|k|^2}$$

Federrath, Klessen, Schmidt (2008a)

dilatational vs. solenoidal

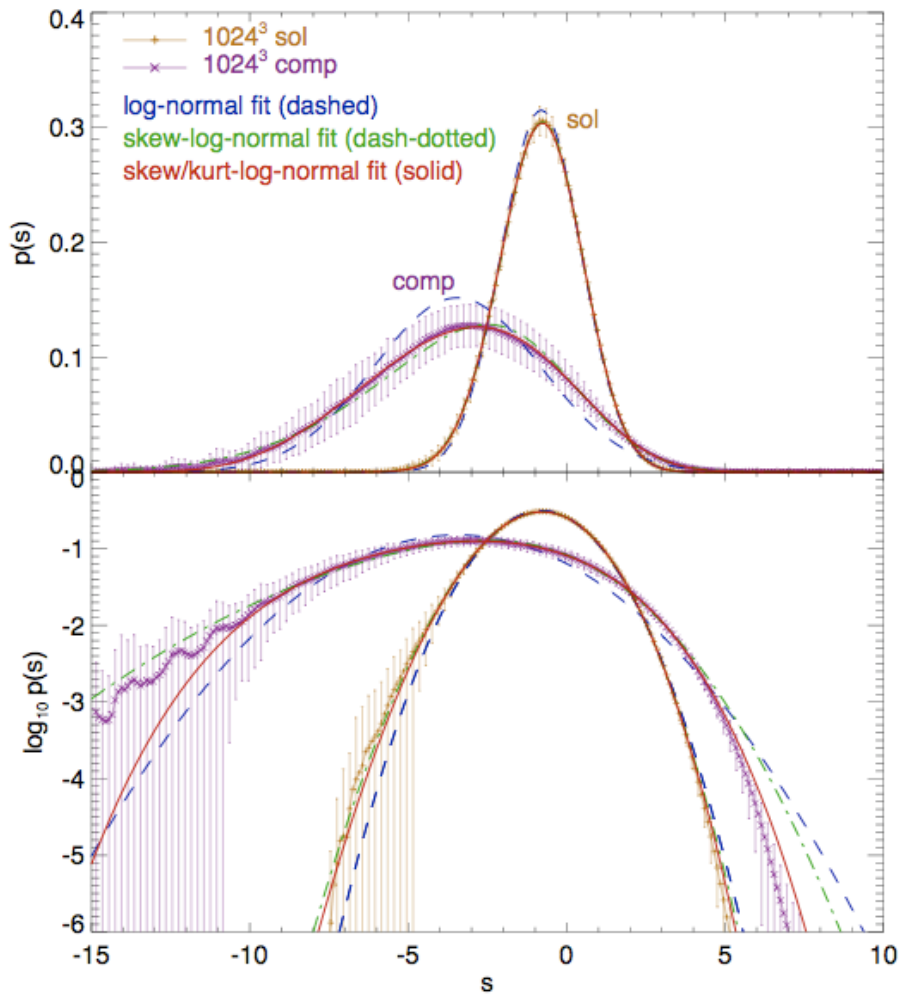

good fit needs 3rd and 4th moment of distribution!

Federrath, Klessen, Schmidt (2008b)

- density pdf depends on "dimensionality" of driving
  → is that a problem for the Krumholz & McKee model of the SF efficiency?
- density pdf of compressive driving is *NOT log-normal*
  → is that a problem for the Padoan & Nordlund IMF model?
- most "physical" sources should be *compressive* (convergent flows from spiral shocks or SN)

effects of chemistry 4

- deliverables / predictions:
  - x-factor estimates (as function of environmental conditions)
  - synthetic line emission maps (in combination with line transfer)
  - pdf's of density, velocity, emissivity / structure functions (to directly connect to observational regime)
  - *COMMENT:* density pdf is *NOT* lognormal! <-- gravity (poster by Kim), driving scheme (Federrath et al. 2008), EOS (Hennebelle & Audit 2009)

initial mass function

initial mass function

- what is the relation between molecular cloud fragmentation and the distribution of stars?
- important quantity: *IMF*
- IMPORTANT CAVEAT:
  "everyone" gets the right IMF
  → better look for secondary indicators
  - *stellar multiplicity*
  - protostellar *spin* (including disk)
  - *spatial distribution* + *kinematics* in young clusters
  - *magnetic field strength* and *orientation*

IMF

- distribution of stellar masses depends on
  - turbulent initial conditions
    --> mass spectrum of prestellar cloud cores
  - collapse and interaction of prestellar cores
    --> competitive accretion and *N*-body effects
  - thermodynamic properties of gas
    --> balance between heating and cooling
    --> EOS (determines which cores go into collapse)
  - (proto) stellar feedback terminates star formation
    ionizing radiation, bipolar outflows, winds, SN

(e.g. Larson 2003, Prog. Rep. Phys.; Mac Low & Klessen, 2004, Rev. Mod. Phys, 76, 125 - 194)

IMF

- distribution of stellar masses depends on
  - turbulent initial conditions
    --> mass spectrum of prestellar cloud cores
  - collapse and interaction of prestellar cores
    --> competitive accretion and *N*-body effects
  - *thermodynamic properties of gas*
    --> balance between heating and cooling
    --> EOS (determines which cores go into collapse)
  - (proto) stellar feedback terminates star formation
    ionizing radiation, bipolar outflows, winds, SN

(e.g. Larson 2003, Prog. Rep. Phys.; Mac Low & Klessen, 2004, Rev. Mod. Phys, 76, 125 - 194)

EOS as function of metallicity

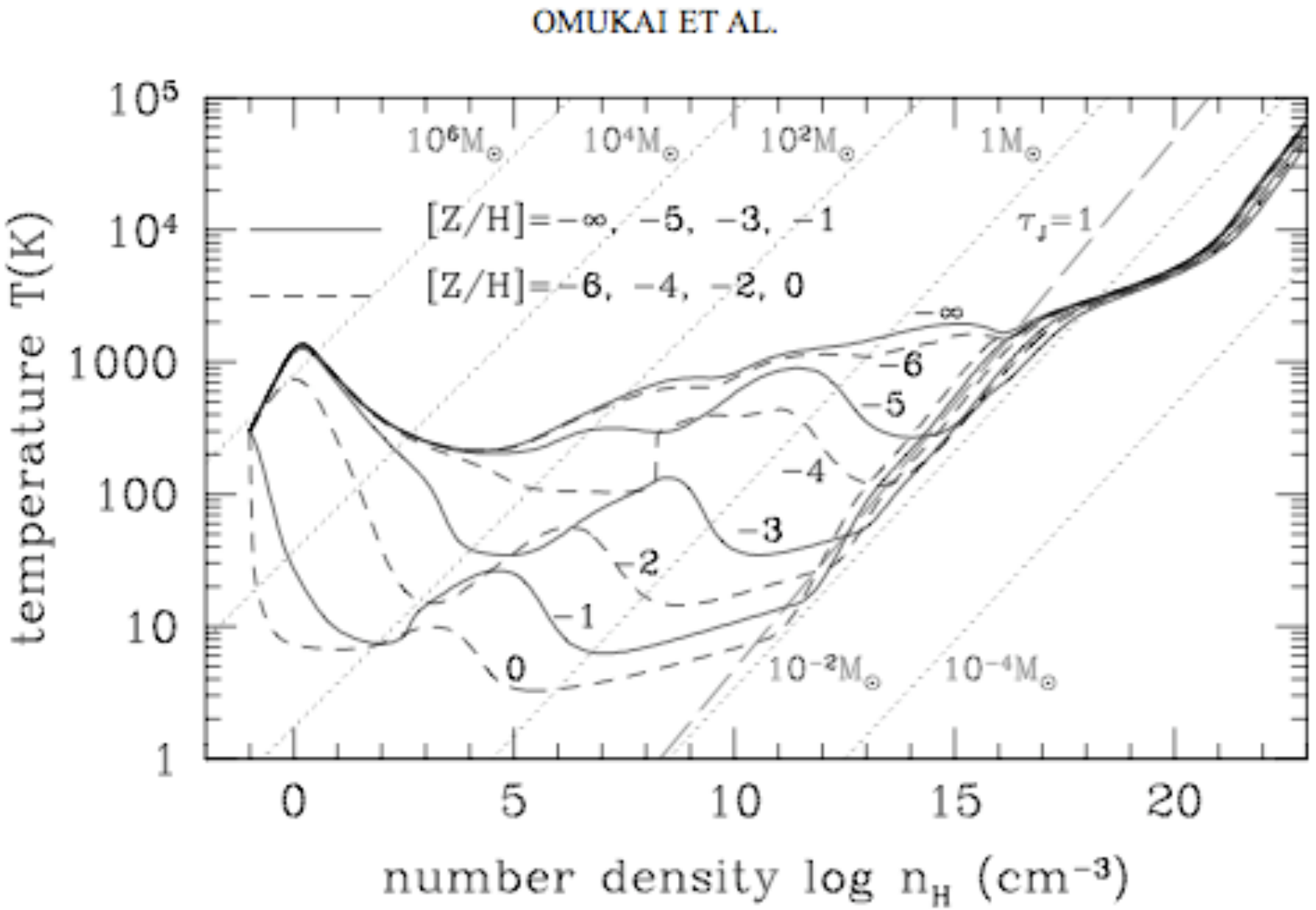

(Omukai et al. 2005)

EOS as function of metallicity

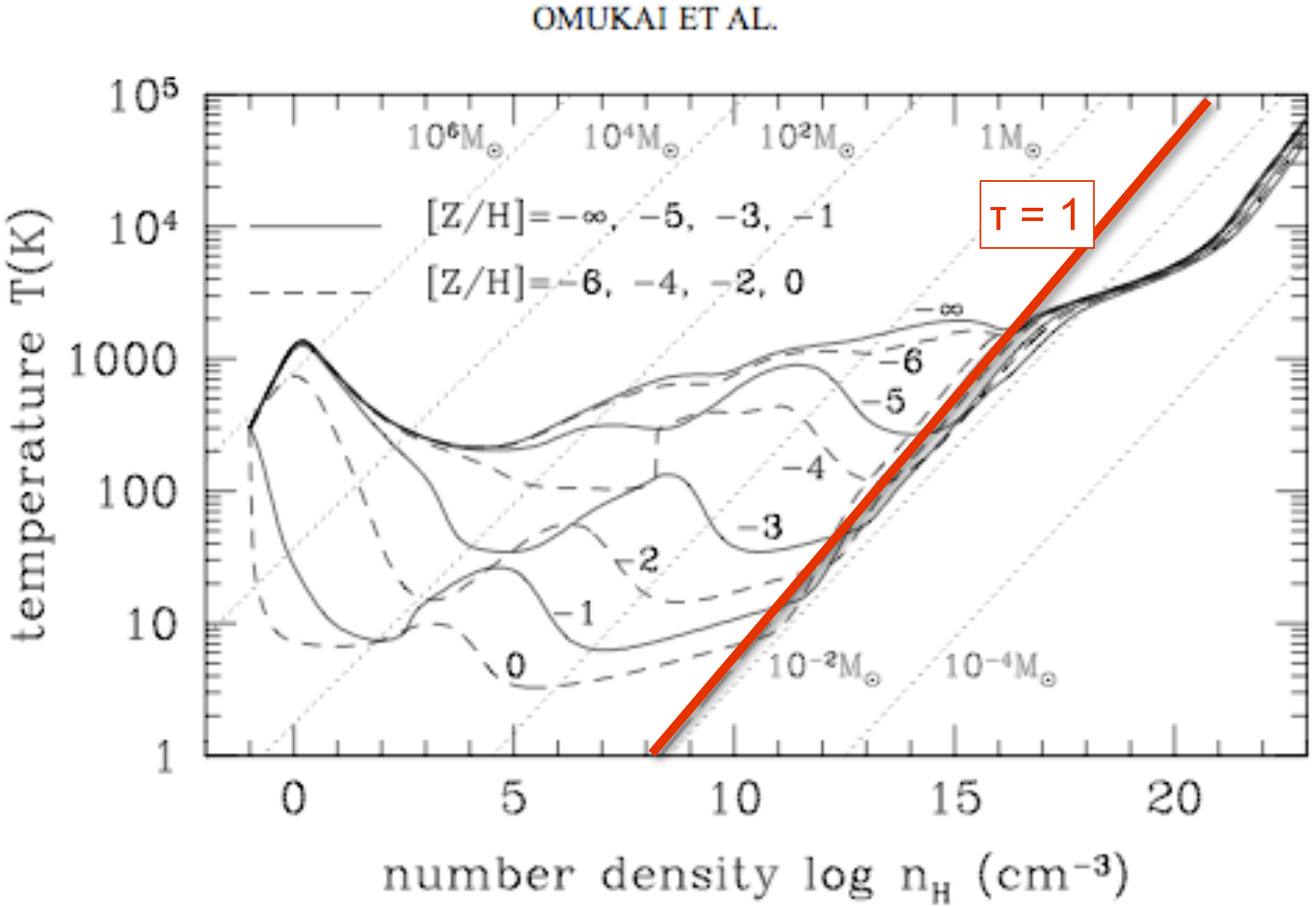

(Omukai et al. 2005)

EOS as function of metallicity

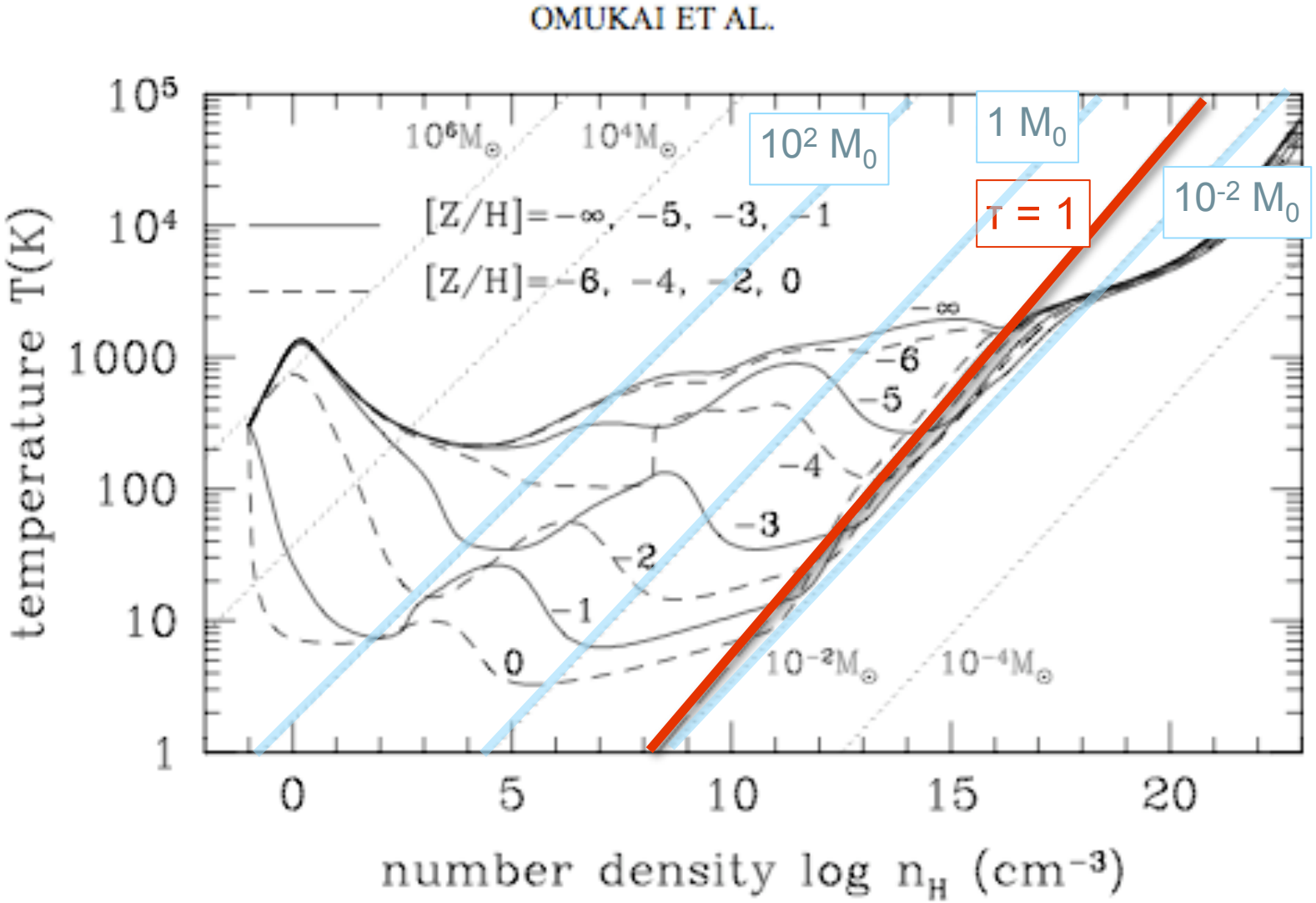

(Omukai et al. 2005)

present-day star formation

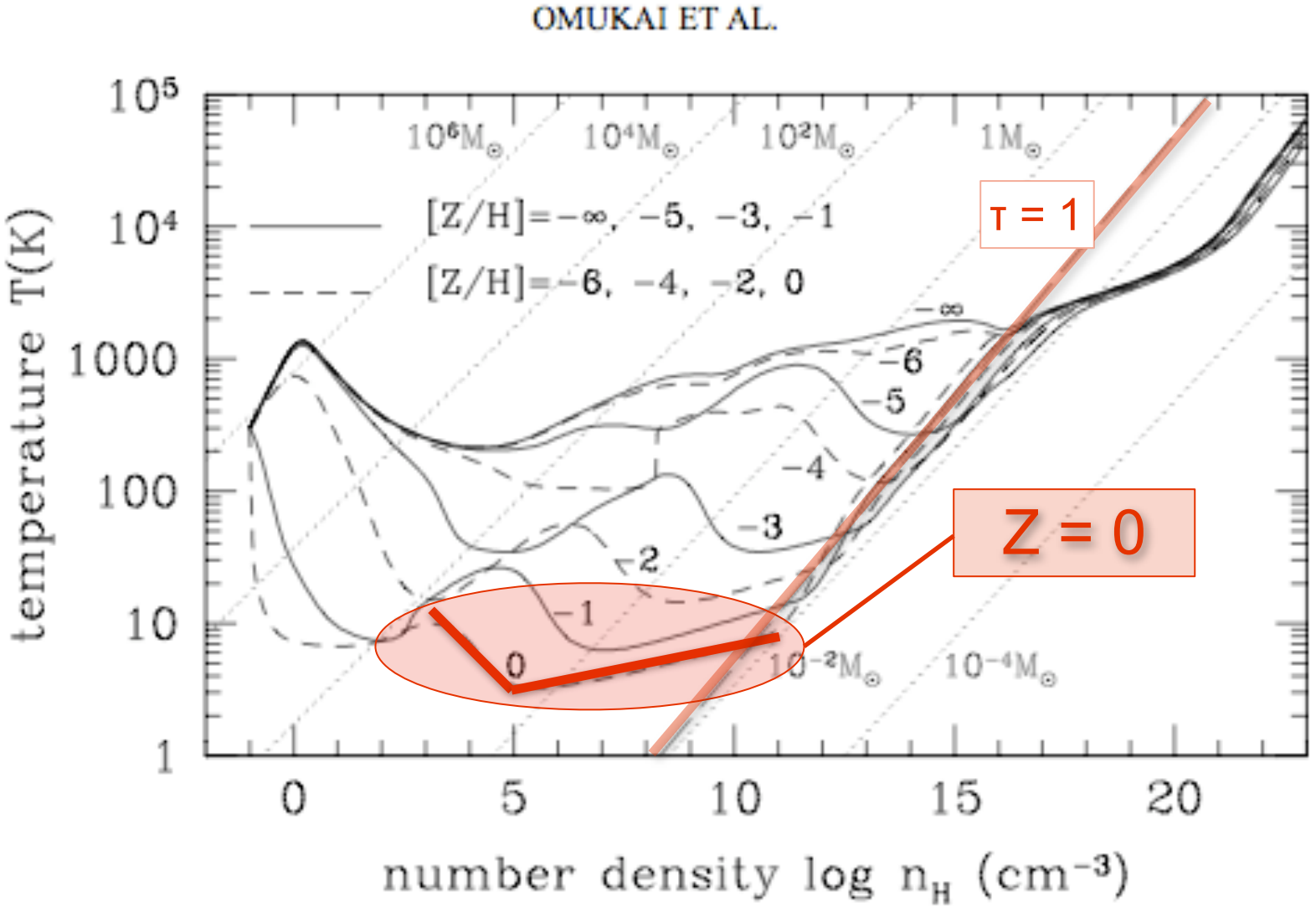

(Omukai et al. 2005, Jappsen et al. 2005, Larson 2005)

present-day star formation

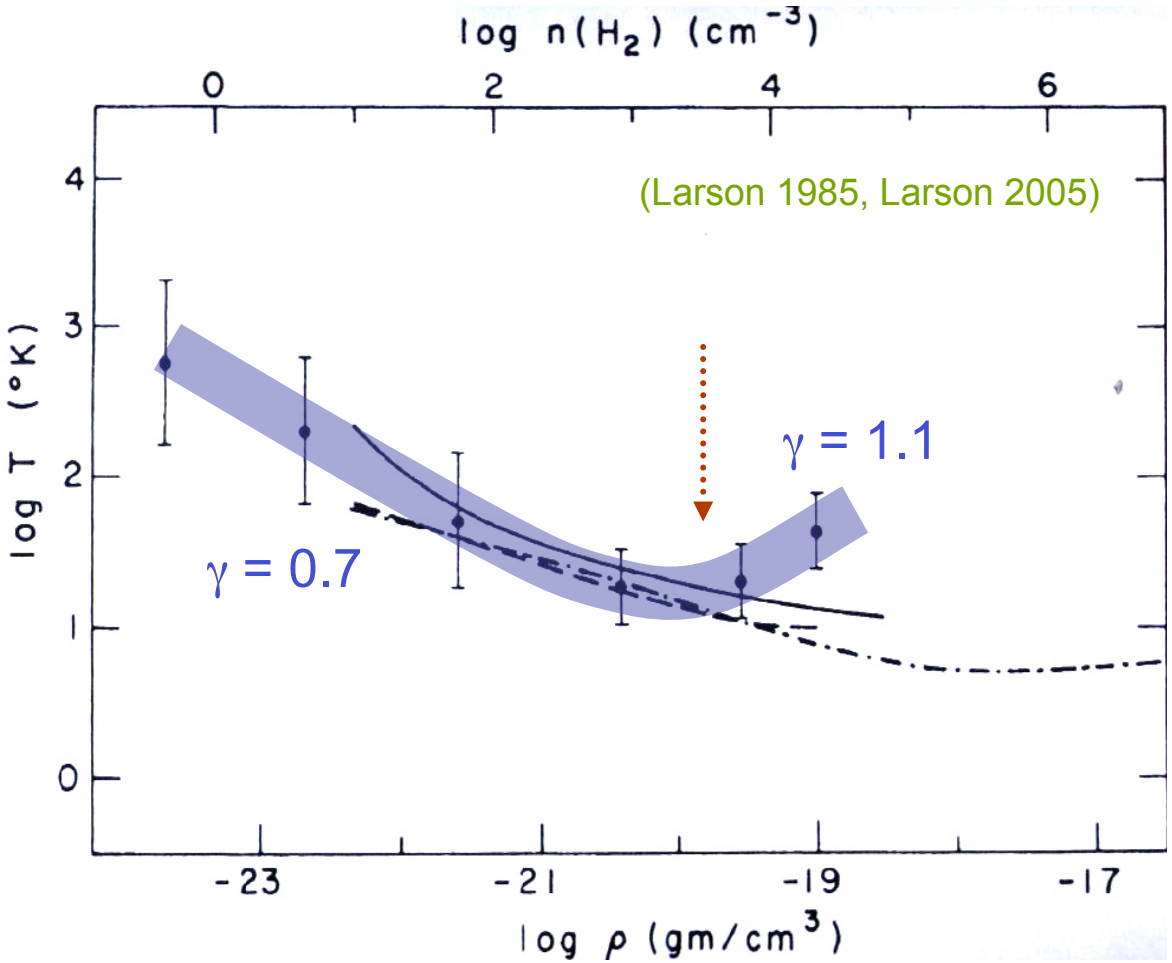

present-day star formation

This kink in EOS is very insensitive to environmental conditions such as ambient radiation field
--> reason for universal for of the IMF? (Elmegreen et al. 2008)

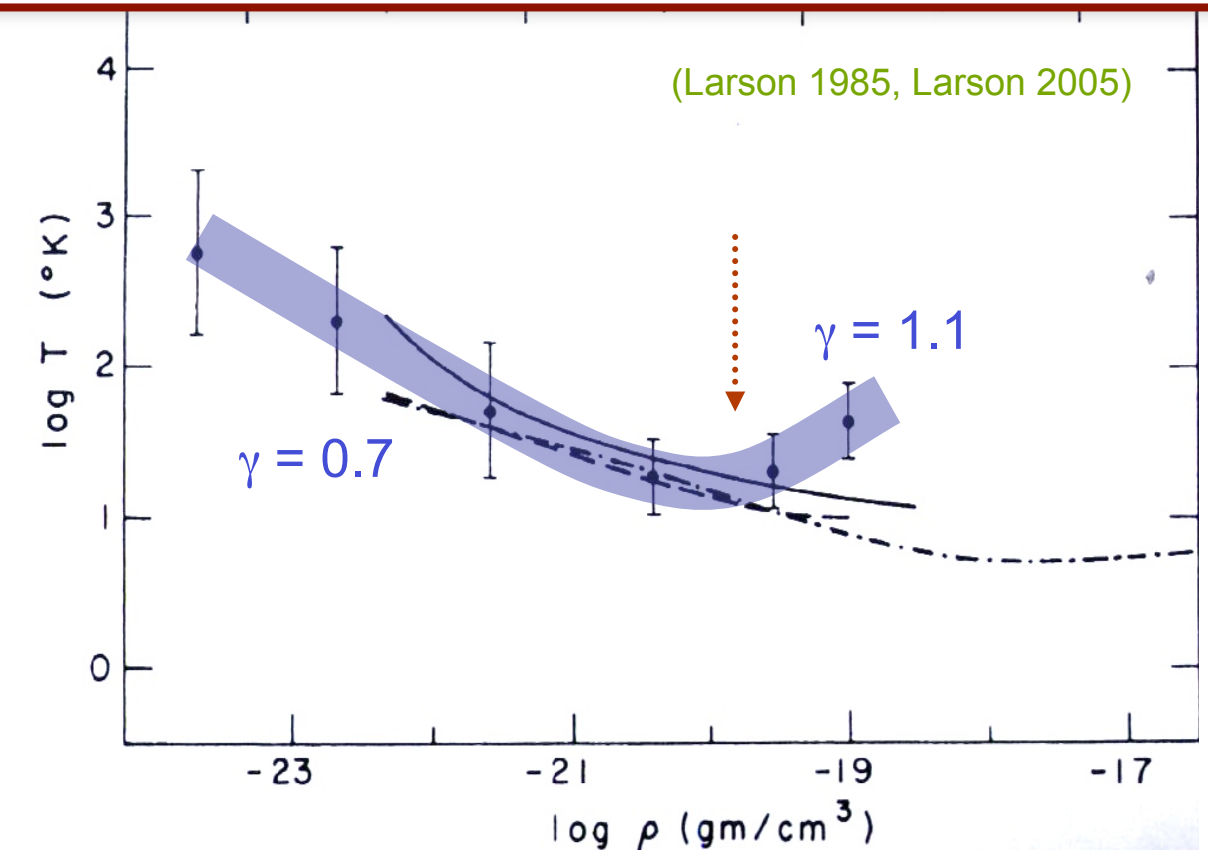

IMF from simple piece-wise polytropic EOS

$\gamma_1 = 0.7$

$\gamma_2 = 1.1$

$$T \sim \rho^{\gamma-1}$$

EOS and Jeans Mass:

$\mathbf{p} \propto \rho^{\gamma} \rightarrow \rho \propto \mathbf{p}^{1/\gamma}$

$\mathbf{M_{jeans}} \propto \gamma^{3/2}\, \rho^{(3\gamma-4)/2}$

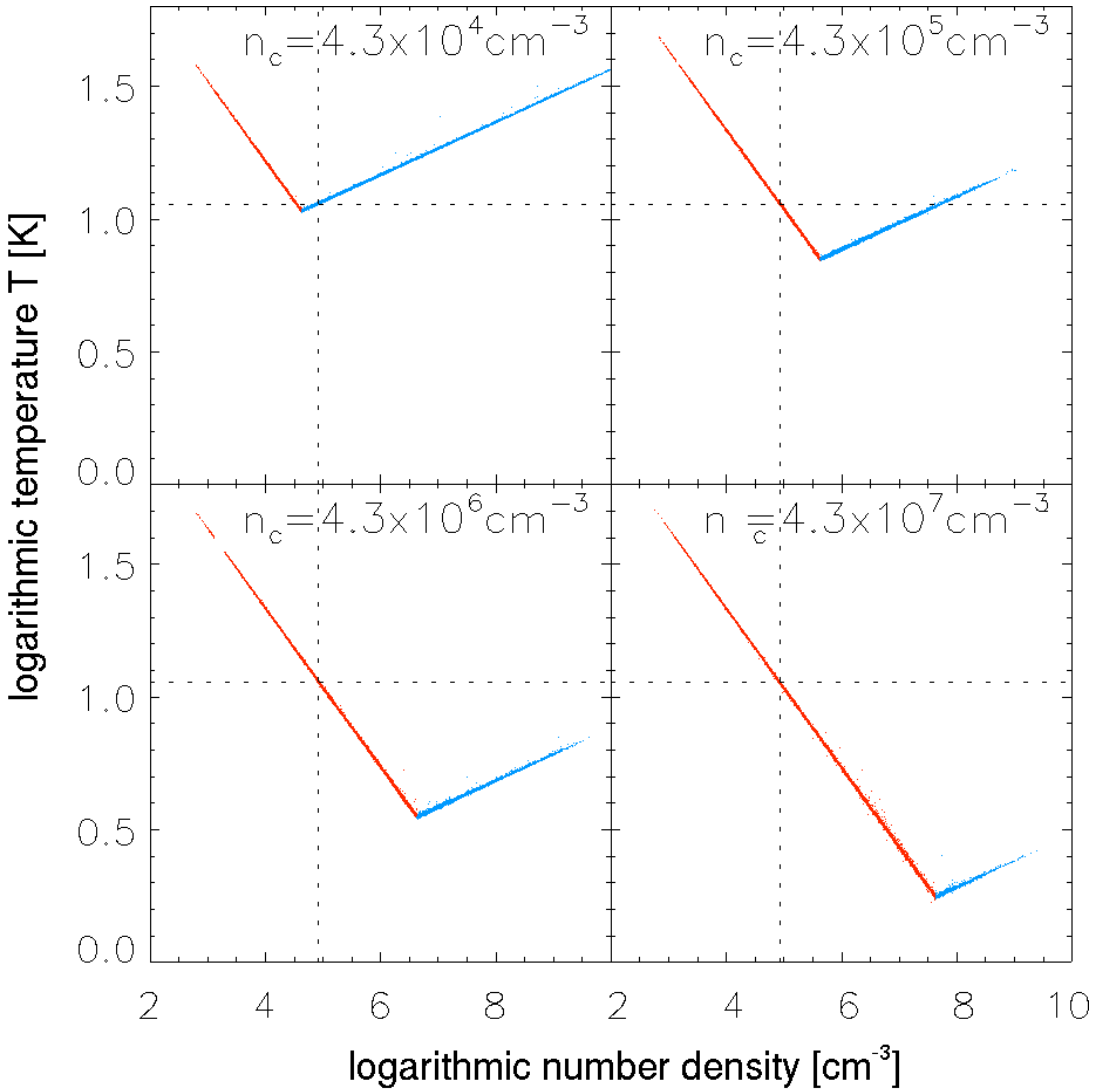

(Jappsen et al. 2005)

IMF from simple piece-wise EOS

critical density ⇧ ⇨ median mass ⇩

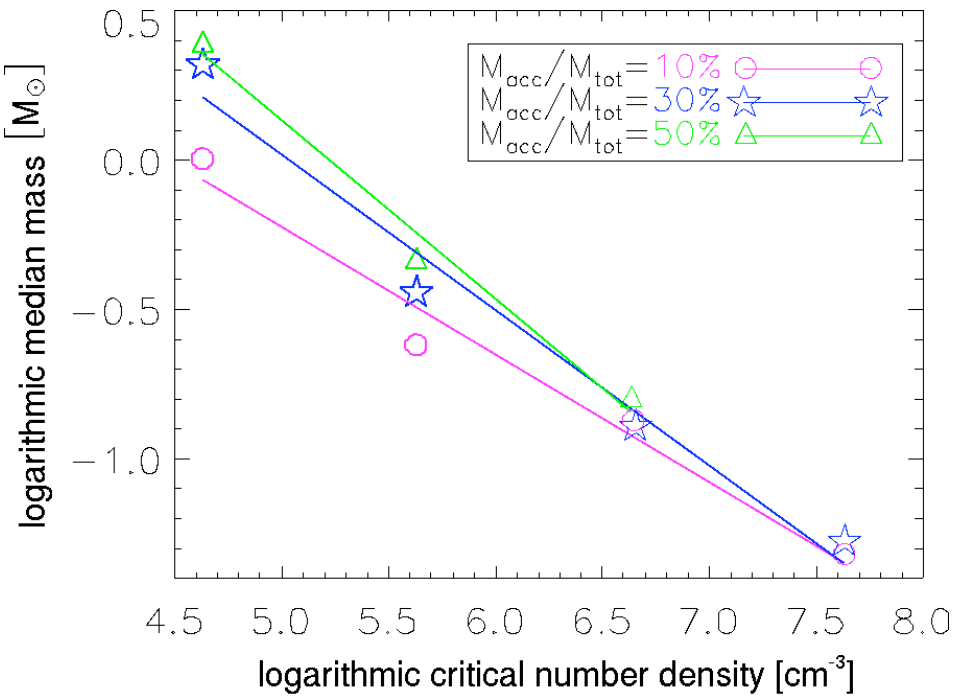

(Jappsen et al. 2005)

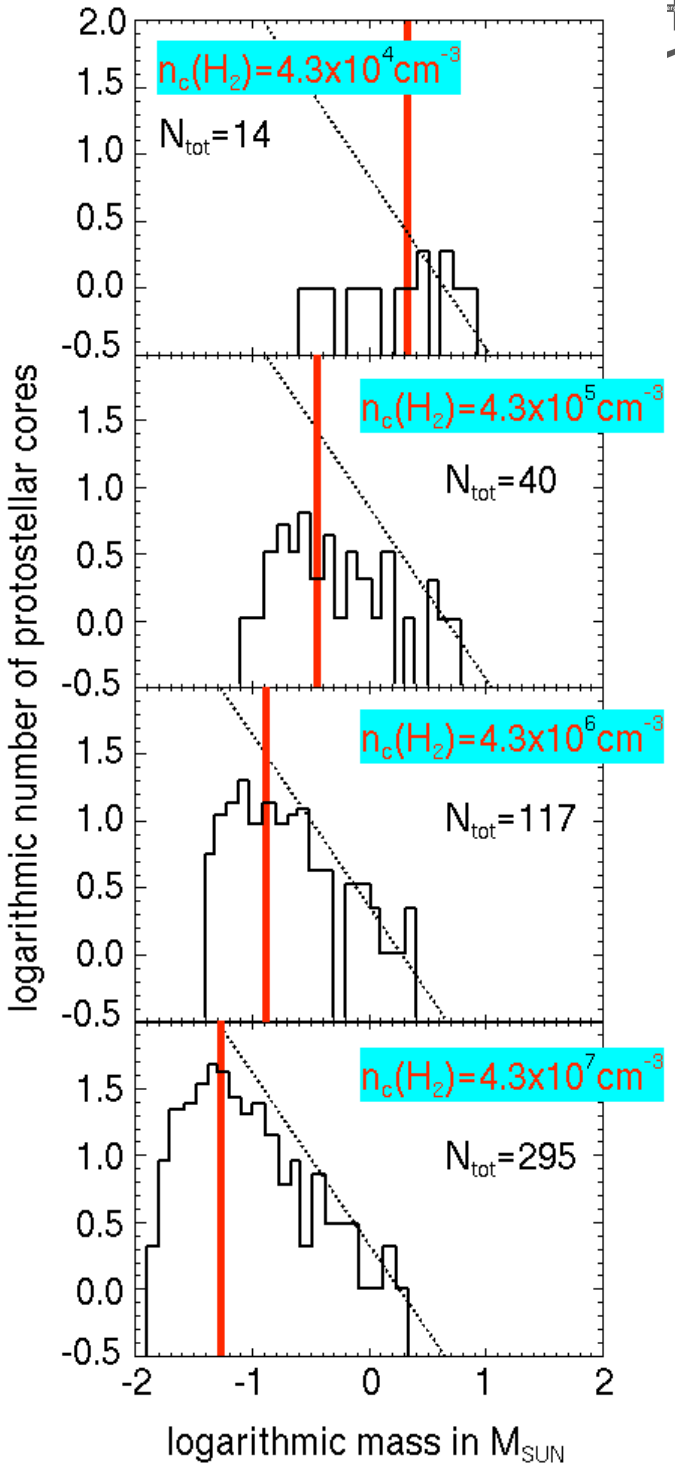

IMF in nearby molecular clouds

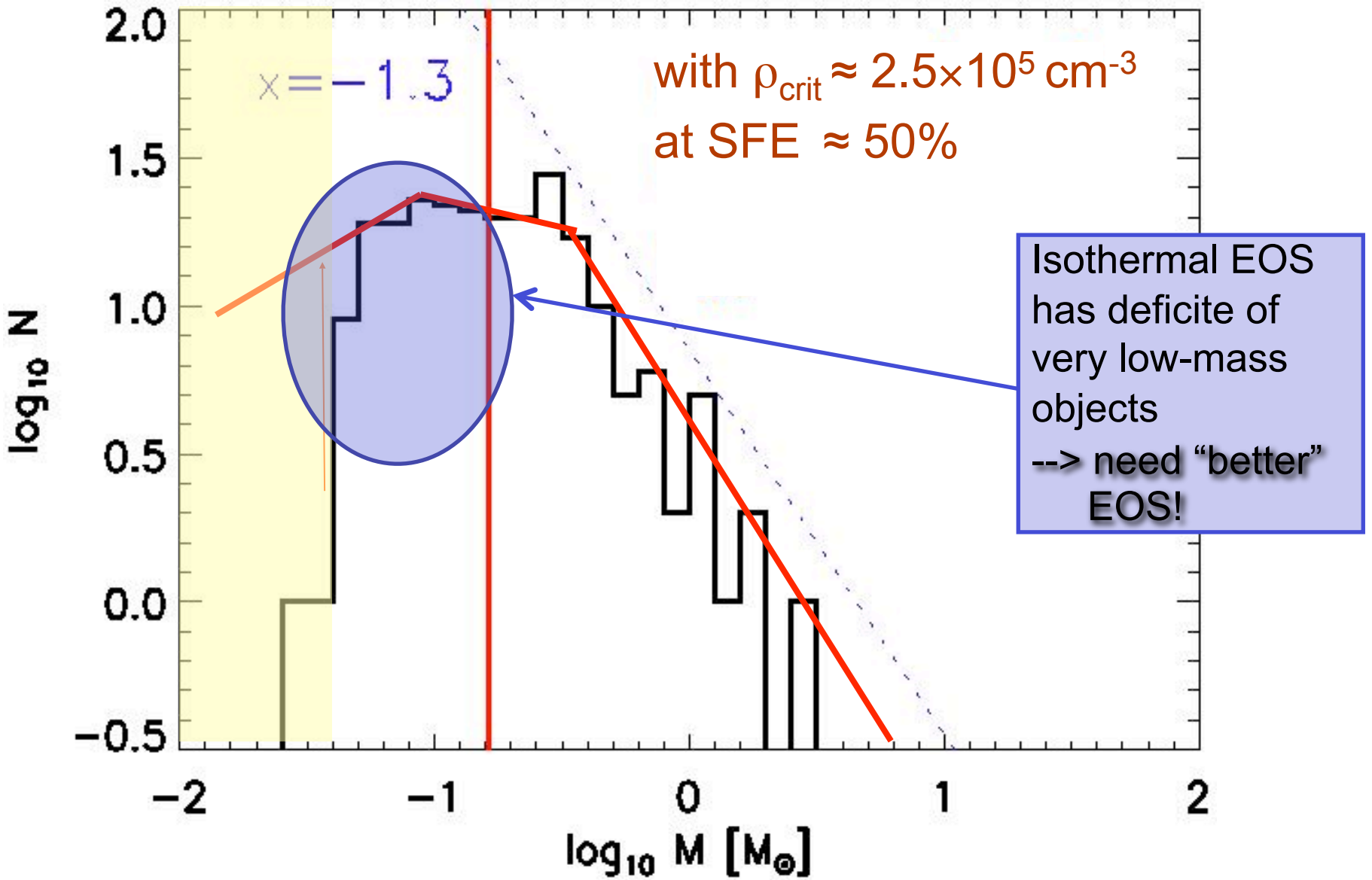

(Jappsen et al. 2005, A&A, 435, 611)c

IMF shape and universality

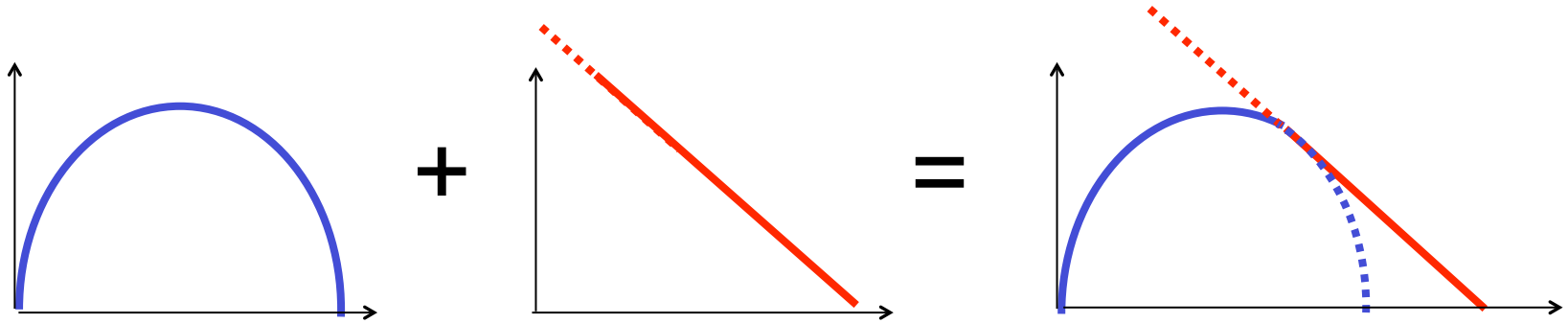

- combine scale free process → *POWER LAW BEHAVIOR*
  - turbulence (Padoan & Nordlund 2002, Hennebelle & Chabrier 2008)
  - gravity in dense clusters (Bonnell & Bate 2006, Klessen 2001)
  - universality: dust-induced EOS kink insensitive to radiation field (Elmegreen et al. 2008)
- with highly stochastic processes → central limit theorem
  → *GAUSSIAN DISTRIBUTION*
  - basically mean thermal Jeans length (or feedback)
  - universality: insensitive to metallicity (Clark et al. 2009, submitted)

dependence on Z at low density

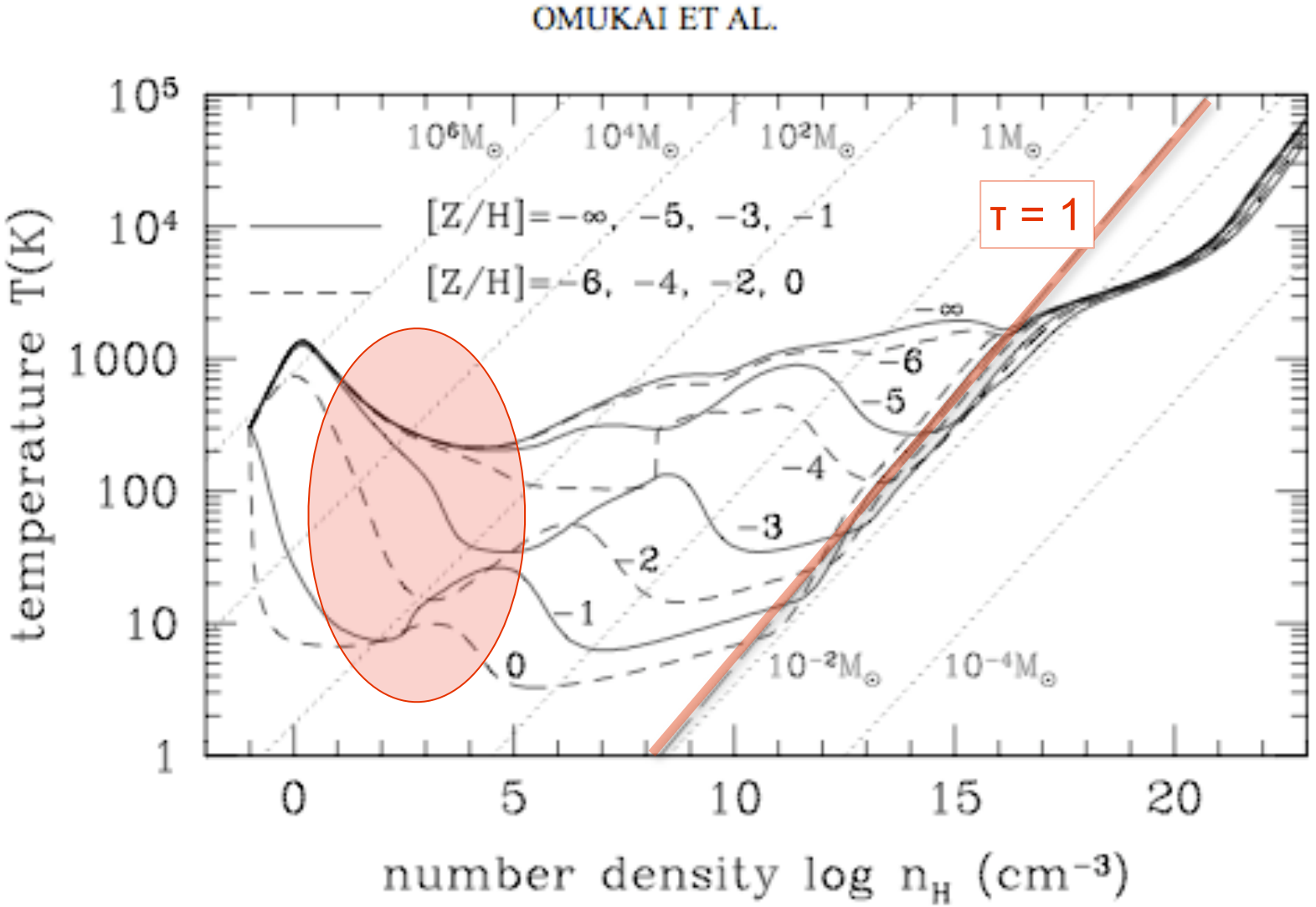

(Omukai et al. 2005)

dependence on Z at low density

- at densities below n ≈ 10^2 cm^{-3} *H_2 cooling* dominates the behavior. (Jappsen et al. 2007)
- fragmentation depends on *initial conditions then*
  - example: *solid-body rotating top-hat* initial conditions with dark matter fluctuations (a la Bromm et al. 1999) fragment no matter what metallicity you take (in regime n ≤ 10^6 cm^{-3})
    → because *unstable disk* builds up
    (Jappsen et al. 2008a)

dependence on Z at low density

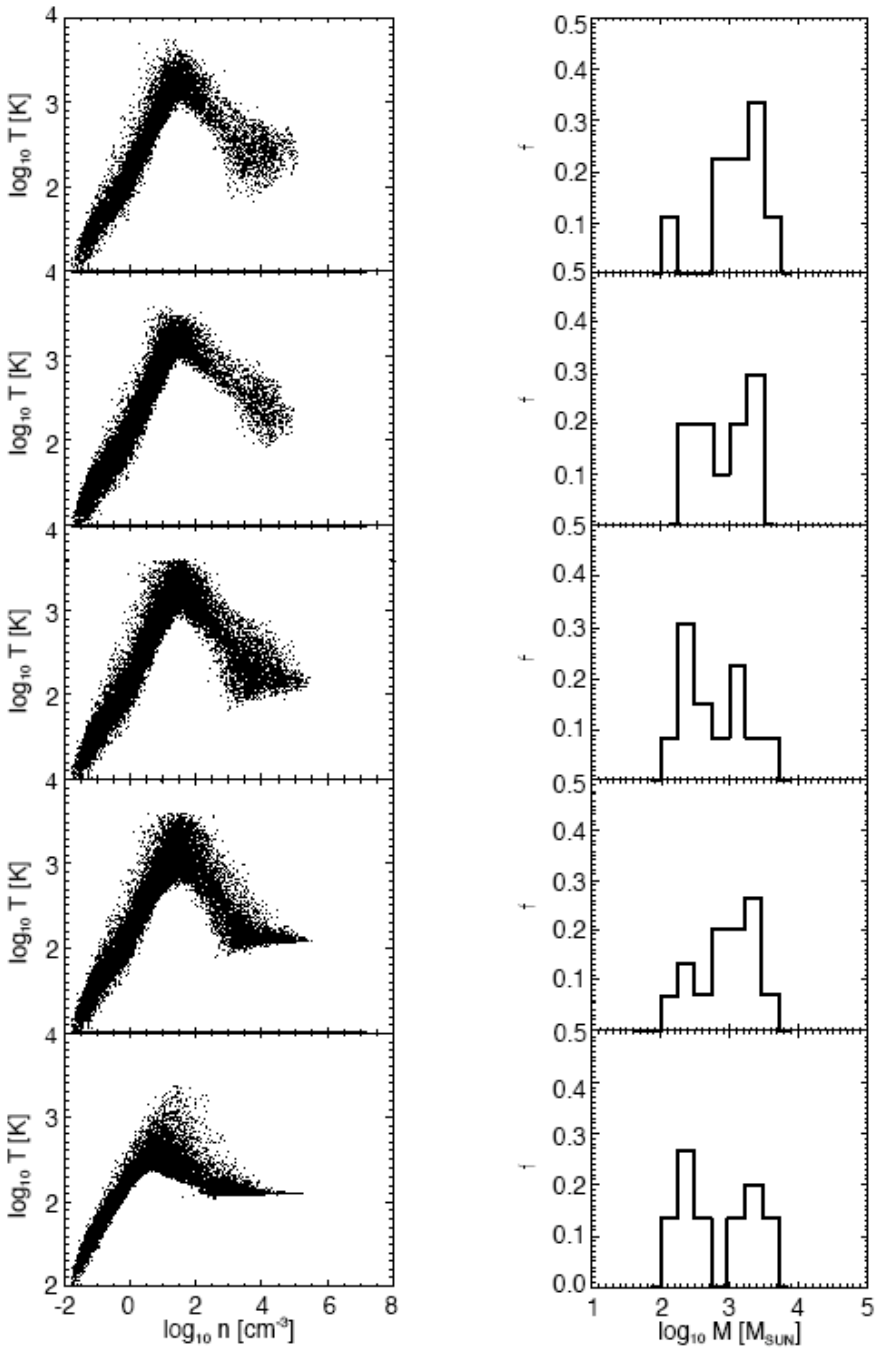

Z = 0

Z = -4

Z = -3

Z = -2

Z = -1

rotating top-hat with dark matter fluctuations fragments, no matter what

(Jappsen et al. 2008a, see also Clark et al. 2008)

dependence on Z at low density

- fragmentation depends on *initial conditions then*
  - example: *centrally concentrated halo* does *not* fragment up to densities of $n \approx 10^6$ cm^{-3} up to metallicities $Z \approx -1$
    (Jappsen et al. 2008b)

implications for Pop III

- star formation will depend on *degree of turbulence* in protogalactic halo
- speculation: *differences in stellar mass function*?
- speculation:
  - low-mass halos → low level of turbulence → relatively massive stars
  - high-mass halos (atomic cooling halos) → high degree of turbulence → wider mass spectrum with peak at lower-masses?

turbulence developing in an atomic cooling halo

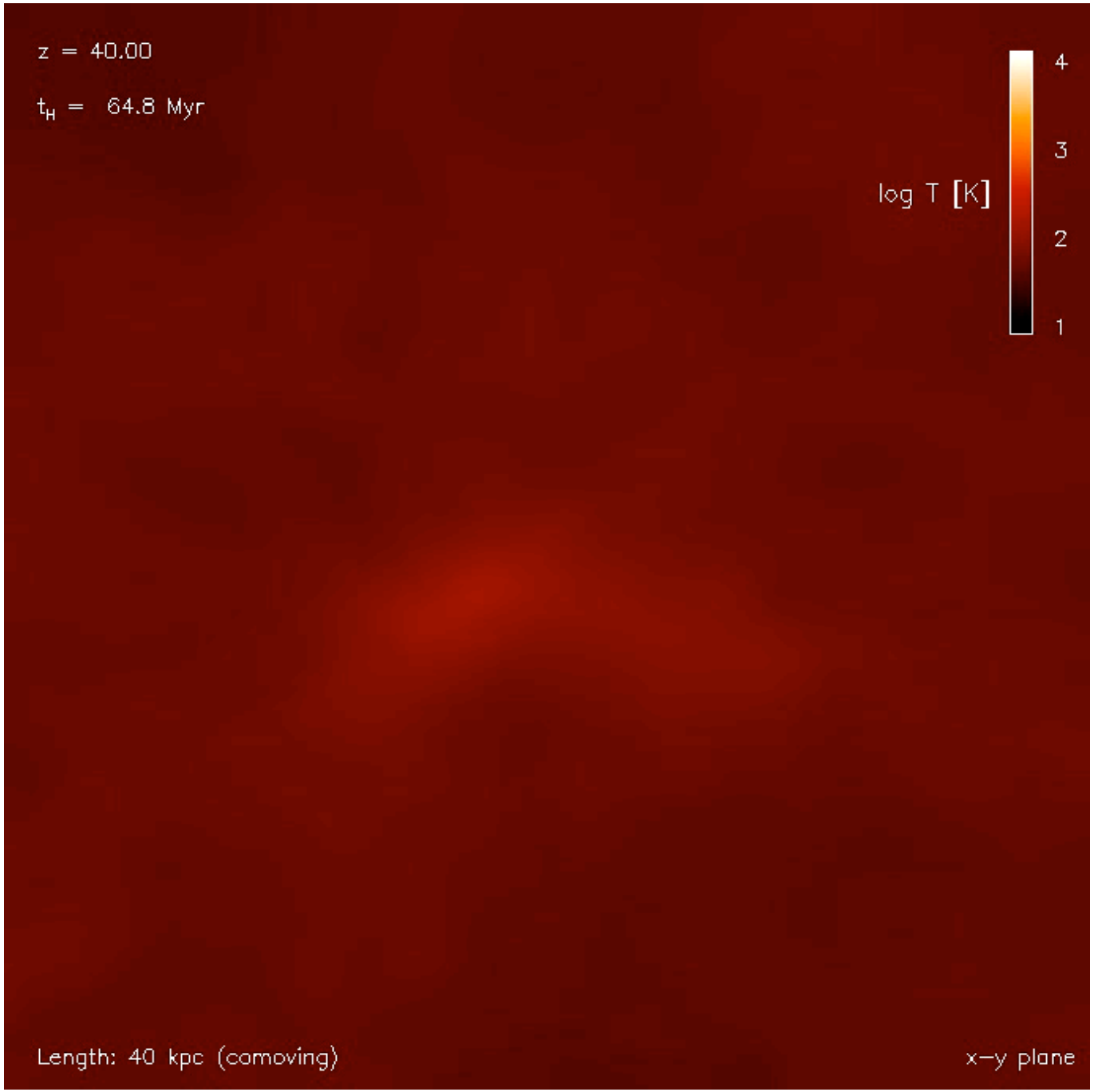

(Greif et al. 2008)

transition: Pop III to Pop II.5

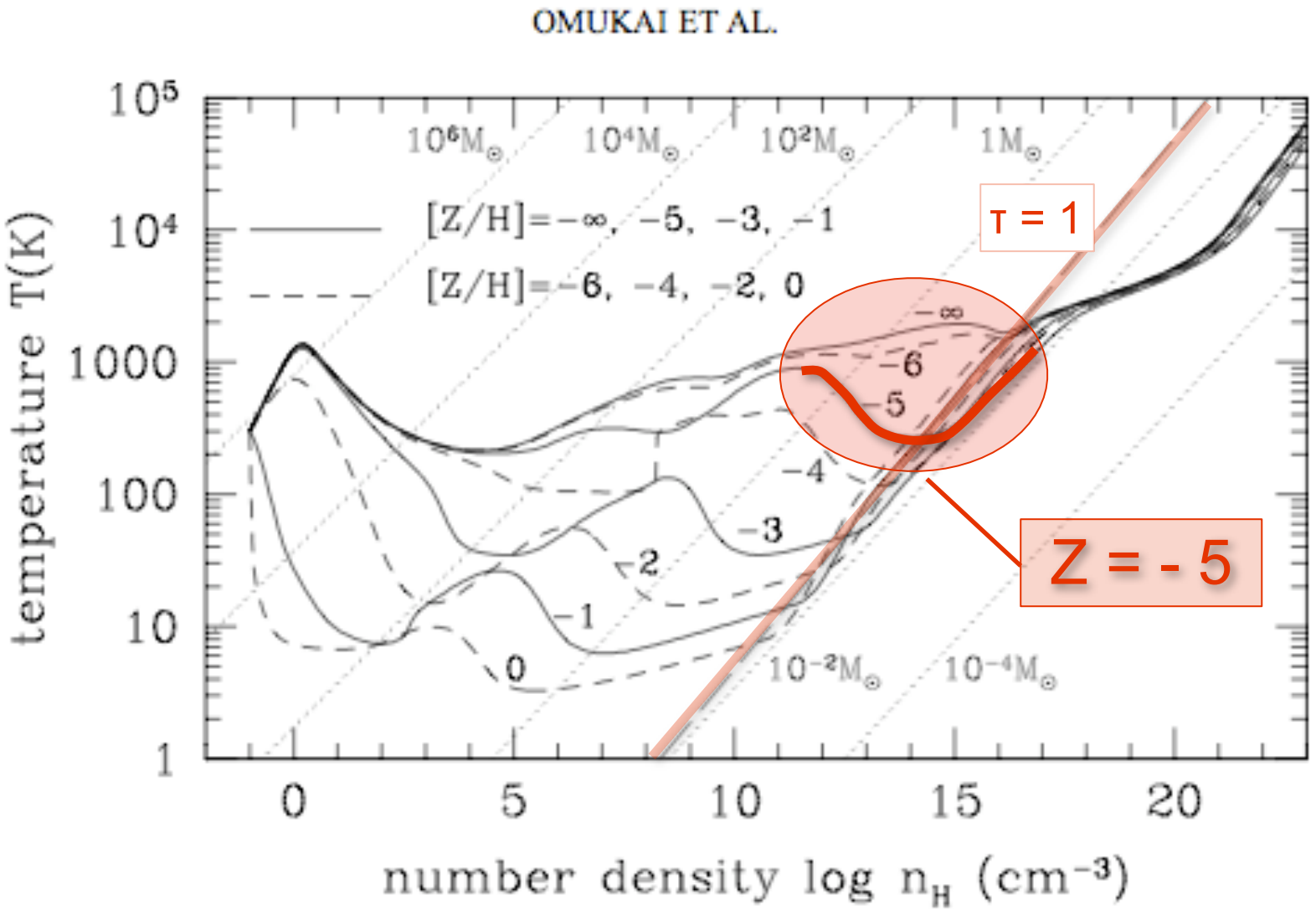

(Omukai et al. 2005)

dust induced fragmentation at $Z=10^{-5}$

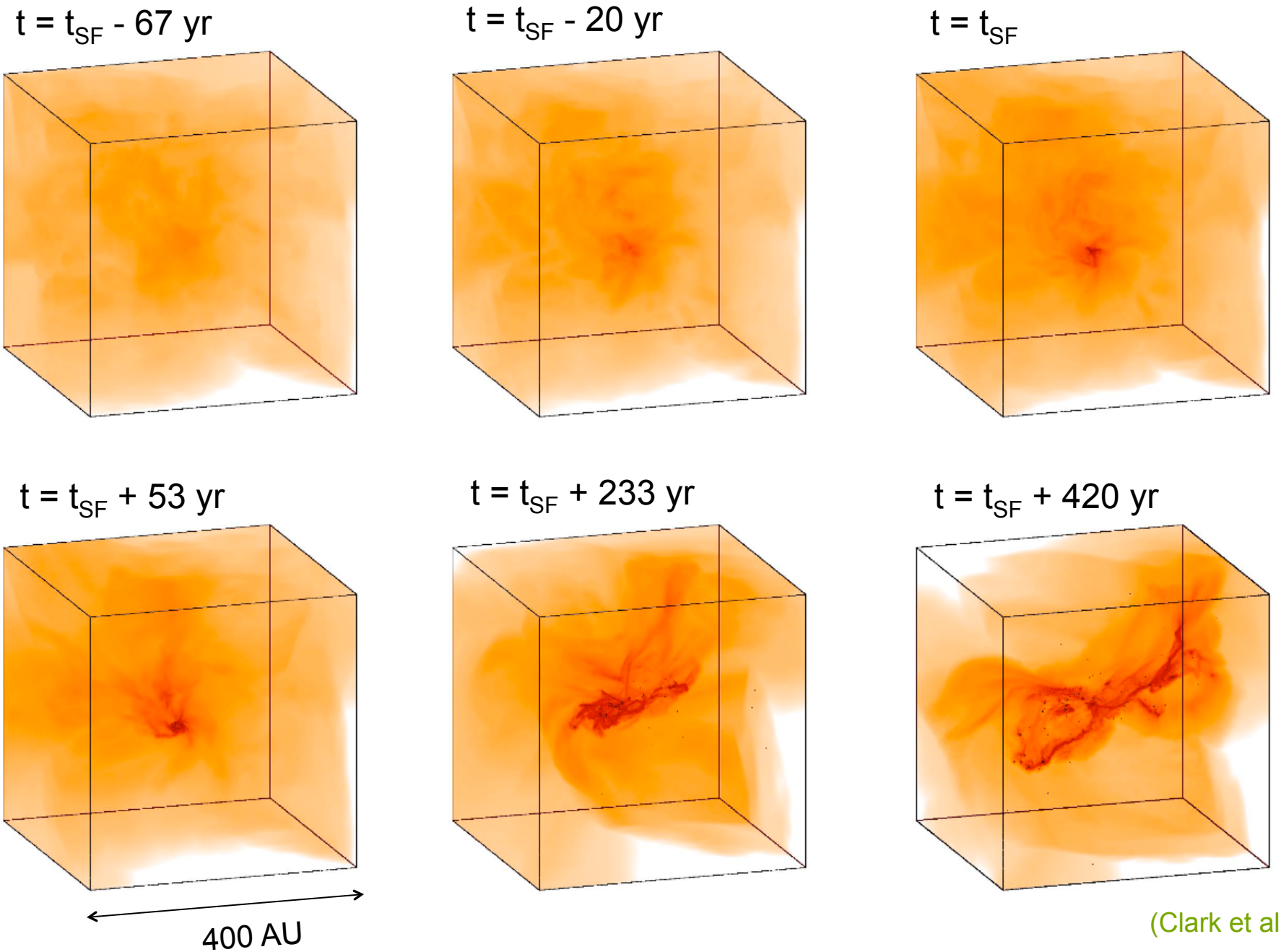

(Clark et al. 2007)

dust induced fragmentation at $Z=10^{-5}$

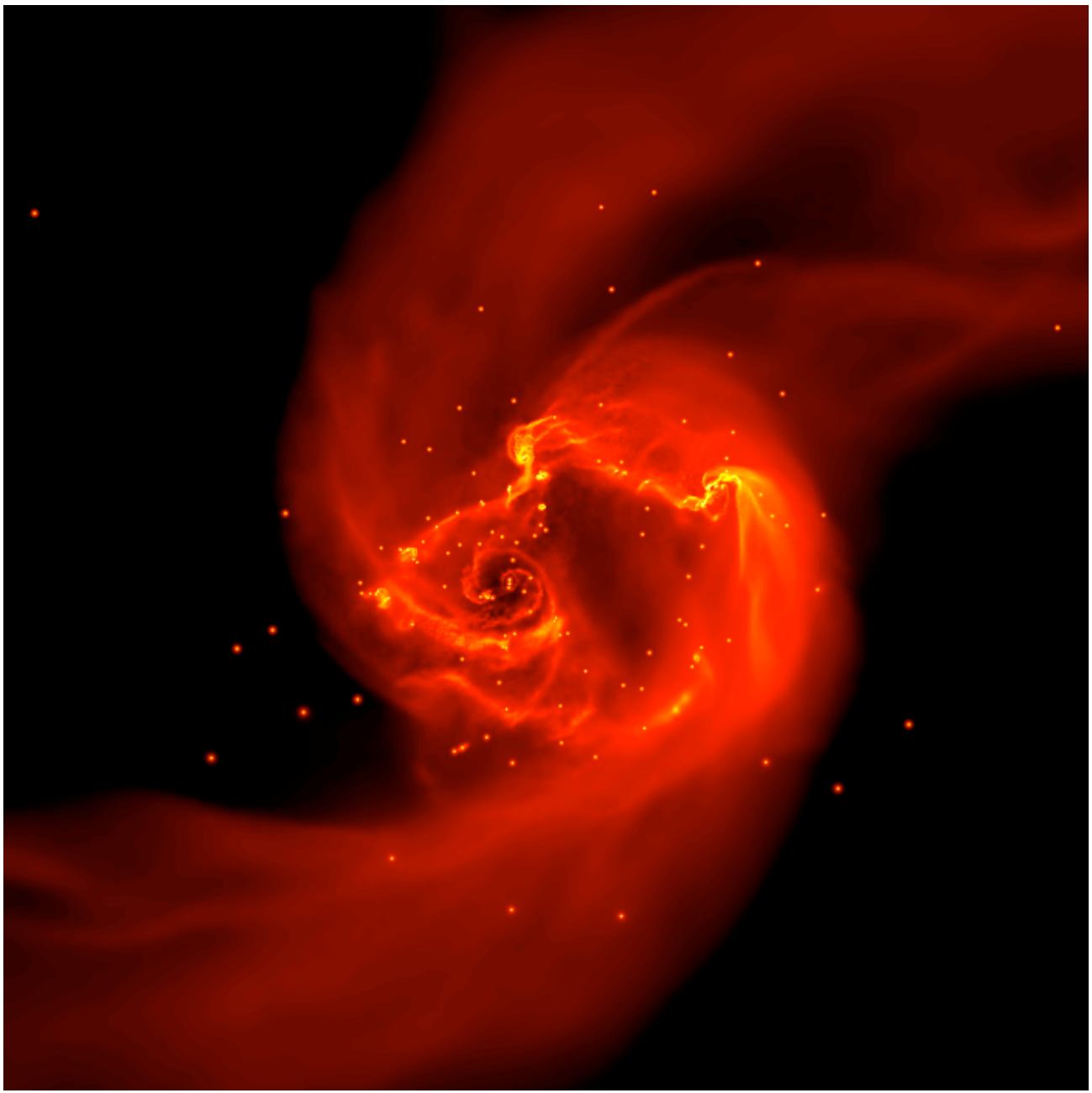

dense cluster of low-mass protostars builds up:

- mass spectrum peaks *below 1* M_{sun}
- cluster VERY dense $n_{stars} = 2.5 \times 10^{9}\ pc^{-3}$
- fragmentation at density $n_{gas} = 10^{12} - 10^{13}\ cm^{-3}$

(Clark et al. 2008, ApJ 672, 757)

dust induced fragmentation at $Z=10^{-5}$

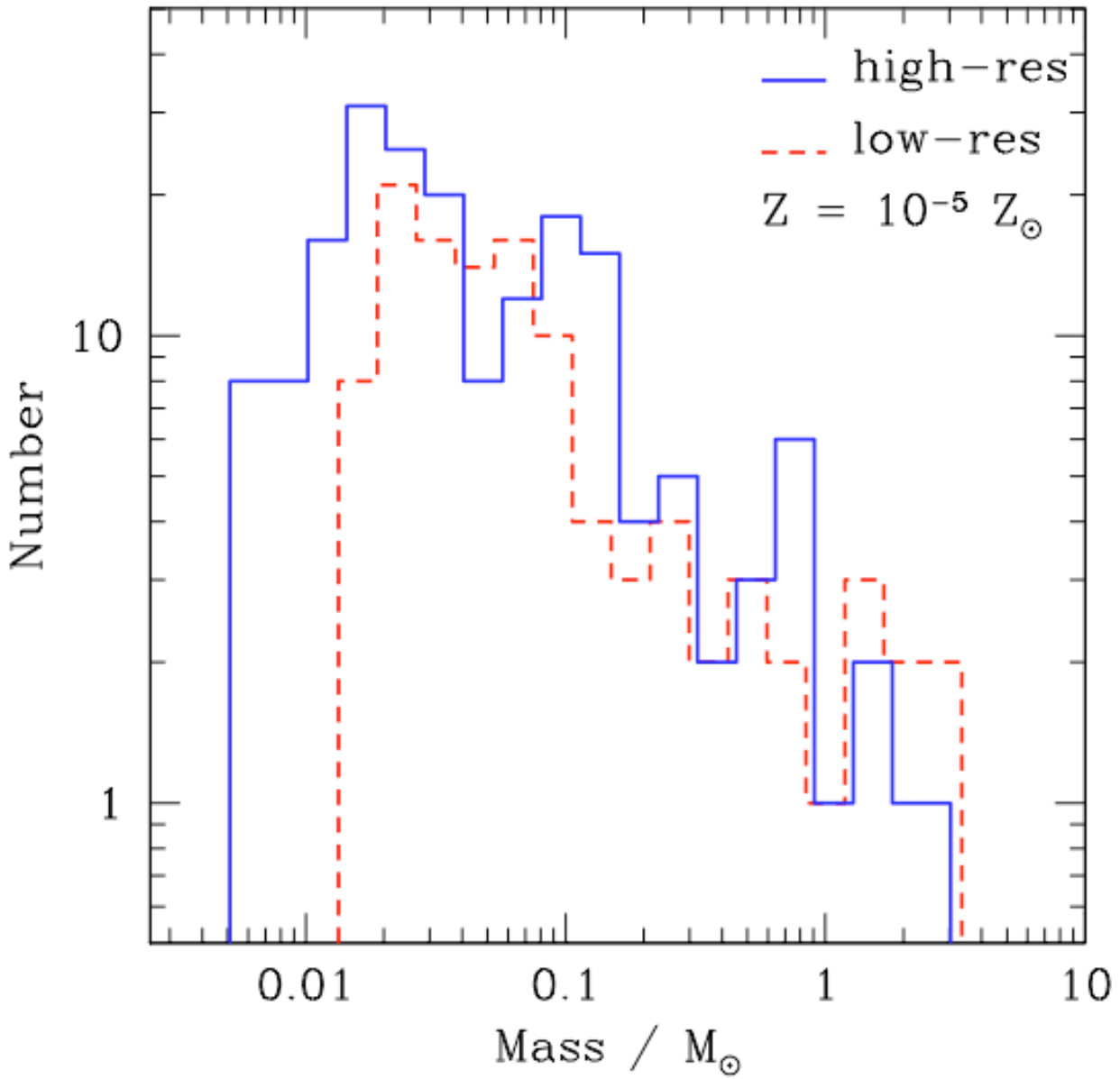

dense cluster of low-mass protostars builds up:

- mass spectrum peaks below 1 M_{sun}
- cluster VERY dense $n_{stars} = 2.5 \times 10^9\ pc^{-3}$

- *predictions:*
  * low-mass stars with [Fe/H] ~ 10^{-5}
  * high binary fraction

(Clark et al. 2008)

dust induced fragmentation at $Z=10^{-5}$

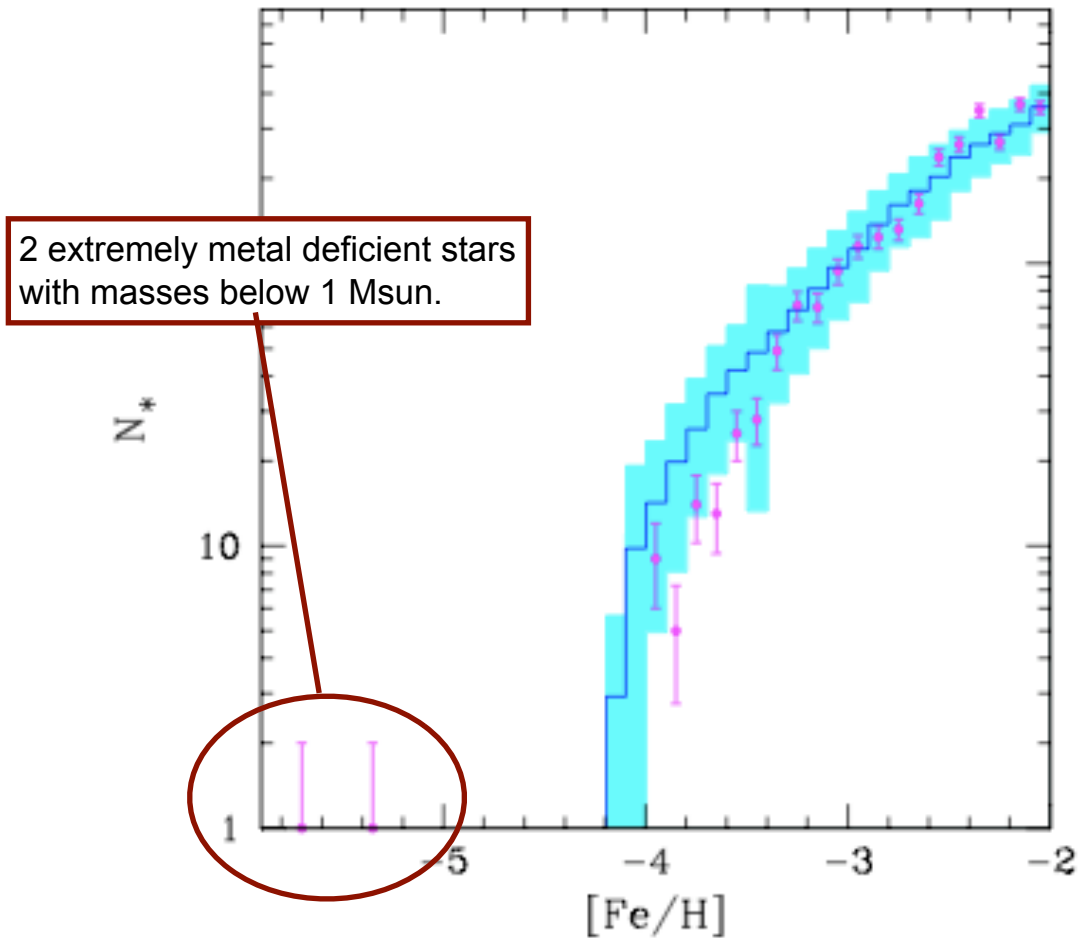

(plot from Salvadori et al. 2006, data from Frebel et al. 2005)

dense cluster of low-mass protostars builds up:

- mass spectrum peaks below 1 M_{sun}
- cluster VERY dense $n_{stars} = 2.5 \times 10^{9}\ pc^{-3}$

- *predictions:*
  * low-mass stars with [Fe/H] ~ 10^{-5}
  * high binary fraction

(Clark et al. 2008)

summary

conclusions

- chemistry and thermodynamics are important:
  - for molecular cloud formation
  - for statistical properties of the ISM (turbulence, density distribution, pressure distribution, etc)
  - for star formation
  - and therefore for the Schmidt law.

conclusions

- chemistry and thermodynamics are important:
  - “YES WE CAN!!”

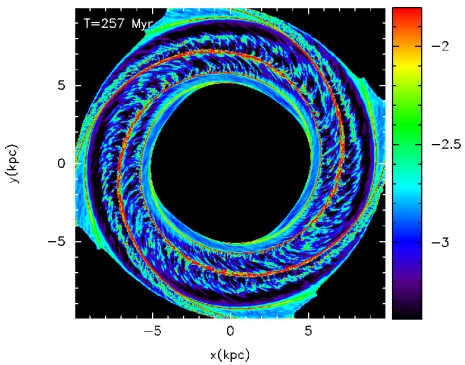

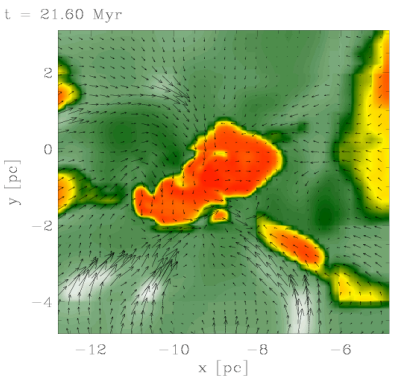

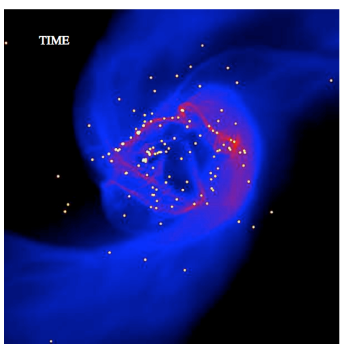

conclusions

- chemistry and thermodynamics are important:
  - YES WE CAN!!
  - *postdictions:*
    - global Schmidt law (from gravity)
    - molecular cloud properties (morphology, kinematics, etc.)
    - IMF (at least roughly)

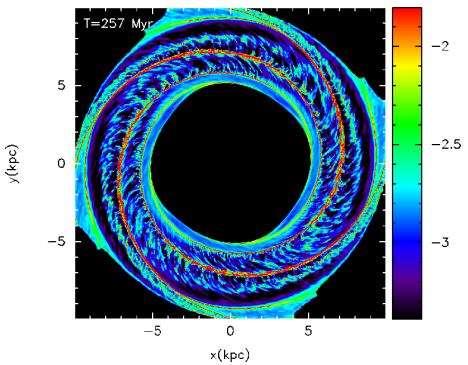

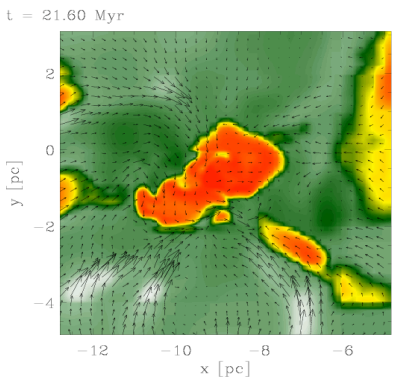

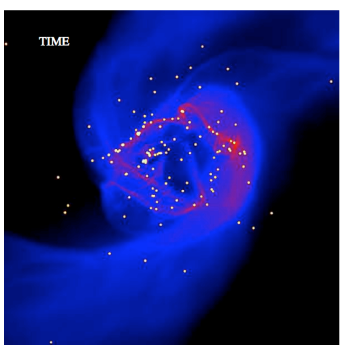

conclusions

- chemistry and thermodynamics are important:
  - density pdf influenced by *Mach number*, but also by *EOS* (wider for softer EOS) and *modes of driving* (rotational / compressive) --> ***SFR, IMF***
  - *observational implications/predictions:*
    - variations of x-factor (location, Fe/H)
    - molecular cloud formation times
    - density pdf *not* log-normal
    - (local) universality of IMF
    - ultra-low metallicity stars with masses below M_{sun} and high binarity

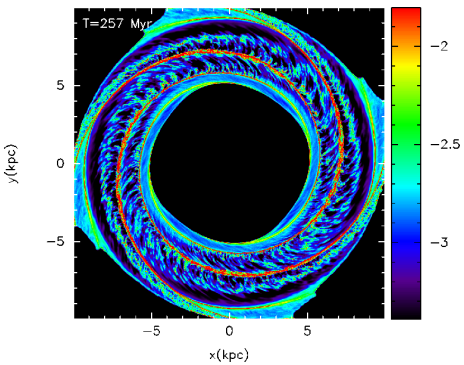

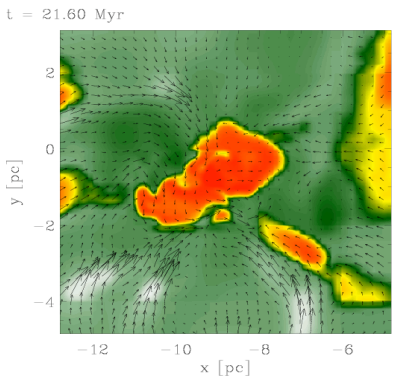

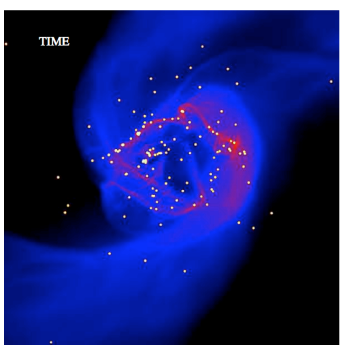

Thanks!